

Three-Dimensional Theories for Light-Matter Interactions

*Faculty of Science
University of Copenhagen
The Niels Bohr Institute*

Ph.D. Thesis
JANUARY 2009

Martin Westring Sørensen

Table of Contents

Foreword	v
Dansk resumé	ix
I Introduction	1
1 Introducing quantum optics with atomic ensembles	3
1.1 The interaction strength problem	4
1.2 The dimensionality and scaling problem	8
1.3 Overview of the thesis	10
II Three-dimensional theory for light-matter interactions	13
2 Introduction	15
3 Model	21
3.1 Interaction with single atoms	21
3.2 Mode expansion	24
3.3 Quantization and commutation relations	27
4 Equations of motion	31
5 General solution and Feynman diagrams	35
5.1 Perturbative expansion	37
5.2 Density correlations.	38

5.3	Green's function and propagator	40
6	Time evolution	45
6.1	Evolution of the spin	45
6.2	Evolution of the light	49
6.3	Photon counting and Stokes operators	52
6.4	Calculation of Stokes operators	54
7	Experimental application and validity	61
7.1	Measurement procedure	61
7.2	Extreme paraxial approximation	62
7.3	Multi-mode coupling	64
7.4	Validity	68
7.4.1	Validity of the simple multi-mode dynamics	68
7.4.2	Validity of perturbation theory	69
8	Conclusion	73
III	Three-dimensional theory for Superradiance	75
9	Introduction	77
10	Equations of motion	79
10.1	Atomic dynamics	80
10.2	Field equation	82
11	Discrete to continuous system	85
12	Diagonalizing the interaction matrix	87
13	Real space representation of the electric field	93
13.1	Short time limit	97
13.2	Finite time, build up of superradiance	98
14	Intensity and the correlation function	101
14.1	Intensity on the symmetry axis	103

14.2 Intensity profile	104
14.3 Total coherent radiation.	108
15 Conclusion	117
IV Qubit protection in nuclear-spin quantum dot memories	119
16 Qubit protection in nuclear-spin quantum dot memories	121
16.1 Fully polarized nuclei.	122
16.2 Decoherence suppression.	125
16.3 Non-perfect spin polarization.	128
V Conclusions	131
17 Conclusions	133
A Appendix for Part 1	135
A.1 Adiabatic elimination	135
A.2 Calculation of infinitely short propagator	137
A.3 Reciprocal equation for Green's function	139
A.4 Lorentz-Lorenz relation	142
A.5 Calculations of second-order Stokes generator	145
A.6 Calculation of second-order Spin-terms	146
A.7 Calculation of spontaneous emission	148
A.8 Beyond paraxial approximation	150
B Appendix for Part 2	151
B.1 Deriving the first order correction to the matrix $M_{k'm'n'}^{kmn}$	151
B.2 Commutation relation for Λ_{mn}^m and Λ_{mn}^{1m}	153
B.3 Beyond the delta function approximation of the Gaussian $\eta(k)$	154
B.4 Additional material to Sec. 14.3	155
B.5 The Sum rule	156
Bibliography	157

Foreword

This thesis is a collection of work done as part my Ph.D. programme at Copenhagen University, Faculty of Science. The work has been done in the period from fall 2005 to winter 2009, and covers in detail a generalized three-dimensional description of the interaction between an electromagnetic field and a realistic collection of atoms. The thesis that I present here is split in four parts, where the first part gives an overview of the problems adressed in the thesis. The second part describes a weakly interacting collection of photons and atoms, whereas the third part describes a strongly interacting system. Part Four of the thesis covers work done in collaboration with Z. Kurucz and M. Fleischhauer at University of Kaiserslautern, J. Taylor at Massachusetts Institute of Technology and M. D. Lukin at Harvard University. The work was done in Kaiserslautern in the fall of 2007. I note that after I left Kaiserslautern the process continued. The work I present in Part Four of this thesis is a preprint of a paper including more than my contribution. Specifically I participated in the development of the theory leading to Eqs. (16.0.1- 16.2.7) of Part Four. I would like to thank Professor Michael Fleischhauer for his hospitality and obligingness during my stay in Kaiserslautern. Also and in particular I am greatly thankfull to Ph.D. Zoltan Kurucz, with whom I primarily worked. Finally I wish to thank my supervisor Anders Sørensen. In spite of our differences I find our collaboration inspirering. It goes without mention that I could not have derived these results without him.

My Ph.D was prolonged by two months as my wife in January 2007 gave birth to our first child. I only hope that eventually I shall be able to give back to my family, some of the time I borrowed for finishing this thesis.

The work presented in Part Two is published in Ref. [1], publications concerning Part Three and Four are in preparation. In the following I present a brief abstract for the bulk of the thesis, Part Two, Three, and Four.

Part Two

We present a full quantum mechanical three dimensional theory describing an electromagnetic field interacting with an ensemble of identical atoms. The theory is constructed such that it describes recent experiments on light-matter quantum interfaces, where the quantum fluctuations of light are mapped onto the atoms and back onto light. We show that the interaction of the light with the atoms may be separated into a mean effect of the ensemble and a deviation from the mean. The mean effect of the interaction effectively gives rise to an index of refraction of the gas. We formally change to a dressed state picture, where the light modes are solutions to the diffraction problem, and develop a perturbative expansion in the fluctuations. The fluctuations are due to quantum fluctuations as well as the random positions of the atoms. In this perturbative expansion we show how the quantum fluctuations are mapped between atoms and light while the random positioning of the atoms give rise to decay due to spontaneous emission. Furthermore we identify limits, where the full three dimensional theory reduce to the one dimensional theory typically used to describe the interaction.

Part Three

We present a three-dimensional theory of Stimulated Raman Scattering (SRS) or superradiance. In particular we address how the spatial and temporal properties of the generated SRS beam, or Stokes beam, of radiation depends on the spatial properties of the gain medium. Maxwell equations for the Stokes field operators and of the atomic operators are solved analytically and a correlation function for the Stokes field is derived. In the analysis we identify a superradiating part of the Stokes radiation that exhibits beam characteristics. We show how the intensity in this beam builds up in time and at some point largely dominates the total Stokes radiation of the gain medium. We show how the superradiance depends on geometric factors such as Fresnel number and gain properties such as optical depth, and that in fact these geometry factors are the only factors describing the coherent radiation.

Part Four

We present a mechanism to protect quantum information stored in an ensemble of nuclear spins in a semiconductor quantum dot. When the dot is charged the nuclear magnetic moments interact with the spin of the excess electron through the hyperfine coupling. If this coupling is made off-resonant it leads to an energy gap between the collective storage

states and all other states. We analyze the collective spin excitations and show that the energy gap protects the quantum memory from local spin-flip and spin-dephasing noise. The protection decreases with increasing spatial correlation length of the noise. Effects of non-perfect initial spin polarization and inhomogeneous hyperfine coupling are discussed.

Dansk resumé

Denne afhandling hører under feltet kvanteoptik inden for diciplinen teoretisk fysik. Afhandlingen er delt i tre dele foruden en introduktion og en konklusion. Disse tre dele består af en tre-dimensionel beskrivelse af lys, der vekselvirker svagt med atomer, en tre-dimensionel teori for en stærkere vekselvirkning mellem lys og atomer, kaldet superradians, og til sidst en beskrivelse af dynamikken i et system bestående af en elektron og en samling atomkerner i en kvante-prik. I det følgende giver vi en mere detaljeret beskrivelse af de enkelte dele.

I Del to udleder vi en fuldstændig, tre-dimensionel beskrivelse af vekselvirkningen mellem et elektromagnetisk felt og en samling identiske atomer. Teorien er konstrueret med henblik på at beskrive eksperimenter udført for nylig om kvante-grænsefladen mellem lys og atomer, hvor kvante-unøjagtigheder fra lyset projekteres på atomerne og bagefter tilbage på lyset. Vi viser, at vekselvirkningen mellem lys og atomer kan deles i en middeleffekt og i en afvigelse fra middeleffekten. Vi viser også at denne middeleffekt blot leder til et brydnings-index for den atomare gas. Vi skifter dernæst til en beskrivelse hvori middeleffekten af vekselvirkningen er inkorporeret i lysets dynamik, og laver en formel perturbations regning i afvigelsen fra middeleffekten. Både de kvantemekaniske unøjagtigheder samt unøjagtigheder fra den tilfældige rummelige fordeling af atomerne er indeholdt i beskrivelsen af afvigelserne fra middeleffekten. I denne perturbative beskrivelse viser vi, hvordan kvante-unøjagtigheder projekteres imellem lys og atomer, samt at den tilfældige rumlige fordeling af atomer leder til et henfald af felt- og atomare excitationer. Til sidst identificerer vi de grænser, hvor den tre-dimensionelle teori reduceres til den en-dimensionelle teori, der typisk bliver brugt til at beskrive denne type vekselvirkning mellem lys og atomer.

I Del tre udleder vi en tre-dimensionel teori om “Stimulated Raman Scattering” (SRS). Vi er specielt interesserede i de rumlige og tidslige egenskaber ved den i vekselvirkningen

genererede SRS stråle eller “Stokes” stråle, og hvordan egenskaberne afhænger af dimensionerne af de atomer, der danner strålen. Vi udleder Maxwell-ligninger for Stokes-feltet og tilsvarende ligninger for atomerne. Disse ligninger bliver løst analytisk, og der bliver udledt en korrelations-funktion for Stokes-feltet. Vi identificerer den del af Stokes-feltet, der giver anledning til en stråle, og viser hvorledes intensiteten i strålen tager til over tid og endeligt bliver den dominerende effekt. Vi viser, hvordan strålen afhænger af geometriske egenskaber ved samlingen af atomer, såsom Fresnel-nummer og optisk dybde, og at netop disse geometriske faktorer er de eneste, der påvirker den genererede stråle.

I Del fire præsenterer vi en mekanisme, der kan beskytte kvanteinformation gemt i en samling kernespin i en halvleder eller kvante-prik. Når kvante-prikken er ladet op med en elektron, vil kernernes magnetiske moment vekselvirke med elektronens spin via den hyperfine kobling. Når denne kobling gøres ikke-resonant med kernespin-overgange fører det til et energi-gab mellem den kollektive hukommelses-tilstand og alle andre kollektive tilstande. Vi analyserer den kollektive spin tilstand og viser at energi-gabet beskytter hukommelsen mod individuelle “spin-flips” og “spin-dephasing” støj. Beskyttelsen aftager når den rumlige korrelations længde af støjen tiltager. Effekten af en samling atomer, der til at begynde med ikke er perfekt polariserede, samt effekten af en ikke-homogen hyperfin kobling, bliver ligeledes analyseret.

Part I

Introduction

*Introducing quantum optics with
atomic ensembles*

Entering the field of quantum optics, one quickly learns that the importance of the wave particle duality of light can not be overstated. An almost overwhelming amount of effects in nature involving the electromagnetic field are explained and explored within the framework of wave theories in the Maxwell equations. This includes grand scale phenomena such as the rainbow, radio signals transmitted to the other end of the universe, but also small scale electrical circuits printed on a silicon plate in a computer processor. At the other end of our intuition, where the particle behavior of light is found, we are able to explain effects such as spontaneous radiative decay of an atom, and the photoelectric effect. It is at the border of classical electrodynamics that quantum optics is found. Should one have a desire to work in the field of quantum optics, it is therefore of paramount importance to understand a description of the electromagnetic field that encompass both the particle and the wave behavior. Statistics on quantum optics shows that the bulk of the research has to do with the interaction between electromagnetic radiation and atom-like systems. This thesis is no exception, as some of the most amazing quantum features of light is found in the interface between radiation and atomic excitation. In this thesis we will show examples of how to derive a description of light suitable for treating both particle and wave effects. We will examine light-atom interactions, where the microscopic quantum effects is still visible even though the system is scaled to involve thousands of

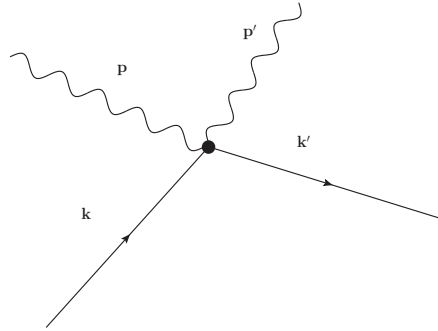


Figure 1.1: A single atom interacting with a single photon.

atoms and photons. The methods for dealing with these atom and photon interaction problems are many and varied, but often falls under the two main problems. The problem of interaction strength, and the dimensionality and scaling problem. In this thesis we will however not discuss the exciting problems of imposing extra boundary conditions to the electromagnetic field, such as including an optical fibre, a photonic crystal, or a nano-wire. Below we shall discuss the two main problems that we are examining in this thesis.

1.1 The interaction strength problem

We will discuss and examine the interaction strength problem by using simple drawings. Let us imagine that the degrees of freedom of an atom can be described by the index \mathbf{k} . That will include the momentum of the atom, the internal energy state and other information we could ascribe to a set of commuting operators. Similarly we imagine that the degrees of freedom for the photon is described by an index \mathbf{p} . In the picture, Fig. 1.1, we draw the evolution of the atom as a straight line and the evolution of the photon as a wiggly line. The picture is understood in the following way. A photon described by the index \mathbf{p} meets an atom described by the index \mathbf{k} . They interact, and after the interaction the atom is no longer described by the index \mathbf{k} but with the index \mathbf{k}' . Similarly the photon is now described by the index \mathbf{p}' . During the interaction the state of the atom and the photon changed. Perhaps the energy of the photon changed, and the internal state of the atom changed. This will of course depend on the details of the interaction.

We readily complicate the picture when allowing the photon to meet the same atom

over and over again, like in an optical cavity. In Fig. 1.2 we have made an illustration of the case where the photon and the atom interact five times. The number of times they interact is chosen with some arbitrariness, we really can not tell if they interact one, five, or say, one hundred times. This is the essence of the interaction strength problem. Depending on this interaction strength, one will either treat the interaction as a pertur-

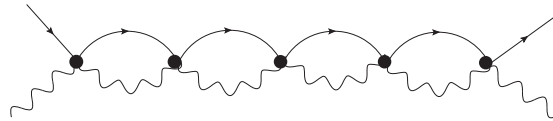


Figure 1.2: Interactions in a cavity

bation to the time-evolution of the system, or as a source driving the time-evolution. In the case of a photon and an atom in a cavity one will typically expect the latter. Since such a system driven by the interaction is of fundamental interest in the quantum optics field we will continue the analysis a little further. Let us say that the problem of an atom in a cavity is described by the situation that either the photon and the atom do not interact, they interact one time, they interact two times, three times and so on, we

can make a drawing that represents this situation. $\rightarrow + \begin{array}{c} \swarrow \\ \bullet \\ \searrow \end{array} + \begin{array}{c} \swarrow \bullet \searrow \\ \swarrow \bullet \searrow \end{array} + \begin{array}{c} \swarrow \bullet \searrow \\ \swarrow \bullet \searrow \\ \swarrow \bullet \searrow \end{array} + \dots$. The drawing can be split, so that we start treating the drawing as a mathematical object $\rightarrow \left\{ \begin{array}{c} \swarrow \\ \bullet \\ \searrow \end{array} + \begin{array}{c} \swarrow \bullet \searrow \\ \swarrow \bullet \searrow \end{array} + \begin{array}{c} \swarrow \bullet \searrow \\ \swarrow \bullet \searrow \\ \swarrow \bullet \searrow \end{array} + \dots \right\} \leftarrow$, and what we see is that the complicated problem of an atom in a cavity can be summarized in a geometrical series $\rightarrow \left\{ \begin{array}{c} \bullet \\ \hline 1 - \begin{array}{c} \swarrow \bullet \searrow \end{array} \end{array} \right\} \leftarrow$.

Often however the problem is to find the proper mathematical description of such drawings, because what seems intuitively clear on drawing might contain mathematical pit holes.

Let us move to the class of systems that are the subject of this thesis. Namely systems that include many atoms and many photons. Before we dig into the large variety of diagrams describing the possible interaction events happening in such a system, we first look at two relatively simple situations. The first situation describes a photon traveling through the ensemble of atoms, and on its way it interacts with a lot of different atoms. We will assume that during this passage the photon never interacts with an atom that have any prior history involving an interaction with a photon. In Fig. 1.3 we show such an interaction sequence. The symmetry and relative simplicity of such kinds of diagrams

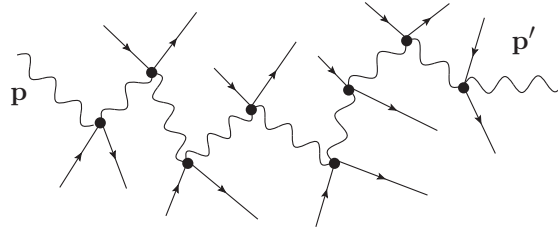


Figure 1.3: A diagram describing the propagation of a photon through an atomic gas. The diagram belongs to a class of diagrams that can be reduced to an index of refraction.

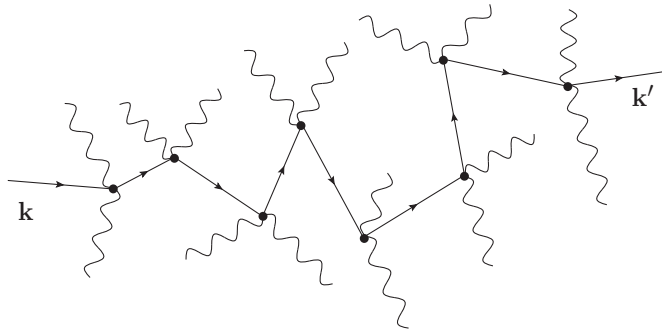


Figure 1.4: A diagram describing the propagation of an atom through an electromagnetic field. This type of diagram belongs to a class of diagrams that reduce to a Stark shift of the internal energy levels of the atom.

enable us to treat them the same way as with the atom in a cavity. The effect of such interactions is to add to the propagation of the photon an index of refraction.

Similarly such a situation exists from the atoms point of view, where an atom is being hit by a number of different photons. This situation is described in Fig. 1.4. In the simple case where the photons are identical, and have not interacted with atoms before, the type of drawings presented above can similarly be summed to represent a Stark shift of the dipole-energy of the atom.

The work presented in this thesis is in the many photon many atom regime, where we understand the Stark shift, and the index of refraction. The physics we focus on is described in the remaining diagrams. As an example we imagine an atom first interacting with a photon and then later with another photon. This photon then interact with two different atoms. In all we have an interaction process involving two different photons and three different atoms. This situation can be represented in a drawing such as Fig. 1.5. The vast number of such interaction sequences is what we will call the interaction strength

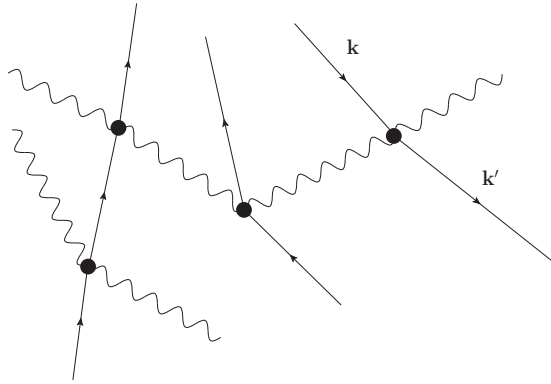


Figure 1.5: A complicated sequence of interactions involving two photons and three atoms.

problem, since sorting out and choosing the relevant interaction sequences is much related to the interaction strength between photons and atoms. This problem is typically split in two cases. The weak interaction problem, and the strong interaction problem. In the weak interaction problem we will in principle consider all kinds of interaction sequences, but introduce a maximal number of interactions that still effects the evolution of the system. This way we only get a finite set of interaction sequences or diagrams, and can in principle analyze all of them. In Part Two of the thesis we demonstrate this approach, by way of analyzing the dynamics of a system that is too complicated to solve exactly, but is sufficiently described by a relatively small number of interaction sequences.

In Part Three of the thesis we will turn to the strong interaction problem. In this regime there is an interaction that we can not treat in an entirely perturbative way. By this we mean that the interaction is so strong that there is no way we can make a cut in the number of interactions and claim that these remaining diagrams contain all the information that is relevant for the dynamics of the system. We could for example imagine that the situation where a photon interacts with an atom and then later with another atom is so probable, that with this interaction sequence all atoms effectively interacts with each other all the time. To find the dynamics of one atom, therefore requires solving the two-particle interaction problem exactly. In Fig. 1.6 we illustrate the meaning of this effective two-particle interaction. An example on such a problem is the superradiance problem which is the topic of Part Three. Solving such a strong interaction problem is often quite complicated, but the formal solution is in principle found in the same way as we did with the atom in a cavity. Let us now turn a little away from the problem involving only the interactions and look a little on the environment in which the interaction takes place.

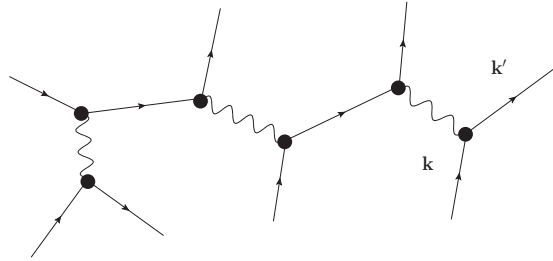


Figure 1.6: A diagram showing an effective two-particle interaction between atoms, involving the emission and absorption of a photon.

1.2 The dimensionality and scaling problem

When we discuss the environment we refer to the situation that the atoms are distributed in a finite region of space. The problems that such a distribution of atoms lead to, we will refer to as the dimensionality and scaling problem. In this discussion we will have to be more specific concerning the interaction between the particles since such a discussion eventually have to compare the length scale of the environment with the length scale of the interaction. Say that the interaction is very short range, e.g. in a collision. We then assume that all the atoms are homogeneously distributed in a box of dimensions much larger than the range of the interactions, and thus we can with high accuracy say that the overall dynamics of the system is not effected by the finite size of the container. In this case the particles interacts only with their nearest neighbors, and thus the majority of them will have the same amount of nearest neighbors and the same dynamical environment.

Let us consider an interaction that does not exhibit this local behavior. We could as an example take the two-particle interaction described in Fig. 1.6. In principle this interaction has an infinite range in the sense that the photon after interacting with the first atom can travel to the end of the universe before it meets another atom and interact. For this type of interaction one can imagine that having a finite sized ensemble of atoms, does effect the overall dynamics of the system. To discuss this problem we will consider a system where the atoms are described by some operator $b(\mathbf{r})$. The operator can tell us about the internal state of an atom at position \mathbf{r} . This information is changed when the atom interacts with a photon. We will assume that the interacting photon originated from another atom, and that the state of the photon depends on the state of the atom it was emitted from. We might therefore find that the change of the state of an atom can be

described by

$$\frac{d}{dt}b_j(t) = \sum_{j'} P^{(+)}(\mathbf{r}_j, \mathbf{r}_{j'}) \beta b_{j'}(t). \quad (1.2.1)$$

The function P is a Green's function that describes the propagation of a photon traveling from $\mathbf{r}_{j'}$ to \mathbf{r}_j . The quantity β describes the coupling strength between a photon and an atom. To discover some of the effects of a finite sized ensemble of atoms we will use the fact that we have no knowledge about the position of the atoms. By this we mean that though the atoms are in principle localized in space, we do not know where, so if we talk about the outcome of some physical measurement, we will have to trace out the position of the atoms. This we will refer to by taking a spatial average. In Sec. 5.2 we discuss and develop such spatial average. In this way we get a continuous function describing the density of atoms. The natural continuous formulation of the problem is

$$\frac{d}{dt}b(\mathbf{r}, t) = \int d^3r' \sqrt{\rho(\mathbf{r})} \bar{P}^{(+)}(\mathbf{r}, \mathbf{r}') \sqrt{\rho(\mathbf{r}')} b(\mathbf{r}') \quad (1.2.2)$$

where the function $\rho(\mathbf{r})$ is the atomic density at position \mathbf{r} . The two limits that we will consider here are first the limit where the atomic ensemble is infinitely big, and second the limit where the atomic ensemble is infinitely small. In the first case we will use the fact that the density is constant, and in the second case that the density is resembling a delta function. The propagator $P^{(+)}$ has a nice description in Fourier space, see e.g. Chap. 5,

$$P(\mathbf{r}, \mathbf{r}') \propto \int d^3k \frac{\mathbf{k}^2 e^{i\mathbf{k}\cdot(\mathbf{r}-\mathbf{r}')}}{\mathbf{k}^2 - k_L^2}, \quad (1.2.3)$$

where we assume that there is some wave number k_L describing the energy scale on which these interaction processes take place. It is therefore convenient to make a Fourier transformation of the Eq. (1.2.2). In the first case of an infinitely big atomic ensemble we arrive at a differential equation stating

$$\frac{d}{dt}b(\mathbf{k}, t) = i\beta' \frac{\mathbf{k}^2}{\mathbf{k}^2 - k_L^2} b(\mathbf{k}, t). \quad (1.2.4)$$

From here we see that in the case of an infinitely sized atomic ensemble, the Fourier components of the operators describing the atoms are decoupled from each other. We see a resonance behavior of the Fourier components that are on resonance with the energy

scale on which the interactions takes place k_L . The nice thing about infinitely size atomic ensembles is then that the dynamics of the atomic operators are decoupled in Fourier space. One can therefore choose to look at some specific Fourier component which makes dimensionality reduction very easy.

In the opposite limit where the sample is infinitely small, the propagator will now only describe a photon traveling an infinitely short distance. This type of propagator is the subject of Chap. 6. There we show that the propagator in the simple case reduces to a decay rate Γ . The atomic operator equation is in this case best described by

$$\frac{d}{dt}b(\mathbf{k}, t) = -\Gamma \int d^3k' b(\mathbf{k}', t). \quad (1.2.5)$$

Now we find that the Fourier components of the atomic operators collectively decays, and the natural way to continue is to define the collective operator as being just the sum of all the Fourier components. This collective operator decays in the same way a single atom operator would. The two results are quite different, in the first case, where we have no localization of the atoms in position-space, we have a perfect localized behavior in momentum-space. Where in the other case we have perfect localized behavior of the atoms in position space, we find that they are completely de-localized in momentum space. For atomic ensembles in the real world we can never really be in any one of the two situations, and discovering the behavior of such a real system is what we refer to as the dimensionality or scaling problem. The reason for calling it a scaling problem is that we would like to know, how fast we go from one limit to the other as we vary the geometry of or system. We also wish to know how the general dynamics of our system scale with the geometry of the system. Both in Part Two and in Part Three of the thesis, this scaling problem is a main concern, which is also the reason for calling the research topic under which this thesis falls, three-dimensional theories for light matter interactions. The general approach we shall use in dealing with this problem is to say that the system is big compared to the wave number k_L but otherwise finite.

1.3 Overview of the thesis

The thesis is divided into three research Parts, Two, Three, and Four. In Part Two we develop a three-dimensional theory for light-matter interactions, where we focus on a weak

interaction, and present the dynamics of the system as a perturbation series. The work presented in Part Two is organized as follows: In Chap. 3 we give the details of the model used to describe the interaction. In Chap. 4 we derive a set of equations of motion describing the system of atoms and light, using Heisenberg's equation of motion. The wave equation describing the light is expressed in a form that ideally suits a perturbative treatment. In Chap. 5 we express the general solution to the wave equation in terms of Green's functions and derive the perturbative expansion of the solution to the wave equations as well as the equation describing the atoms. This is represented in terms of Feynman diagrams. In addition we develop the appropriate theoretical tools to describe point particle effects such as density correlations, and derive a formal expression for the Green's function. In Chap. 6 we present our results where we discuss higher order effects such as spin decay and light scattering. We define operators that describe photon-measurements, and demonstrate how these are calculated in the theory. In Chap. 7 we discuss various limits where the general three dimensional theory reduce to the usually employed one dimensional model [2]. We also describe how a detailed understanding of the spatial modes can be used to achieve storage and retrieval of information in several transverse modes of light and atoms simultaneously. In Chap. 8 we conclude the work, and in Appendix A we give several details omitted from the main text.

In Part Three we look at a system of strongly interacting atoms and photons. This system can not be expressed correctly as a finite perturbation series, and we therefore turn to an eigenvalue description of the dynamics of the system. The analysis begins with the basic set of equations describing the interaction of light with atoms. The atoms are treated as non-moving point particles and the radiation fields are considered in the so-called length gauge with operators suited to a macroscopic description. See Chap. 3 for a discussion of this choice. We will then in Chap. 10 derive effective equations of motion for both the radiation field and the atoms. These equations are directly comparable to the equations used in Ref. [3]. Having established the equations of motion we will in Chap. 11 change from the point particle picture to a continuous description. This again follows methods described in Sec. 5.2. In Chap. 12 we make a formal diagonalization of the matrix describing the interaction between atoms mediated by the light. This diagonalization means that we have to find a basis that will simplify the interaction. In Chap. 13 we will look at the radiated field and see how this is evolving as the atoms are interacting. Finally in Chap. 14 we look at the intensity of the radiated field and present the final results. We shall in addition to the analytical results make a comparison with numerical calculations

for the superradiance starting with the point particle equations of motion derived in Chap. 4. In Chap. 15 we conclude the work. Calculations omitted from the text is found in Appendix B.

In Part Four we look at a system consisting of a single electron, and a collection of nuclear spins confined in a quantum dot. The electron spin is coupled to the nuclear spin by the Fermi contact interaction Hamiltonian. The spin state of the electron is via the interaction Hamiltonian mapped onto the collection of nuclear spin. We first derive a description of the collective nuclear spin states. These states include the state of the collective nuclear spin after a successful mapping of the electron state via the interaction Hamiltonian. We then look at mechanisms responsible for destroying the stored electronic spin state in the collective nuclear spin system. First we look at the effect of an inhomogeneous distribution of nuclear spin in the quantum dot. Then we look at the effect of coupling the nuclear spins to a noisy classical magnetic field. After that we look at the effect of nuclear spin diffusion due to dipole-dipole interactions between nuclear spins. Finally we look at the problem of mapping the electron spin to non-perfect polarized nuclear spin.

Finally in Part Five we summarize the main results presented in the thesis.

Part II

Three-dimensional theory for light-matter interactions

Introduction

For several applications in quantum information science, such as long distance quantum communication [4], it is essential to create an interface linking the photonic states used for transmitting quantum information to a material state suitable for storing and processing the information. The generation of the required strong coherent coupling of light to a single emitter has proven difficult to achieve in practise, although substantial progress has been made [5–9]. In recent years optically dense atomic ensembles has emerged as a promising alternative [2, 10–24]. In this approach one can for instance use classical laser pulses to engineer a suitable interaction such that an incoming light field is reversibly stored into the coherence between, e.g., two stable ground states in the atoms [11].

Some experiments on atomic ensembles uses atoms that are enclosed inside a cavity to enhance the coupling [20]. In this situation the cavity defines a unique mode of the light field and the theoretical description consists of describing a single optical mode coupled to the atomic ensembles. Most experiments are, however, performed with atoms in free space not enclosed in a cavity, and in this situation the theoretical description is more complicated. Typically this situation is described in a one dimensional approximation, where one only considers a single transverse mode and solves a one dimensional propagation equation for this mode [2, 14, 15].

In this paper we explore the range of validity of the one-dimensional approximation

by making a full three dimensional description of the interaction between light and an atomic ensemble. Our calculations directly apply to an experimental situations similar to the ones described in Refs. [10–13], where the light is detuned far from the atomic transition, but we expect the general features of our results to be valid for a much broader class of problems.

Some justification for the one-dimensional description may be found in the literature on superfluorescence, e.g. Refs. [3, 25, 26]. In this context it was found that the one-dimensional description is valid provided that the Fresnel number is of order unity $\mathcal{F} \equiv A/\lambda L \approx 1$, where A is the transverse beam area, λ is the wavelength of the light, and L is the length of the ensemble. Based on this work it has been argued that it is also necessary to have a Fresnel number of order unity in order for the one-dimensional approximation to be applicable to the quantum interfaces between light and atomic ensembles [2, 14, 15]. It is, however, essential to realize that the physical situations are very different in the two cases. The work on superfluorescence typically concerns the temporal distribution of the output light measured by impinging the outgoing light on a photodetector. Because the photodetector just measures the incoming flux I , this is essentially a multi-mode measurement

$$I \propto \sum_m \hat{a}_m^\dagger \hat{a}_m, \quad (2.0.1)$$

where the the sum is over all modes m hitting the detector, and each of these modes are described by the photon creation (annihilation) operators \hat{a}_m^\dagger (\hat{a}_m). In particular the sum here includes all transverse modes. This is in contrast to the quantum interface work, where one is interested in the outgoing state of a single light mode, e.g., in Refs. [10–13] the measurement is essentially a homodyne measurement of a single mode, defined by the field of the strong classical laser. In other experiments the outgoing light is sent through a single mode optical fiber, which filters out everything except a single transverse mode. Furthermore the superfluorescence work applies to a nonperturbative situation with a large optical gain, whereas the quantum interfaces typically operates in the few excitation regime. The previous analysis is thus not applicable to the present situation and it is therefore not to be expected that the condition $\mathcal{F} \sim 1$ is the right condition for the validity of the one-dimensional approximation. In fact, the experiments in Refs. [10–12] are performed with $\mathcal{F} \sim 10^4$, and still give very good agreement with the one-dimensional description. Here we make a full three dimensional description of the experiments in Refs. [10–12], and we find that it reduces to the one-dimensional description in the paraxial approximation

provided that $\mathcal{F} \gg 1$.

In a related work a three dimensional description was also presented in Ref. [27]. Whereas our procedure assumes non-moving atoms, i.e., cold atoms, that work considered the opposite limit, where the motion of the atoms wash out any spatial structure of the atomic spin state. Unlike the situation in Ref. [27], where the motion of the atoms always lead to certain inefficiencies, the fact that we consider stationary atoms, allows us to identify certain limits, where we exactly reproduce the simple result of the one dimensional theory as discussed in Chap. 7.2.

Our theory is developed as a perturbative expansion of the interaction between light and the atomic ensembles. It is, however, essential to be very careful about the way this perturbative expansion is performed. Below we shall present results up to second order in the interaction between the light and the atoms. We shall use an effective Hamiltonian, where the excited atomic state has been eliminated, i.e., a Hamiltonian of the form

$$H \sim \sum_{\mathbf{k}, \mathbf{k}'} \sum_i g_{\mathbf{k}, \mathbf{k}'} u_{\mathbf{k}}(\mathbf{r}_i) u_{\mathbf{k}'}^*(\mathbf{r}_i) \hat{a}_{\mathbf{k}'}^\dagger \hat{a}_{\mathbf{k}}, \quad (2.0.2)$$

where $g_{\mathbf{k}, \mathbf{k}'}$ is a coupling constant for the two modes \mathbf{k} , and \mathbf{k}' described by photon creation (annihilation) operators $\hat{a}_{\mathbf{k}}^\dagger$ ($\hat{a}_{\mathbf{k}}$) with mode functions $u_{\mathbf{k}}$, and \mathbf{r}_i is the position of the i th atom. If we take the mode functions to be simple plane waves with an input field in a certain mode \mathbf{k}_0 and calculate the intensity in a certain direction described by \mathbf{k}_1 , we find the intensity

$$I \propto \left| \sum_i e^{i\Delta\mathbf{k} \cdot \mathbf{r}_i} \right|^2 = \sum_{i,j} e^{i\Delta\mathbf{k} \cdot (\mathbf{r}_i - \mathbf{r}_j)}, \quad (2.0.3)$$

where $\Delta\mathbf{k} = \mathbf{k}_1 - \mathbf{k}_0$. The standard way to proceed from here is to say that the exponential varies rapidly when $i \neq j$ and therefore neglect all terms except $i = j$ so that one is left with something proportional to the number of atoms N_A , which is known as spontaneous emission. For the problem we are interested in here, we are, however, mainly concerned with the properties of the light in the forward direction, where $\Delta\mathbf{k} \approx 0$. In this case it seems unjustified to neglect the cross terms which give rise to collective scattering scaling as N^2 . Since N is typically a very big number, the presence of such large N^2 contributions may limit the applicability of perturbation theory.

In order to avoid the problems associated with this collective scattering, we use a

different basis for our perturbative expansion: instead of starting from the eigenmodes of the propagation equation in vacuum, we use the solutions to the classical diffraction problem in the presence of the medium, i.e., we take into account that the atoms give rise to an index of refraction of the gas, which changes the propagation of the light. Specifically, we write the Hamiltonian as

$$H = \langle \mathcal{H} \rangle_{\text{atoms}} + \delta H, \quad (2.0.4)$$

where $\langle \mathcal{H} \rangle_{\text{atoms}}$ is the quantum mechanical expectation value of the Hamiltonian with respect to the atomic spin state averaged over the random positions of the atoms. This averaged Hamiltonian gives rise a continuous quadratic Hamiltonian in the light field operators similar to a Hamiltonian describing the interaction with a dielectric medium. When we formally change to the interaction picture with respect to this averaged Hamiltonian, we obtain a new set of basis modes. Doing perturbation theory on these modes, the only effect on the light comes from the quantum mechanical fluctuations and the fluctuations caused by the random position of the atoms. These fluctuations are described by the Hamiltonian $\delta H = H - \langle \mathcal{H} \rangle_{\text{atoms}}$. When we average the first order term in the perturbative expansion with respect to the position of the atoms the resultant expression describe that the quantum fluctuations of the atoms are mapped onto the light in analogy with the results derived in a one-dimensional theory in Ref. [2].

If we go to second order in the interaction, our expression will give terms quadratic in δH . In order to take the spatial average of such terms we need to know the density correlation function of the atoms. Inserting the density correlation function for an ideal gas we no longer find the collective scattering terms described above, i.e., the collective scattering is essentially the classical diffraction of the light, which is explicitly taken into account by our average Hamiltonian, and therefore it does not appear in our perturbation theory. The spatial average of the second order term does, however, produce a new term associated with the point particle nature of the atoms and their random positions. This term is equivalent to the results obtained by just keeping the $i = j$ terms in Eq. (2.0.3), and represents the effect of spontaneous emission.

Unlike most approaches to the interaction between atoms and light, which derive coupled equations for the atomic states and the electric field, our approach considers the electric displacement field \mathbf{D} instead of the electric field. The reason we chose to use the

displacement field is that it is convenient to work with a purely transverse field, which is the case for the displacement field due to the macroscopic Maxwell equation $\nabla \cdot \mathbf{D} = 0$, whereas this is not necessarily the case for the electric field in a medium. Formally the two approaches are equivalent and may be related through a unitary transformation [28].

The full theory is quite involved. Readers who are mainly interested in the consequences of our theory for experimental implementations are therefore advised to skip to Chap. 7, where we discuss such consequences. The sections prior to this mainly focus on building the theoretical frame using a first-principles strategy.

Model

The model we consider describes the interaction between an ensemble of atoms and an incoming light field. The atomic ensemble is considered to be an ideal gas of identical atoms. The atoms are described as non-moving randomly distributed point particles and the interaction with the light field is described within the dipole-approximation. Each atom is assumed to have a ground level of total spin F . In addition we assume that the atoms have no other stable ground states to which they can decay. See Fig. 3.1. We shall assume that the electric fields are sufficiently far-detuned that we may adiabatically eliminate the excited states, and work with an effective Hamiltonian involving only the ground states. In the following we first discuss the interaction between light and a single atom, and then move on to discuss the interaction with an ensemble of atoms.

3.1 Interaction with single atoms

The aim of this work is to describe the interaction between an electromagnetic field and an ensemble of identical atoms. The problem is therefore both to deal with the microscopic behaviour of a single atom, and also the collective effect of many atoms. We choose here to work in the so called length gauge, where the basic interaction is given as the product

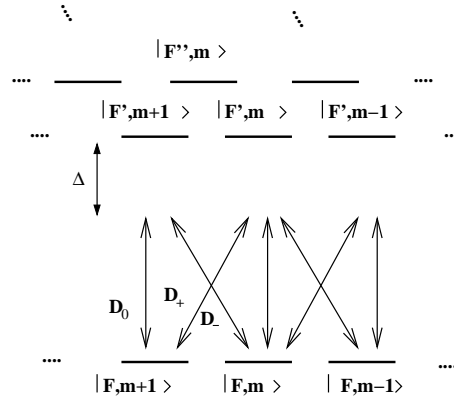


Figure 3.1: Example of an atomic level structure. The atoms have a single ground level with spin F and one or more excited levels. The fields have a large detuning Δ so that the excited states may be adiabatically eliminated and we obtain an effective ground state Hamiltonian Eq. (3.1.3).

of the displaced electric field and the polarization of the media [28]*.

$$\mathcal{H}_{\text{int}} = - \sum_j^{\text{Atoms}} \frac{1}{\epsilon_0} \mathbf{D}(\mathbf{r}_j, t) \cdot \mathbf{P}(\mathbf{r}_j, t). \quad (3.1.1)$$

Our gauge choice ensures $\nabla \cdot \mathbf{D}(\mathbf{r}, t) = 0$. We will assume that the fields have a large detuning and do not saturate the atomic transition, so that the excited levels may be adiabatically eliminated. This procedure is described in Appendix A.1. The polarization of the atomic ensemble then depends linearly on the displaced electric field, that is $\mathbf{P}(\mathbf{r}, t) = \bar{\bar{V}}[\hat{\mathbf{J}}]\mathbf{D}(\mathbf{r}, t)$. We introduce here the argument $\hat{\mathbf{J}}$ to indicate that the interaction matrix $\bar{\bar{V}}[\hat{\mathbf{J}}]$ depends on the spin of the atoms. Next we write the displaced electric field as a sum of a positively oscillating part and a negatively oscillating part,

$$\mathbf{D}(\mathbf{r}, t) = \mathbf{D}^{(+)}(\mathbf{r}, t) + \mathbf{D}^{(-)}(\mathbf{r}, t). \quad (3.1.2)$$

In Appendix A.1 we show that the effective interaction Hamiltonian, assuming such linear

*We have here a formally divergent term, the dipole self-energy. One can, however, show that this term has no effect on the dynamics of the system.

dependence of the polarization on the displaced electric field, reads

$$\mathcal{H}_{\text{int}} = -\frac{1}{2\epsilon_0} \sum_j^{\text{Atoms}} \left(\left[\bar{V}[\hat{\mathbf{J}}_j]^t \mathbf{D}_j^{(-)} \right] \cdot \mathbf{D}_j^{(+)} + \mathbf{D}_j^{(-)} \cdot \left[\bar{V}[\hat{\mathbf{J}}_j] \mathbf{D}_j^{(+)} \right] \right), \quad (3.1.3)$$

where we have also employed the rotating wave approximation. Here the superscript t denotes matrix transposition.

Since the Hamiltonian must be rotationally invariant it can only contain irreducible tensors of at most rank two. In the vector representation the interaction may thus in general be written as

$$\bar{V}[\hat{\mathbf{J}}_j] = \beta \left(c_0 \hat{\mathbf{J}}_j^2 - ic_1 \hat{\mathbf{J}}_j \times + c_2 \times \hat{\mathbf{J}}_j \right) \cdot (\hat{\mathbf{J}}_j \times). \quad (3.1.4)$$

The meaning of the notation is that when inserted into the Hamiltonian the result of, e.g., the last term of the right hand side of Eq. (3.1.4) is

$$\beta c_2 \sum_j^{\text{Atoms}} (\mathbf{D}^{(-)}(\mathbf{r}_j, t) \times \hat{\mathbf{J}}_j) \cdot (\hat{\mathbf{J}}_j \times \mathbf{D}^{(+)}(\mathbf{r}_j, t)). \quad (3.1.5)$$

Note that we have here chosen a description which has a simple analytical representation, but this means the c_2 term is not a pure rank two irreducible tensor, but consist of a combination of tensors of rank zero, one and two. In matrix form the interaction may be written:

$$\bar{V}[\hat{\mathbf{J}}] = \beta \begin{bmatrix} (c_0 - c_2)\hat{\mathbf{J}}^2 + c_2\hat{J}_x^2 & ic_1\hat{J}_z + c_2\hat{J}_y\hat{J}_x & -ic_1\hat{J}_y + c_2\hat{J}_z\hat{J}_x \\ -ic_1\hat{J}_z + c_2\hat{J}_x\hat{J}_y & (c_0 - c_2)\hat{\mathbf{J}}^2 + c_2\hat{J}_y^2 & ic_1\hat{J}_x + c_2\hat{J}_z\hat{J}_y \\ ic_1\hat{J}_y + c_2\hat{J}_x\hat{J}_z & -ic_1\hat{J}_x + c_2\hat{J}_y\hat{J}_z & (c_0 - c_2)\hat{\mathbf{J}}^2 + c_2\hat{J}_z^2 \end{bmatrix}. \quad (3.1.6)$$

In general the atoms may have several exited levels as shown in Fig. 3.1. The effect of several exited levels can be included in the coefficients c_0 , c_1 and c_2 that will then depend on the detuning. For atoms with $F = \frac{1}{2}$ or for an alkali atom, where the fields are detuned by more than the hyperfine structure of the exited state, the c_2 term disappears [29] and the interaction matrix is given by

$$\bar{V}[\hat{\mathbf{J}}_j] = \beta \left(c_0 \hat{\mathbf{J}}_j^2 - ic_1 \hat{\mathbf{J}}_j \times \right). \quad (3.1.7)$$

Here c_0 and c_1 are constants which depend on the atomic structure as well as the detuning. The coupling constant β in Eq. (3.1.7) is given by

$$\beta = \frac{\pi\gamma}{2\Delta k_{\perp}^3}, \quad (3.1.8)$$

where γ is the linewidth of the excited level, Δ the detuning of the laser field with respect to the atomic transition, and k_{\perp} is the wave vector. With this choice of β the coefficients c_0 , c_1 and c_2 will be of order unity or less. Throughout this paper we shall only consider the simple interaction in (3.1.7). A discussion of the effect of the c_2 term is given in Refs. [23, 24] in a one dimensional description.

We will consider a perturbative regime, where the product of the atomic density ρ and β is small $\beta\rho \ll 1$, and make a perturbative expansion in β . Note, however, that this condition does not imply that the total effect of the interaction is small. On the contrary, we are most interested in situations, where the integrated effect of the interaction significantly alters the light beam as it passes through the sample. To take into account these collective effects we explicitly include, e.g., the diffraction of the light caused by the propagation through a medium. To describe these effects we discuss in the following section how to quantize the field in a medium.

3.2 Mode expansion

To quantize the electromagnetic fields we could: i) impose the canonical commutation relations on the vector potential and displaced electric field. Or ii) expand the electromagnetic fields on an orthonormal set of spatial mode-functions $\{\mathbf{f}_{\mathbf{k}}\}$ conveniently chosen to diagonalize the Hamiltonian (in vacuum this is the set of plane waves), and then quantizing the mode-amplitudes. Here we will use the latter. The Hamiltonian describing the electromagnetic field in a medium is given by [28]

$$\mathcal{H} = \frac{1}{2} \int d^3r \left\{ \frac{\mathbf{D}^2}{\epsilon_0} + \frac{(\nabla \times \mathbf{A})^2}{\mu_0} \right\} + \mathcal{H}_{\text{int}}, \quad (3.2.1)$$

where \mathcal{H}_{int} is given in equation (3.1.3). A careful analysis of how to quantize the electromagnetic field in a medium, is given in Ref. [30], and here we shall only go through the steps briefly.

By introducing the spin field

$$\hat{\mathbf{J}}(\mathbf{r}, t) = \sum_j^{\text{Atoms}} \hat{\mathbf{J}}_j \delta(\mathbf{r} - \mathbf{r}_j), \quad (3.2.2)$$

the Hamiltonian may be put in an all-integral form. The main idea in our approach is to divide the full Hamiltonian into a spatially averaged part, and a point particle part, describing the fluctuations from the average caused by the atoms being point particles. For now we only consider the spatially averaged part of the theory. We will use calligraphic font to denote that we have made a spatial average. We thus write the spatially averaged interaction from equation (3.1.7) as

$$\bar{\mathcal{V}}[\bar{\mathbf{J}}] = \beta\rho(\mathbf{r})\left(c_0 \bar{\mathbf{J}}^2 - ic_1 \bar{\mathbf{J}}(\mathbf{r}) \times\right). \quad (3.2.3)$$

Here a bar denotes a single-atom operator, that is $\bar{\mathbf{J}}(\mathbf{r})$ is the spin operator of a single atom at position \mathbf{r} . We use the bar to distinguish between the spatially averaged single-atom spin operator, and the general spin field in equation (3.2.2). The two may be related by $\langle \hat{\mathbf{J}}(\mathbf{r}, t) \rangle_{\text{s.a.}} = \rho(\mathbf{r})\bar{\mathbf{J}}(\mathbf{r}, t)$, where $\langle \cdot \rangle_{\text{s.a.}}$ denotes spatial average. The function $\rho(\mathbf{r})$ denotes the average atomic density, which in this model is a continuous scalar field.

In the following we will define a mean Hamiltonian, where we have taken into account the quantum mechanical average of the spatially averaged interaction. We then write the Hamiltonian as a sum of the average Hamiltonian and a point particle Hamiltonian

$$\mathcal{H} = \mathcal{H}_0 + \mathcal{H}_{\text{pp}}, \quad (3.2.4)$$

where

$$\mathcal{H}_0 = \frac{1}{2} \int d^3r \left\{ \frac{\mathbf{D}(\bar{\mathcal{M}}^t \mathbf{D}^{(-)} + \bar{\mathcal{M}} \mathbf{D}^{(+)})}{\epsilon_0} + \frac{(\nabla \times \mathbf{A})^2}{\mu_0} \right\}, \quad (3.2.5)$$

$$\mathcal{H}_{\text{pp}} = - \frac{1}{2\epsilon_0} \int d^3r \mathbf{D} \cdot \left(\bar{m}[\hat{\mathbf{J}}]^t \mathbf{D}^{(-)} + \bar{m}[\hat{\mathbf{J}}] \mathbf{D}^{(+)} \right), \quad (3.2.6)$$

$$\bar{\mathcal{M}} = \mathbb{I} - \bar{\mathcal{V}}[\bar{\mathbf{J}}], \quad (3.2.7)$$

and

$$\bar{m}[\hat{\mathbf{J}}] = \bar{V}[\hat{\mathbf{J}}] - \bar{\mathcal{V}}[\mathbf{J}]. \quad (3.2.8)$$

Here we simply write \mathbf{J} (without the hat) to denote that this is now a classical field describing the classical expectation of the spin of the atoms. In analogy with Ref. [30] we introduce the mode functions $\{\mathbf{f}_{\mathbf{k}}\}$ defined by:

$$\nabla \times \nabla \times \bar{\mathcal{M}}\mathbf{f}_{\mathbf{k}}(\mathbf{r}) = \frac{\omega_{\mathbf{k}}^2}{c^2} \mathbf{f}_{\mathbf{k}}(\mathbf{r}), \quad (3.2.9a)$$

$$\nabla \cdot \mathbf{f}_{\mathbf{k}}(\mathbf{r}) = 0. \quad (3.2.9b)$$

We also define the appropriate inner product on the space spanned by these mode functions:

$$\langle \phi(\mathbf{r}) | \psi(\mathbf{r}) \rangle = \int d^3r \phi(\mathbf{r})^* \cdot \bar{\mathcal{M}}\psi(\mathbf{r}). \quad (3.2.10)$$

We will assume that the average interaction term $\bar{\mathcal{V}}[\mathbf{J}]$ does not evolve in time, and our appropriate mode-functions are therefore time independent vector fields. One can show that the functions $\mathbf{f}_{\mathbf{k}}$ span a complete orthonormal basis for the space in which we work. To diagonalize the Hamiltonian we expand the vector potential and the displaced electric field in these mode functions

$$\mathbf{D}(\mathbf{r}, t) = - \sum_{\mathbf{k}} \sqrt{\epsilon_0} p_{\mathbf{k}}(t) \mathbf{f}_{\mathbf{k}}^*(\mathbf{r}) \quad (3.2.11a)$$

$$\mathbf{A}(\mathbf{r}, t) = \sum_{\mathbf{k}} c \sqrt{\mu_0} q_{\mathbf{k}}(t) (1 - \bar{\mathcal{V}}[\mathbf{J}]) \mathbf{f}_{\mathbf{k}}(\mathbf{r}). \quad (3.2.11b)$$

The minus sign in Eq. (3.2.11a) is conventional and stems from the relation between the displaced electric field and the canonical conjugate field given in terms of the vector potential.

The reality condition on the displaced electric field $[\mathbf{D}(\mathbf{r}, t)]^\dagger = \mathbf{D}(\mathbf{r}, t)$ allows us to write

$$\mathbf{D}(\mathbf{r}, t) = - \sum_{\mathbf{k}} \frac{\sqrt{\epsilon_0}}{2} (p_{\mathbf{k}}^\dagger(t) \mathbf{f}_{\mathbf{k}}(\mathbf{r}) + p_{\mathbf{k}}(t) \mathbf{f}_{\mathbf{k}}^*(\mathbf{r})). \quad (3.2.12)$$

Using the results in Eqs. (3.2.9) and (3.2.10) and the expansion in equation (3.2.11), the Hamiltonian attains the desired diagonal form

$$\begin{aligned}\mathcal{H}_0 &= \frac{1}{2} \int d^3r \left\{ \frac{\mathbf{D}(1 - \bar{\bar{V}}[\mathbf{J}])\mathbf{D}}{\epsilon_0} + \frac{(\nabla \times \mathbf{A})^2}{\mu_0} \right\} \\ &= \frac{1}{2} \sum_{\mathbf{k}} \{ p_{\mathbf{k}}^\dagger(t) p_{\mathbf{k}}(t) + \omega_{\mathbf{k}}^2 q_{\mathbf{k}}^\dagger(t) q_{\mathbf{k}}(t) \}.\end{aligned}\quad (3.2.13)$$

The mode functions $\{\mathbf{f}_{\mathbf{k}}\}$ are thus the spatial basis diagonalizing the spatially averaged Hamiltonian, and as we shall see the proper basis describing the diffraction problem.

The splitting in equation (3.2.4) allows us to consider the problem as comprised of two types of properties. The effect of single atoms, and the spatially averaged Hamiltonian. The effect of the spatially averaged Hamiltonian is well understood in terms of the mode-functions defined in equation (3.2.9). The point particle effect we will discuss in greater detail when considering the equations of motion for the full system. Before deriving these equations of motion we, however, briefly need to discuss the commutation relations describing the system.

3.3 Quantization and commutation relations

Above we expanded the fields in convenient spatial modes. The coordinates $p_{\mathbf{k}}(t)$ and $q_{\mathbf{k}}(t)$ are canonically conjugate variables, and we can thus quantize our theory by imposing the commutation relations

$$[q_{\mathbf{k}}(t), p_{\mathbf{k}'}(t)] = i\hbar\delta_{\mathbf{k}\mathbf{k}'}.\quad (3.3.1)$$

It will however be convenient to have the commutation relations for the fields which we may derive from the mode-amplitude commutation relations. It will also be convenient to separate the displaced electric field into a positively and a negatively oscillating part $\mathbf{D} = \mathbf{D}^{(+)} + \mathbf{D}^{(-)}$, where $\mathbf{D}^{(-)}$ is in accordance with convention chosen so that it only contains terms oscillating like $e^{i\omega_{\mathbf{k}}t}$. Our choice of gauge is reflected in the transversality of the mode functions defined in Eq. (3.2.9). We expect this transversality condition to be represented in the commutation relations as well. With the quantization procedure above

one finds the following expression for the negative frequency part of the relevant fields

$$\hat{\mathbf{D}}^{(-)}(\mathbf{r}, t) = -i \sum_{\mathbf{k}} \sqrt{\frac{\hbar\omega_{\mathbf{k}}\epsilon_0}{2}} \hat{a}_{\mathbf{k}}^{\dagger} e^{i\omega_{\mathbf{k}}t} \mathbf{f}_{\mathbf{k}}^*(\mathbf{r}) \quad (3.3.2a)$$

$$\hat{\mathbf{A}}^{(-)}(\mathbf{r}, t) = \sum_{\mathbf{k}} c \sqrt{\frac{\hbar\mu_0}{2\omega_{\mathbf{k}}}} \hat{a}_{\mathbf{k}}^{\dagger} e^{i\omega_{\mathbf{k}}t} (1 - \bar{\mathcal{V}}[\mathbf{J}])^t \mathbf{f}_{\mathbf{k}}^*(\mathbf{r}). \quad (3.3.2b)$$

The positive frequency part may be found by Hermitian conjugation. The above result is found from equation (3.2.12) along with the definitions of creation and annihilation operators given by

$$q_{\mathbf{k}}(t) = \sqrt{\frac{\hbar}{2\omega_{\mathbf{k}}}} \left\{ \hat{a}_{\mathbf{k}}(t) + \sum_{\mathbf{k}'} U_{\mathbf{k}\mathbf{k}'}^* \hat{a}_{\mathbf{k}'}^{\dagger}(t) \right\} \quad (3.3.3a)$$

$$p_{\mathbf{k}}(t) = i \sqrt{\frac{\hbar\omega_{\mathbf{k}}}{2}} \left\{ \hat{a}_{\mathbf{k}}^{\dagger}(t) - \sum_{\mathbf{k}'} U_{\mathbf{k}\mathbf{k}'} \hat{a}_{\mathbf{k}'}(t) \right\}, \quad (3.3.3b)$$

where the matrix $U_{\mathbf{k}\mathbf{k}'}$ is defined as

$$U_{\mathbf{k}\mathbf{k}'} = \int d^3r \bar{\mathcal{M}} \mathbf{f}_{\mathbf{k}}(\mathbf{r}) \cdot \mathbf{f}_{\mathbf{k}'}(\mathbf{r}). \quad (3.3.4)$$

A detailed discussion of this procedure is found in Ref. [30].

From these definitions and the commutation relations (3.3.1) we obtain

$$[\hat{a}_{\mathbf{k}}(t), \hat{a}_{\mathbf{k}'}^{\dagger}(t)] = \delta_{\mathbf{k}\mathbf{k}'}. \quad (3.3.5)$$

Going to the field operators we get

$$[\hat{\mathbf{D}}^{(+)}(\mathbf{r}, t), \hat{\mathbf{A}}^{(+)}(\mathbf{r}', t)] = 0 \quad (3.3.6)$$

$$[\hat{\mathbf{D}}^{(+)}(\mathbf{r}, t), \hat{\mathbf{A}}^{(-)}(\mathbf{r}', t)] = \frac{i\hbar}{2} \bar{\delta}^T(\mathbf{r}, \mathbf{r}'), \quad (3.3.7)$$

where

$$\bar{\delta}^T(\mathbf{r}, \mathbf{r}') = \sum_{\mathbf{k}} \mathbf{f}_{\mathbf{k}}(\mathbf{r}) [\bar{\mathcal{M}}^t \mathbf{f}_{\mathbf{k}}^*(\mathbf{r}')]. \quad (3.3.8)$$

Here $\bar{\delta}^T(\mathbf{r}, \mathbf{r}')$ is a generalized transverse delta function [30]. This may be seen by consid-

ering its action on some transverse vector field ($\nabla \cdot \boldsymbol{\psi}(\mathbf{r}, t) = 0$). Since $\{\mathbf{f}_{\mathbf{k}}\}$ is a complete basis on the set of transverse fields, we may expand $\boldsymbol{\psi}(\mathbf{r}, t)$ as

$$\boldsymbol{\psi}(\mathbf{r}, t) = \sum_{\mathbf{k}} \hat{C}_{\mathbf{k}}(t) \mathbf{f}_{\mathbf{k}}(\mathbf{r}). \quad (3.3.9)$$

If we calculate the effect of the transverse delta-function on a transverse field we find

$$\begin{aligned} \int d^3 r' \bar{\delta}^T(\mathbf{r}, \mathbf{r}') \cdot \boldsymbol{\psi}(\mathbf{r}', t) &= \\ \int d^3 r' \sum_{\mathbf{k}\mathbf{k}'} \hat{C}_{\mathbf{k}}(t) \mathbf{f}_{\mathbf{k}}(\mathbf{r}) [\bar{\mathcal{M}}^t \mathbf{f}_{\mathbf{k}'}^*(\mathbf{r}') \cdot \mathbf{f}_{\mathbf{k}}(\mathbf{r}')] \sum_{\mathbf{k}\mathbf{k}'} \hat{C}_{\mathbf{k}}(t) \mathbf{f}_{\mathbf{k}'}(\mathbf{r}') \delta_{\mathbf{k}\mathbf{k}'} &= \\ &= \boldsymbol{\psi}(\mathbf{r}, t), \end{aligned} \quad (3.3.10)$$

where we have used the orthonormality condition of the basis-functions.

We shall also need the equal-space commutation relations

$$[\hat{\mathbf{D}}^{(+)}(\mathbf{r}, t), \hat{\mathbf{D}}^{(-)}(\mathbf{r}, t')].$$

A formal expression of this commutation relation can be found from Eq. (3.3.2a) to be

$$[\hat{\mathbf{D}}^{(+)}(\mathbf{r}, t), \hat{\mathbf{D}}^{(-)}(\mathbf{r}, t')] = \frac{\hbar \epsilon_0}{2} \bar{\eta}(\mathbf{r}, t, t'), \quad (3.3.11)$$

where

$$\bar{\eta}(\mathbf{r}, t, t') = \sum_{\mathbf{k}} \omega_{\mathbf{k}} \mathbf{f}_{\mathbf{k}}(\mathbf{r}) \mathbf{f}_{\mathbf{k}}^*(\mathbf{r}) e^{-i\omega_{\mathbf{k}}(t-t')}. \quad (3.3.12)$$

In vacuum $\bar{\eta}(\mathbf{r}, t, t')$ is simple to evaluate, but for complex systems it is nontrivial to gain knowledge of the basis-functions $\{\mathbf{f}_{\mathbf{k}}\}$. In Appendix A.2 we calculate $\bar{\eta}$ using the rotating-wave approximation and the local density approximation, where we assume that $\rho(\mathbf{r})$ varies slowly with respect to \mathbf{r} .

Equations of motion

In this section we derive the equations of motion for the system, and consider their general properties. In the previous section we discussed that the theory could be divided into an average part and a part representing the deviation from the average. To derive the equations of motion we will, however, work with the full Hamiltonian and later make the splitting into the average part and the deviations from it. The strategy we will use is to first derive the quantum mechanical Maxwell equations, and then to combine them into an effective wave equation for the field.

We will now as an example derive one of the quantum mechanical Maxwell equations from Heisenberg's equation of motion:

$$\begin{aligned}
 \frac{d}{dt}\hat{\mathbf{D}}(\mathbf{r}) &= \frac{i}{\hbar}[\hat{\mathcal{H}}, \hat{\mathbf{D}}(\mathbf{r})] \\
 &= \frac{i}{2\hbar\mu_0} \int d^3r' [(\nabla \times \hat{\mathbf{A}}(\mathbf{r}'))^2, \hat{\mathbf{D}}(\mathbf{r})] \\
 &= \frac{i}{2\hbar\mu_0} \int d^3r' \{(\nabla \times \nabla \times \hat{\mathbf{A}}(\mathbf{r}')) \cdot [\hat{\mathbf{A}}(\mathbf{r}'), \hat{\mathbf{D}}(\mathbf{r})] \\
 &\quad + [\hat{\mathbf{A}}(\mathbf{r}'), \hat{\mathbf{D}}(\mathbf{r})] \cdot (\nabla \times \nabla \times \hat{\mathbf{A}}(\mathbf{r}'))\}. \tag{4.0.1}
 \end{aligned}$$

Here we have used the Hamiltonian given in Eq.(3.2.1), and the boundary condition that the physical fields vanish at infinity. To shorten the notation we have suppressed the ex-

explicit time dependence. The commutation relation may be found from (3.3.6) and (3.3.7) to be

$$[\hat{\mathbf{A}}(\mathbf{r}'), \hat{\mathbf{D}}(\mathbf{r})] = -i\hbar\bar{\delta}^T(\mathbf{r}, \mathbf{r}'). \quad (4.0.2)$$

Since the field $\nabla \times \hat{\mathbf{A}}$ is transverse by definition, this gives us the first quantum mechanical Maxwell equation.

$$\frac{d}{dt}\hat{\mathbf{D}}(\mathbf{r}) = \frac{1}{\mu_0}\nabla \times \hat{\mathbf{B}}(\mathbf{r}), \quad (4.0.3)$$

where

$$\hat{\mathbf{B}}(\mathbf{r}) = \nabla \times \hat{\mathbf{A}}(\mathbf{r}). \quad (4.0.4)$$

Similarly we may derive the Maxwell equation $\nabla \times \hat{\mathbf{E}} = -\partial_t \hat{\mathbf{B}}$, where $\hat{\mathbf{E}} = -d\hat{\mathbf{A}}/dt = \hat{\mathbf{D}} - \hat{\mathbf{P}}$. The remaining Maxwell equations $\nabla \cdot \hat{\mathbf{B}} = 0$ and $\nabla \cdot \hat{\mathbf{D}} = 0$ follow immediately from the definition of $\hat{\mathbf{B}}$ in Eq. (4.0.4) and from the transversality of $\hat{\mathbf{D}}$.

Because of the nature of the interaction part of the Hamiltonian, it is convenient to consider the two frequency components of the displaced electric field separately. The quantum mechanical Maxwell equations may be combined into a single wave equation

$$\left(\frac{d^2}{dt^2} + c^2\nabla \times \nabla \times\right)\hat{\mathbf{D}}^{(-)}(\mathbf{r}, t) = c^2 \int d^3r' \nabla \times \nabla \times \bar{\delta}^T(\mathbf{r}, \mathbf{r}') \cdot \bar{\mathbf{V}}[\hat{\mathbf{J}}]^t \hat{\mathbf{D}}^{(-)}(\mathbf{r}', t), \quad (4.0.5)$$

where the positive frequency part can be found by Hermitian conjugation. Similarly we may derive equations for the spin of the atoms, and for the simple interactions given in Eq. (3.1.7), one finds

$$\frac{d}{dt}\hat{\mathbf{J}}(\mathbf{r}, t) = \frac{i\beta c_1}{\hbar\epsilon_0}\hat{\mathbf{J}}(\mathbf{r}, t) \times (\hat{\mathbf{D}}^{(-)}(\mathbf{r}, t) \times \hat{\mathbf{D}}^{(+)}(\mathbf{r}, t)). \quad (4.0.6)$$

In the remainder of this article we will solve these coupled partial differential equations.

The expression in Eq. (4.0.5) is a second order differential equation in time. The solution of this equation will in general not only depend on the initial value $\mathbf{D}(\mathbf{r}, t = t_0)$, but also the time derivative $\partial_t \mathbf{D}(\mathbf{r}, t)|_{t=t_0}$. In deriving our interaction we have, however, already used the rotating wave approximation, where we ignore the dynamics on a time

scale similar to the inverse of the optical frequency. Similarly we shall here make a slowly-varying-envelope approximation and write the displaced electric field as

$$\hat{\mathbf{D}}(\mathbf{r}, t) = \tilde{\mathbf{D}}^{(-)}(\mathbf{r}, t)e^{i\omega_L t} + \tilde{\mathbf{D}}^{(+)}(\mathbf{r}, t)e^{-i\omega_L t}, \quad (4.0.7)$$

where $\tilde{\mathbf{D}}^{(\pm)}$ are slowly varying in time. If we ignore the second derivative of the slowly varying operators ($\partial_t^2 \tilde{\mathbf{D}}^{(\pm)}(\mathbf{r}, t) \approx 0$), then Eq. (4.0.5) reduces to a first-order differential equation in time.

Since we are heading towards a perturbation theory in the point-particle part of the Hamiltonian (3.2.4), we will add and subtract the average part of the source term in Eq. (4.0.5). That is we write

$$\bar{\bar{\mathbf{V}}}[\hat{\mathbf{J}}] = \bar{\mathbf{V}}[\hat{\mathbf{J}}] - \bar{\mathcal{V}}[\mathbf{J}] + \bar{\mathcal{V}}[\mathbf{J}] \equiv \bar{\bar{m}}[\hat{\mathbf{J}}] + \bar{\mathcal{V}}[\mathbf{J}]. \quad (4.0.8)$$

The idea in this separation is that now $\bar{\mathcal{V}}[\mathbf{J}]$ represents the average effect of the ensemble, which may have a big effect, whereas $\bar{\bar{m}}[\hat{\mathbf{J}}]$ represents the fluctuations around this average. To take advantage of this we first consider the average term

$$\int d^3 r \nabla \times \nabla \times \bar{\delta}^T(\mathbf{r}, \mathbf{r}') \cdot \bar{\mathcal{V}}[\mathbf{J}]' \hat{\mathbf{D}}^{(-)}(\mathbf{r}', t). \quad (4.0.9)$$

This term is continuous and we may use partial integration twice. Using the expression for the general transverse delta-function one finds

$$\begin{aligned} & \int d^3 r \nabla \times \nabla \times \bar{\delta}^T(\mathbf{r}, \mathbf{r}') \cdot \bar{\mathcal{V}}[\mathbf{J}]' \hat{\mathbf{D}}^{(-)}(\mathbf{r}', t) \\ &= \nabla \times \nabla \times \bar{\mathcal{V}}[\mathbf{J}]' \hat{\mathbf{D}}^{(-)}(\mathbf{r}, t). \end{aligned} \quad (4.0.10)$$

This term we will move to the left hand side of Eq. (4.0.5), and we are left with a diffusion equation involving only the fluctuations as a source term on the right hand side

$$\begin{aligned} & (2i\omega_L \frac{d}{dt} - \omega_L^2 + c^2 \nabla \times \nabla \times \bar{\bar{M}}^t) \tilde{\mathbf{D}}^{(-)}(\mathbf{r}, t) \\ &= c^2 \int d^3 r \nabla \times \nabla \times \bar{\delta}^T(\mathbf{r}, \mathbf{r}') \cdot \bar{\bar{m}}[\hat{\mathbf{J}}]' \tilde{\mathbf{D}}^{(-)}(\mathbf{r}', t). \end{aligned} \quad (4.0.11)$$

If we put the right hand side of this equation to zero, i.e., ignore the fluctuations, this equation describes the propagation and diffraction of the field in a medium. For instance

if we take the simplest case where the medium is isotropic so that the matrix $\bar{\bar{V}}[\mathbf{J}]$ is just a scalar, this equation describes the propagation through a medium with an index of refraction given by $n = 1/\sqrt{1 - \bar{\bar{V}}[\mathbf{J}]}$, see Ref. [30].

General solution and Feynman diagrams

In this section we discuss the solution of Eq. (4.0.11) in terms of its Green's function. Let us for convenience define the differential operator

$$\mathcal{D} = 2i\omega_L \frac{d}{dt} - \omega_L^2 + c^2 \nabla \times \nabla \times \bar{\mathcal{M}}'(\mathbf{r}). \quad (5.0.1)$$

We then define the Green's function by

$$\mathcal{D}\bar{G}^{(-)}(\mathbf{r}, t|\mathbf{r}_0, t_0) = \bar{\delta}^T(\mathbf{r}, \mathbf{r}_0)\delta(t - t_0). \quad (5.0.2)$$

The right hand side of this equation describes an identity functional on the inner product space we are working in. We want the Green's function to describe an evolution of the system forward in time. We therefore define a cut-off on the Green's function in time

$$\bar{G}^{(-)}(\mathbf{r}, t|\mathbf{r}_0, t_0) = 0 \quad \text{for } t < t_0. \quad (5.0.3)$$

The general solution to Eq. (4.0.11) in terms of Green's functions is discussed in detail in Appendix A.3, and reads

$$\begin{aligned} \tilde{\mathbf{D}}^{(-)}(\mathbf{r}, t) &= 2i\omega_L \int d^3 r' \bar{M}^t(\mathbf{r}') \bar{G}^{(-)}(\mathbf{r}, t|\mathbf{r}', t_0) \cdot \tilde{\mathbf{D}}^{(-)}(\mathbf{r}', t_0) \\ &+ c^2 \iint_{t_0}^{t^+} d^3 r' dt' \bar{M}^t(\mathbf{r}') \bar{G}^{(-)}(\mathbf{r}, t|\mathbf{r}', t') \cdot \int d^3 r'' \nabla' \times \nabla' \times \bar{\delta}^T(\mathbf{r}', \mathbf{r}'') \cdot \bar{m}[\hat{\mathbf{J}}]^t \tilde{\mathbf{D}}^{(-)}(\mathbf{r}'', t'). \end{aligned} \quad (5.0.4)$$

The upper limit is understood to be $t^+ = \lim_{\varepsilon \rightarrow 0} [t + \varepsilon]$. Before continuing a few comments are in order. Here we have used the boundary conditions, that all fields vanish at infinity, i.e., we imagine that at time $t = 0$ we have generated an optical pulse inside the volume we are describing, which travels toward the atomic medium. Alternatively we could have described the incoming field by a boundary term. The positive frequency part may be found by Hermitian conjugation.

Let us now consider the last term of Eq. (5.0.4). We notice that the involved fields are all continuous and differentiable with respect to the primed spatial coordinates. Using partial integration twice and introducing the propagator defined by

$$\bar{P}^{(-)}(\mathbf{r}, t|\mathbf{r}', t') = \nabla' \times \nabla' \times \bar{M}^t(\mathbf{r}') \bar{G}^{(-)}(\mathbf{r}, t|\mathbf{r}', t') \quad (5.0.5)$$

the last term of Eq. (5.0.4) may be written as

$$c^2 \iint_{t_0}^t d^3 r' dt' \int d^3 r'' \bar{P}^{(-)}(\mathbf{r}, t|\mathbf{r}', t') \cdot \bar{\delta}^T(\mathbf{r}', \mathbf{r}'') \bar{m}[\hat{\mathbf{J}}]^t \tilde{\mathbf{D}}^{(-)}(\mathbf{r}'', t'). \quad (5.0.6)$$

Due to the cross product in Eq. (5.0.5) the propagator is transverse with respect to primed coordinates and the transverse delta function in (5.0.6) may be integrated out, giving

$$c^2 \iint_{t_0}^t d^3 r' dt' \bar{P}^{(-)}(\mathbf{r}, t|\mathbf{r}', t') \cdot \bar{m}[\hat{\mathbf{J}}]^t \tilde{\mathbf{D}}^{(-)}(\mathbf{r}', t'). \quad (5.0.7)$$

The first term of the right hand side of equation (5.0.4) we will denote as $\tilde{\mathbf{D}}_0^{(-)}(\mathbf{r}, t)$

$$\tilde{\mathbf{D}}_0^{(-)}(\mathbf{r}, t) = 2i\omega_L \int d^3 r' \bar{M}^t(\mathbf{r}') \bar{G}^{(-)}(\mathbf{r}, t|\mathbf{r}', t_0) \cdot \tilde{\mathbf{D}}^{(-)}(\mathbf{r}', t_0). \quad (5.0.8)$$

If there were no deviation from the mean, i.e. $\bar{m}[\hat{\mathbf{J}}] = 0$, the solution would simply be

$\tilde{\mathbf{D}}^{(-)}(\mathbf{r}, t) = \tilde{\mathbf{D}}_0^{(-)}(\mathbf{r}, t)$. $\tilde{\mathbf{D}}_0^{(-)}(\mathbf{r}, t)$ thus denotes the solution to the diffraction problem, where the atomic medium is treated as a continuous medium with a diffraction matrix $\bar{\bar{\mathcal{M}}}$.

5.1 Perturbative expansion

Below we shall develop a perturbative expansion in the deviation from the mean due to quantum fluctuations and from the fact that the medium is not continuous but consists of a large number of point particles. The starting point for the perturbative expansion will be the *field equation*


$$\tilde{\mathbf{D}}^{(-)}(\mathbf{r}, t) = \tilde{\mathbf{D}}_0^{(-)}(\mathbf{r}, t) + c^2 \iint_{t_0}^t d^3 r' dt' \bar{\bar{P}}^{(-)}(\mathbf{r}, t | \mathbf{r}', t') \cdot \bar{\bar{m}}[\hat{\mathbf{J}}]' \tilde{\mathbf{D}}^{(-)}(\mathbf{r}', t'). \quad (5.1.1)$$

In addition to this we shall also need the solution to the equations of motion for the spin (4.0.6), which may be formally solved to give the *spin equation*

$$\hat{\mathbf{J}}(\mathbf{r}, t) = \hat{\mathbf{J}}(\mathbf{r}, t_0) + \frac{i\beta c_1}{\hbar \epsilon_0} \int_{t_0}^t dt' \hat{\mathbf{J}}(\mathbf{r}, t') \times (\tilde{\mathbf{D}}^{(-)}(\mathbf{r}, t') \times \tilde{\mathbf{D}}^{(+)}(\mathbf{r}, t')). \quad (5.1.2)$$

These are the equations we wish to treat using the Born approximation, where we make an expansion in the interaction parameter β . (In Eq. (5.1.1) the interaction $\bar{\bar{m}}[\hat{\mathbf{J}}]'$ is proportional to the expansion parameter β .)

In terms of notation this expansion gets extremely cumbersome. It is therefore convenient to introduce Feynman diagrams to represent the various terms of the expansion. We will be dealing with two types of interactions: the one given in Eq. (5.1.1) which we will represent with a shaded circle, and the one given in Eq. (5.1.2) which we will represent with a shaded triangle. The field equation, we diagrammatically represent as



$$, \quad (5.1.3)$$

and the spin equation is represented as

The diagram shows an equation: a double straight line with an arrow pointing right equals a single straight line with an arrow pointing right plus a loop diagram. The loop diagram consists of a wavy line on top and a straight line with an arrow pointing left on the bottom, connected by two vertical lines. A dot is at the right end of the straight line in the loop diagram. The equation is labeled (5.1.4).

The orientation of the diagram is such that time is going from left to right, and the evaluation at time t is marked by a dot. Spin propagation is represented by a line with an arrow pointing in the positive-time direction. A wiggly line represents propagation of the displaced electric field. The arrow denotes whether the line represent the photon-generating part of the field, $\tilde{\mathbf{D}}^{(-)}(\mathbf{r}, t)$, where the arrow points forward in time, or the photon-annihilating part of the field, where the arrow points backward in time. The full solution to the spin $\hat{\mathbf{J}}(t)$ is denoted with a double straight line, and the full solution to the displaced electric field is denoted with a double wiggly line.

The field equation and the spin equation can be represented as a perturbation series, and in the following we shall discuss the effect of the terms in this perturbation series. An important feature of our system is the random distribution of the atoms in the ensemble. The equations that we have derived so far apply to each realization of the atomic distribution $\{\mathbf{r}_1, \mathbf{r}_2, \dots, \mathbf{r}_N\}$. However since we have no control of the position of the atoms we will have to make a spatial average of our equations, that is of the terms in the perturbation series. To do this we need to know the density correlations of the gas.

5.2 Density correlations.

We assume that we are dealing with an ideal gas, i.e., we assume that the distribution of the atoms is completely random but has a distribution given by the possible spatially varying density $\rho(\mathbf{r})$, and we assume that there are no correlations between the positions of different atoms. The correlation function for the density distribution $\rho(\mathbf{r}) = \sum_j \delta(\mathbf{r} - \mathbf{r}_j)$

is thus

$$\begin{aligned}
\langle \rho(\mathbf{r})\rho(\mathbf{r}') \rangle_{\text{s.a.}} &= \left\langle \sum_{jl} \delta(\mathbf{r} - \mathbf{r}_j)\delta(\mathbf{r}' - \mathbf{r}_l) \right\rangle_{\text{s.a.}} \\
&= \sum_{j \neq l} \langle \delta(\mathbf{r} - \mathbf{r}_j)\delta(\mathbf{r}' - \mathbf{r}_l) \rangle_{\text{s.a.}} + \sum_j \delta(\mathbf{r} - \mathbf{r}') \langle \delta(\mathbf{r} - \mathbf{r}_j) \rangle_{\text{s.a.}} \\
&= \langle \rho(\mathbf{r}) \rangle_{\text{s.a.}} \langle \rho(\mathbf{r}') \rangle_{\text{s.a.}} + \delta(\mathbf{r} - \mathbf{r}') \langle \rho(\mathbf{r}) \rangle_{\text{s.a.}}.
\end{aligned} \tag{5.2.1}$$

Here $\langle \cdot \rangle_{\text{s.a.}}$ denotes spatial averaging. In the last step we used that the distribution is independent for different atoms, and we ignored the small difference between N_A^2 and $N_A(N_A - 1)$, where N_A is the number of atoms. We have also neglected the effect that two different atoms can not be found at the same point in space. While this may seem insignificant for a low density gas, we show in Appendix A.4 that including this effect to all orders in the perturbation series gives the Lorentz-Lorenz correction to the index of refraction.

Below we shall also use the correlation functions for the spin. Similar to the calculation above we find

$$\langle \hat{J}_n(\mathbf{r})\hat{J}_m(\mathbf{r}') \rangle_{\text{s.a.}} = \rho(\mathbf{r})\rho(\mathbf{r}')\bar{J}_n(\mathbf{r})\bar{J}_m(\mathbf{r}') + \rho(\mathbf{r})\delta(\mathbf{r} - \mathbf{r}')\bar{J}_n(\mathbf{r})\bar{J}_m(\mathbf{r}), \tag{5.2.2}$$

where the index n, m refer to the spatial components of the operators. To shorten notation we have written $\rho(\mathbf{r})$ instead of $\langle \rho(\mathbf{r}) \rangle_{\text{s.a.}}$. As discussed previously the bar denotes a single atom operator. We will preserve the quantum mechanical behavior of the operators by not taking the quantum mechanical mean. The first term on the right hand side of Eq. (5.2.2) arises from the contribution from different atoms (signified by the prime on the second spin operator). In the second term on the other hand the two operators refer to the same atom, and the operator product should be evaluated for a single atom. For example for a spin- $\frac{1}{2}$ system, we have the following relation between products of spin operators on single atoms

$$\bar{J}_n(\mathbf{r})\bar{J}_m(\mathbf{r}) = \frac{i}{2}\epsilon_{nml}\bar{J}_l(\mathbf{r}). \tag{5.2.3}$$

The generalization to even higher-order density correlations is straight-forward.

These considerations become important when we calculate the spatial average of the

second-order terms of the perturbation series. Let us as an example consider the second order term of the spin equation representing a photon first interacting with one atom and then later with the atom in consideration.

$$(5.2.4)$$

When taking spatial average this term generates two terms in the perturbative expansion as indicated with the arrow in Eq. (5.2.4). The first term involving the spin of two different atoms we will refer to as a coherent interaction, which we will discuss later. The second term involving the delta function corresponds to the incoherent interaction (for reasons which will become clear below). We include this situation in the diagrammatic notation by introducing a hatched star and a loop signifying the infinitely short propagation stemming from the delta-function term of the correlation function Eq. (5.2.2), i.e.

$$\int d^3r \bar{P}^\pm(\mathbf{r}, t | \mathbf{r}', t') \cdot \psi(\mathbf{r}', t') \delta(\mathbf{r} - \mathbf{r}') = \bar{P}^\pm(\mathbf{r}, t | \mathbf{r}, t') \cdot \psi(\mathbf{r}, t'). \quad (5.2.5)$$

The loop is placed on the top of the star when it comes from the positively oscillating propagator $\bar{P}^{(-)}$, and in the bottom of the star when we refer to the negatively oscillating propagator $\bar{P}^{(+)}$. A star scales with the expansion coefficient β squared since it involves two interactions. In the next section we will calculate the infinitely short propagator appearing in these expressions in the local density approximation.

5.3 Green's function and propagator

In this section we first derive a formal expression for the Green's function. Within our inner product space the Green's function is defined by (5.0.1) and (5.0.2). Expanding our

Green's function in the basis $\mathbf{f}_k^*(\mathbf{r})$ we find the representation

$$\bar{G}^{(-)}(\mathbf{r}, t|\mathbf{r}', t') = \sum_{\mathbf{k}} \mathbf{f}_k^*(\mathbf{r})\mathbf{f}_k(\mathbf{r}')g_k^{(-)}(t, t'). \quad (5.3.1)$$

We have here expanded on the complex conjugated set $\mathbf{f}_k^*(\mathbf{r})$ to match the expansion of the displaced electric field in Eq. (3.3.2a). The transverse delta-function has the representation

$$\bar{\delta}^T(\mathbf{r}, \mathbf{r}') = \sum_{\mathbf{k}} \mathbf{f}_k^*(\mathbf{r})\mathbf{f}_k(\mathbf{r}') \quad (5.3.2)$$

where we are now working in the inner-product space with inner product defined in Eq. (3.2.10). The scalar function $g_k^{(-)}(t, t')$ is defined by

$$\left(2i\omega_L \frac{d}{dt} - \omega_L^2 + \omega_k^2\right)g_k^{(-)}(t, t') = \delta(t - t'), \quad (5.3.3)$$

along with the condition that the function $g_k(t, t')$ vanish for $t < t'$. We will consider the following form of the scalar function, where we explicitly write this cut-off in terms of a step function

$$g_k^{(-)}(t, t') = C e^{i\gamma_k(t-t')} \Theta(t - t'). \quad (5.3.4)$$

The coefficients γ_k and C is found by inserting this result into equation (5.3.3).

$$\gamma_k = \frac{\omega_k^2 - \omega_L^2}{2\omega_L} \approx \omega_k - \omega_L \quad (5.3.5a)$$

$$C = \frac{-i}{2\omega_L}. \quad (5.3.5b)$$

The Green's function is thus given by

$$\bar{G}^{(-)}(\mathbf{r}, t|\mathbf{r}', t') = -i \sum_{\mathbf{k}} \mathbf{f}_k^*(\mathbf{r})\mathbf{f}_k(\mathbf{r}') \frac{e^{i(\omega_k - \omega_L)(t-t')}}{2\omega_L} \Theta(t - t'). \quad (5.3.6)$$

Next we will look at the infinitely short propagator in Eq. (5.2.5). Using the Green's function given in equation (5.3.6) along with definition (3.2.9a) and (5.0.5) the propagator

may be written as

$$\bar{P}^{(-)}(\mathbf{r}, t|\mathbf{r}, t') = \frac{-i}{2\omega_L c^2} \sum_{\mathbf{k}} \omega_{\mathbf{k}}^2 \mathbf{f}_{\mathbf{k}}^*(\mathbf{r}) \mathbf{f}_{\mathbf{k}}(\mathbf{r}) e^{i(\omega_{\mathbf{k}} - \omega_L)(t-t')}, \quad (5.3.7)$$

where we have omitted the step function since it automatically gives unity for the integration limits we are using here. We will now relate this infinitely short propagator to some already known parameter. If we go back and consider the general result for the equal-space commutator, this may in terms of the basis-functions $\{\mathbf{f}_{\mathbf{k}}\}$ be written as:

$$[\tilde{\mathbf{D}}^{(-)}(\mathbf{r}, t); \tilde{\mathbf{D}}^{(+)}(\mathbf{r}, t')] = -\frac{\hbar\epsilon_0}{2} \sum_{\mathbf{k}} \omega_{\mathbf{k}} \mathbf{f}_{\mathbf{k}}^*(\mathbf{r}) \mathbf{f}_{\mathbf{k}}(\mathbf{r}) e^{i(\omega_{\mathbf{k}} - \omega_L)(t-t')}. \quad (5.3.8)$$

Comparing with (5.3.7) we immediately get a formal relationship between this commutator and the infinitely short propagator

$$\left(\frac{d}{dt'} - i\omega_L\right)[\tilde{\mathbf{D}}^{(-)}(\mathbf{r}, t); \tilde{\mathbf{D}}^{(+)}(\mathbf{r}, t')] = -\hbar\epsilon_0\omega_L c^2 \bar{P}^{(-)}(\mathbf{r}, t|\mathbf{r}, t'). \quad (5.3.9)$$

Using Eq. (3.3.11) this relation can also be written as

$$\bar{P}^{(-)}(\mathbf{r}, t|\mathbf{r}, t') = \frac{1}{2c^2} \left(\frac{d}{dt'} - i\omega_L\right) \bar{\eta}^{*t}(\mathbf{r}, t, t'). \quad (5.3.10)$$

To illustrate how the infinitely short propagator enters into the equations we will again consider the second order term in the spin equation represented in Eq. (5.2.4). The term prior to spatial average is given as

$$\frac{i\beta c_1 c^2}{\hbar\epsilon_0} \int_{t_0}^t dt' \hat{\mathbf{J}} \times \left[\iint_{t_0}^{t'} dt'' d^3 r' \left\{ \bar{P}^{(-)}(\mathbf{r}, t'|\mathbf{r}', t'') \bar{m}[\hat{\mathbf{J}}] \tilde{\mathbf{D}}_0^{(-)}(\mathbf{r}', t'') \right\} \times \tilde{\mathbf{D}}_0^{(+)}(\mathbf{r}, t') \right]. \quad (5.3.11)$$

After spatial average we get two terms, representing the coherent and the incoherent interaction. The incoherent interaction may then be written as

$$\frac{i\beta c_1}{2\hbar\epsilon_0} \int_{t_0}^t dt' \int_{t_0}^{t'} dt'' \bar{\mathbf{J}}(\mathbf{r}) \times \left[\left(\frac{\partial}{\partial t''} - i\omega_L\right) [\bar{\eta}^{*t}(\mathbf{r}, t', t'')] \bar{V}^t[\bar{\mathbf{J}}] \tilde{\mathcal{D}}_0^{(-)}(\mathbf{r}, t'') \right] \times \tilde{\mathcal{D}}_0^{(+)}(\mathbf{r}, t'). \quad (5.3.12)$$

To simplify notation, we have signified spatial averaging with calligraphic letters, e.g.

$\langle \mathbf{D}(\mathbf{r}, t) \rangle_{\text{s.a.}} \equiv \mathcal{D}(\mathbf{r}, t)$. This convention will be used in the remainder of this article.

We have now developed all the necessary theoretical tools to describe the system. In the next section we shall use these tools to discuss a perturbative expansion of the evolution of the system.

Time evolution

This section is divided into three parts. In the first part we examine the general behaviour of the atomic spin in the presence of a light field. The aim is to understand the effect of the loops introduced in the Feynman diagrams. In the second part we consider the light field and we show how the theory introduce a decay of the field strength of the light as it interacts with the atoms. Again this is connected to the loops introduced in the Feynman diagrams. Finally we will introduce and discuss Stokes operators, which are the appropriate operators for describing the experiments in Ref. [10–12].

6.1 Evolution of the spin

In this section we will consider the spin equation in detail for the simple interaction (5.1.2). We will begin our analysis by considering the first order term in the perturbative expansion of the solution to the spin equation, formally given by the diagram



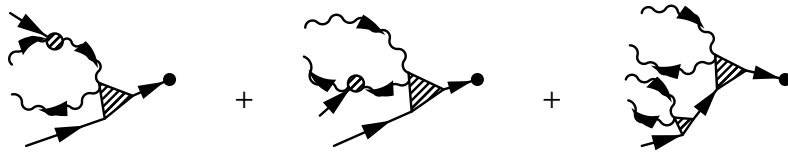
(6.1.1)

This term gives no extra contributions when doing the spatial averaging, and we read-

ily write down the expression describing this term

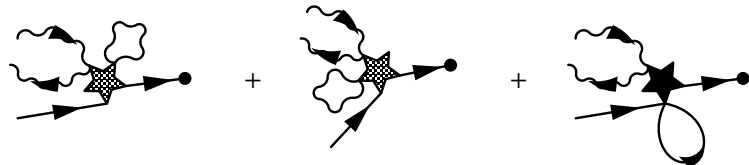
$$\frac{i\beta c_1 \rho(\mathbf{r})}{\hbar \epsilon_0} \int_{t_0}^t dt' \bar{\mathbf{J}}(\mathbf{r}, t_0) \times (\tilde{\mathcal{D}}_0^{(-)}(\mathbf{r}, t') \times \tilde{\mathcal{D}}_0^{(+)}(\mathbf{r}, t')). \quad (6.1.2)$$

We now continue with the second order terms represented by the following Feynman diagrams



$$. \quad (6.1.3)$$

When taking spatial average of these terms, we have argued that the first two diagrams will give an additional set of Feynman diagrams containing loops and stars. It still remains to consider the last diagram of Fig (6.1.3), representing two photons interacting with the same atom at time t and t' . In this diagram it is necessary to pay special attention to the case where the two interactions happen at the same time $t = t'$. The contribution of this term is proportional to $\mathcal{D}^{(-)}(t'')\mathcal{D}^{(+)}(t'')\mathcal{D}^{(-)}(t')\mathcal{D}^{(+)}(t')$ which is not normal-ordered, and it will be convenient to separate it into normal-ordered terms. When commuting $\mathcal{D}^{(-)}(\mathbf{r}, t'')$ and $\mathcal{D}^{(+)}(\mathbf{r}, t')$ we once again get an infinitely short propagator c.f. (3.3.11). This extra term we will denote by a filled star with a loop. This commutator term will produce an interaction which is linear in the field intensity (involves $\mathcal{D}^{(-)}\mathcal{D}^{(+)}$) whereas the normally ordered term ($\mathcal{D}^{(-)}\mathcal{D}^{(-)}\mathcal{D}^{(+)}\mathcal{D}^{(+)}$) will be quadratic in the intensity. Ignoring for now this quadratic term as well as the coherent interactions, the second order diagrams for the spin equation after spatial average reads



$$, \quad (6.1.4)$$

which can also be written as

$$\text{Diagram} \times \left\{ \text{Diagram}_1 + \text{Diagram}_2 + \text{Diagram}_3 \right\} \times \text{Diagram}_4 \quad (6.1.5)$$

The interpretation of the diagrams is given below.

To simplify the expression we will make the slowly varying envelope approximation which simplifies Eq. (5.3.10) to

$$\bar{P}^{(-)}(\mathbf{r}, t | \mathbf{r}, t') \approx \frac{-i\omega_L}{2c^2} \bar{\eta}^{*t}(\mathbf{r}, t, t'). \quad (6.1.6)$$

Secondly we shall evaluate η in a local density approximation, where we assume that $\eta(\mathbf{r}, t, t')$ is the same as if we were in an infinite medium with a constant density $\rho(\mathbf{r})$ and spin density $\mathbf{J}(\mathbf{r})$. By doing this we ignore the reflection of the field on the surface of the ensemble or other inhomogeneities. The infinitely short propagator which expresses the amplitude for the field to be found at the same position at some later time, therefore becomes a delta-function in time. This approximation is valid provided that the diffraction matrix $\bar{M}(\mathbf{r})$ varies slowly on the scale of the wavelength of the light. Furthermore $\bar{\eta}(\mathbf{r}, t, t')$ also contain the Lamb shift which we ignore for simplicity. A detailed calculation of $\bar{\eta}$ is presented in Appendix A.2, where we find

$$\begin{aligned} \bar{P}^{(-)}(\mathbf{r}, t | \mathbf{r}, t') &= \frac{-i\delta(t-t')}{c^2} \begin{bmatrix} \varrho_{\parallel}(\mathbf{r}) & 0 & 0 \\ 0 & \varrho_{\perp}(\mathbf{r}) & -i\varrho_{\Gamma}(\mathbf{r}) \\ 0 & i\varrho_{\Gamma}(\mathbf{r}) & \varrho_{\perp}(\mathbf{r}) \end{bmatrix} \\ &\equiv \frac{-i\delta(t-t')}{c^2} \bar{A}^{(-)}(\mathbf{r}), \end{aligned} \quad (6.1.7)$$

where the coefficients ϱ_{\parallel} , ϱ_{\perp} and ϱ_{Γ} may be found in Eq. (A.2.13). Here the result is given in an Euclidean basis, where \mathbf{J} is assumed to be along the the x -axis. The result may also be expressed in a coordinate-independent form as

$$\bar{P}^{(-)}(\mathbf{r}, t | \mathbf{r}, t') = \frac{-i\delta(t-t')}{c^2} \left\{ \varrho_{\perp}(\mathbf{r}) - i\gamma(\mathbf{r}) \hat{\mathbf{j}} \times + [\varrho_{\parallel}(\mathbf{r}) - \varrho_{\perp}(\mathbf{r})] \hat{\mathbf{j}} (\hat{\mathbf{j}} \cdot \right\}, \quad (6.1.8)$$

where $\hat{\mathbf{j}}$ is a unit vector parallel to \mathbf{J} . This infinitely short propagator is inserted into the second-order terms in the spin equation. The second-order incoherent interaction given

in Eq. (6.1.5) then reads

$$\begin{aligned} \frac{\beta^2}{\hbar\epsilon_0} \int_{t_0}^t dt' \left\{ c_1 c_0 \bar{\mathbf{J}}^2 \left[\bar{\mathbf{A}}^{(-)} \mathcal{D}_0^{(-)} (\bar{\mathbf{J}} \cdot \mathcal{D}_0^{(+)}) - \mathcal{D}_0^{(-)} (\bar{\mathbf{J}} \cdot \bar{\mathbf{A}}^{(+)} \mathcal{D}_0^{(+)}) + H.c. \right] \right. \\ \left. + \frac{c_1^2}{2} \left[\bar{\mathbf{A}}^{(+)} \mathcal{D}_0^{(-)} (\bar{\mathbf{J}} \cdot \mathcal{D}_0^{(+)}) - (\mathcal{D}_0^{(-)} \cdot \mathcal{D}_0^{(+)}) \bar{\mathbf{A}}^{(-)} \bar{\mathbf{J}} \right. \right. \\ \left. \left. - \text{Tr}[\bar{\mathbf{A}}^{(-)}] \mathcal{D}_0^{(-)} (\bar{\mathbf{J}} \cdot \mathcal{D}_0^{(+)}) + \mathcal{D}_0^{(-)} (\bar{\mathbf{J}} \cdot \bar{\mathbf{A}}^{(-)} \mathcal{D}_0^{(+)}) + H.c. \right] \right\}, \quad (6.1.9) \end{aligned}$$

where we have suppressed the space and time dependencies.

In the simple case, where the matrix $\bar{\mathbf{A}}^{(\pm)}$ is proportional to the identity matrix, ($\varrho_{\Gamma} \approx 0$, $\varrho_{\parallel} \approx \varrho_{\perp} = \varrho$), which is the case to lowest order, the terms proportional to $c_1 c_0$ cancels and the expression reduces to

$$-\frac{\beta^2 c_1^2 \varrho}{2\hbar\epsilon_0} \int_{t_0}^t dt' \left[(\mathcal{D}_0^{(-)} \cdot \mathcal{D}_0^{(+)}) \bar{\mathbf{J}} + \mathcal{D}_0^{(-)} (\bar{\mathbf{J}} \cdot \mathcal{D}_0^{(+)}) + H.c. \right]. \quad (6.1.10)$$

This term scale with the power of the incident light, and linearly polarized light will affect the spin component parallel to the field with twice the rate than the perpendicular spin components. To see this we may introduce a decay-rate $\Gamma_{\mathcal{D}}$, and writing expression (6.1.10) on a differential form, we thus see that the term indeed describes a decay of the spin-components.

$$\partial_t \bar{J}_x = -2\Gamma_{\mathcal{D}} \bar{J}_x \quad (6.1.11a)$$

$$\partial_t \bar{J}_y = -\Gamma_{\mathcal{D}} \bar{J}_y \quad (6.1.11b)$$

$$\partial_t \bar{J}_z = -\Gamma_{\mathcal{D}} \bar{J}_z \quad (6.1.11c)$$

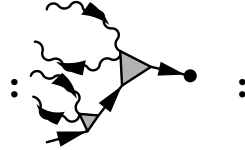
where

$$\Gamma_{\mathcal{D}} = \frac{\beta^2 c_1^2 \varrho}{\hbar\epsilon_0} \langle \mathcal{D}_{0,x}^{(-)} \mathcal{D}_{0,x}^{(+)} \rangle,$$

and where we have assumed that the light is linearly polarized in the x -direction.

Let us now turn to the coherent part of the interaction represented by the Feynman diagrams in Eq. (6.1.3). The first two terms containing a dot are by construction very small, and will vanish when taking the quantum mechanical average, as discussed in

Sec. 5.2. The only important second-order coherent interaction is therefore the following Feynman diagram for normal-ordered fields.



$$(6.1.12)$$

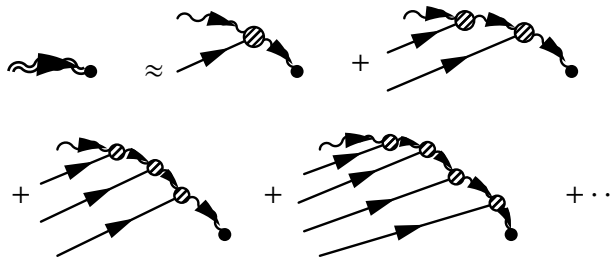
Suppressing the spatial dependence of the displaced electric field, this normal-ordered coherent interaction is given in vector representation by

$$-\frac{\beta^2 c_1^2}{\hbar^2 \epsilon_0^2} \int_{t_0}^t dt' \left\{ \tilde{\mathcal{D}}_0^{(-)}(t') (\tilde{\mathcal{D}}_0^{(-)}(t) \cdot \tilde{\mathcal{D}}_0^{(+)}(t')) (\tilde{\mathbf{J}}_0 \cdot \tilde{\mathcal{D}}_0^{(+)}(t)) \right. \\ \left. - (\tilde{\mathcal{D}}_0^{(-)}(t) \cdot \tilde{\mathcal{D}}_0^{(-)}(t')) (\tilde{\mathbf{J}}_0 \cdot \tilde{\mathcal{D}}_0^{(+)}(t)) \tilde{\mathcal{D}}_0^{(+)}(t') + H.c. \right\}. \quad (6.1.13)$$

In the case of linearly polarized light, say $\tilde{\mathcal{D}}_0^{(-)} \parallel \mathbf{e}_x$ this term vanishes, but this is in general not the case. In Sec. 7 we examine the term in some simplified system.

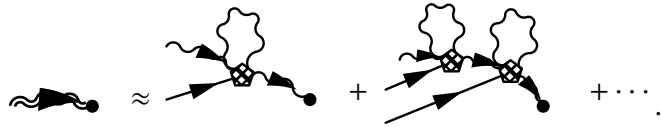
6.2 Evolution of the light

The treatment of the displaced electric field is similar to the spin, but there are a few important differences. Let us consider the negative-frequency part of the field, and write the expansion of the displaced electric field ignoring for now the evolution of the spin



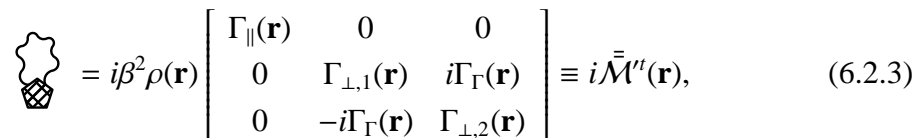
$$(6.2.1)$$

When we take spatial average of diagrams like these, we introduce delta-function correlations between vertex points. So far we have treated the atoms in the ideal gas approximation, where we ignore any correlation in the position of the atoms but in reality we should include a short-range correlation functions describing that two different atoms cannot be at the same position. In Appendix A.4 we show that including this leads to the Lorentz-Lorenz or Clausius-Mossotti relation. In the following we will only discuss loops, where two consecutive vertex points are evaluated for the same atom. Since we have subtracted the quantum mechanical average from the vertex, no first-order vertex will give a contribution to the evolution of the light, and therefore these second-order loop diagrams are the most important effects apart from the diffraction effects included in the mode-functions $\{\mathbf{f}_q\}$. Later in section 6.4 we shall discuss the operator nature of the light field and then we keep the first-order vertex in the calculations. In the current approximation Eq. (6.2.1) reduces to



$$(6.2.2)$$

We have here introduced an interaction denoted by a hatched pentagon which scales with $\beta^2 \rho k_L^3$, and describes two \otimes connected by the infinitely short propagator. Using the results for the infinitely short propagator, and taking quantum mechanical average this interaction reads on matrix form



$$(6.2.3)$$

where the coefficients entering the matrix are given by

$$\Gamma_{\parallel}(\mathbf{r}) = c_0^2 \mathbf{J}^4 \varrho_{\parallel} + c_1^2 \varrho_{\perp} (J_z^2 + J_y^2), \quad (6.2.4a)$$

$$\Gamma_{\perp,1}(\mathbf{r}) = c_0^2 \mathbf{J}^4 \varrho_{\perp} + 2c_0 c_1 \varrho_{\Gamma} \mathbf{J}^2 J_x + c_1^2 (\varrho_{\parallel} J_z^2 + \varrho_{\perp} J_x^2), \quad (6.2.4b)$$

$$\Gamma_{\perp,2}(\mathbf{r}) = c_0^2 \mathbf{J}^4 \varrho_{\perp} + 2c_0 c_1 \varrho_{\Gamma} \mathbf{J}^2 J_x + c_1^2 (\varrho_{\parallel} J_y^2 + \varrho_{\perp} J_x^2), \quad (6.2.4c)$$

$$\Gamma_{\Gamma}(\mathbf{r}) = \varrho_{\perp} 2c_1 c_0 \mathbf{J}^2 J_x - \varrho_{\parallel} \frac{c_1^2}{2} J_x + \varrho_{\Gamma} (c_0^2 \mathbf{J}^2 + c_1^2 J_x^2). \quad (6.2.4d)$$

We have here suppressed the spatial dependence to shorten notation. The series in Eq. (6.2.2) can be included in the differential equation describing the displaced electric field,

$$\begin{aligned} & \left(2i\omega_L \frac{d}{dt} - \omega_L^2 + c^2 \nabla \times \nabla \times [\bar{M}^t(\mathbf{r}) + i\bar{M}^n(\mathbf{r})] \right) \tilde{\mathbf{D}}^{(-)}(\mathbf{r}, t) \\ & = c^2 \int d^3 r' \nabla \times \nabla \times \bar{\delta}^T(\mathbf{r}, \mathbf{r}') \cdot \bar{m}[\hat{\mathbf{J}}]_{\text{mod}}^t \tilde{\mathbf{D}}^{(-)}(\mathbf{r}', t), \end{aligned} \quad (6.2.5)$$

where the perturbation is modified accordingly. Because of the anti-Hermitian matrix, we see that these types of loop diagrams correspond to a decay of the field, i.e. the differential operator on the left side describes the propagation through a lossy medium. On the basis of this analysis and the analysis in Sec. 6.1 we thus link the loops in the Feynman diagrams with the decay associated with spontaneous emission.

It remains to discuss the effect of light interacting with an atom that was previously subject to an interaction such that the atomic spin state has been changed. In terms of Feynman diagrams this is described as



(6.2.6)

We shall postpone the analysis of this term and discuss it in connection with relating the fields to photon counting operators below.

6.3 Photon counting and Stokes operators

So far we have mainly been concerned with calculating the field $\tilde{\mathbf{D}}(\mathbf{r}, t)$. For experiments which eventually involves counting photons we are more interested in quantities like photon flux, and in particular the flux in some particular polarizational state. We shall now discuss how to describe such photon counting experiments within our theory.

The general idea in this subsection is that we shall assume that we are able to measure the light-flux in a certain spatial mode by projecting the light field onto the mode and then integrating the flux of the light field at some detector plane, that we assume to be far away from the atomic ensemble. We will formulate such a measuring process in terms of an inner product,

$$\langle\langle \phi(\mathbf{r}, t) | \psi(\mathbf{r}, t) \rangle\rangle \equiv \int_{-\infty}^{\infty} dt \int_{\mathbb{R}^2} d^2 r_{\perp} \phi^{\dagger}(\mathbf{r}, t) \cdot \psi(\mathbf{r}, t). \quad (6.3.1)$$

We assume that the fields in general have some axis of propagation say \mathbf{r}_{\parallel} . The spatial integral is then performed in some plane perpendicular to this axis at some point r_{\parallel} on this axis. This measuring process could be realized by e.g. sending the light field through a single mode optical fibre prior to detection.

We are interested in the polarization of the field which is conveniently described by the so called Stokes operators defined below. These operators can be derived from a Stokes generator defined in a bra-ket-notation by

$$\bar{S} \equiv |\tilde{\mathbf{D}}^{(-)}(\mathbf{r}, t)\rangle\rangle\langle\langle \tilde{\mathbf{D}}^{(-)}(\mathbf{r}, t)|, \quad (6.3.2)$$

which we represent as the following diagram



$$(6.3.3)$$

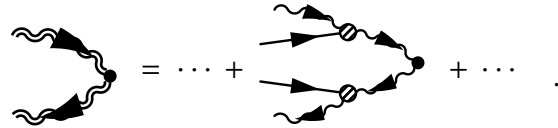
Measuring certain light-modes according to the inner product in Eq. (6.3.1), correspond to picking out a certain matrix element of the Stokes generator. As an example we assume that in some experiment we are able to measure the photon flux of some linear polarization

in some mode say $\tilde{\mathbf{f}}_{\mathbf{q},x}(\mathbf{r}, t)$ after the interaction with the atoms. The time dependence is here $\tilde{\mathbf{f}}_{\mathbf{q},x}(\mathbf{r}, t) = \mathbf{f}_{\mathbf{q},x}(\mathbf{r})e^{-i(\omega_{\mathbf{q},x}-\omega_L)t}$. The integrated photon flux measured at the detector plane, is then given by

$$\frac{2c^2}{\hbar\epsilon_0\omega_L} \langle\langle \tilde{\mathbf{f}}_{\mathbf{q},x}^* | \bar{\mathcal{S}} | \tilde{\mathbf{f}}_{\mathbf{q},x} \rangle\rangle, \quad (6.3.4)$$

where we normalize the outcome to count the number of photons. We have here taken a spatial average of the Stokes generator as indicated by the calligraphic font.

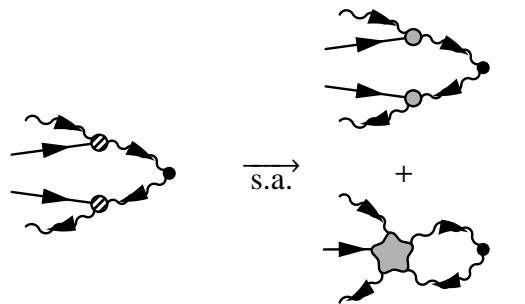
Expanding this operator to second order, gives an additional term not covered by the analysis above. This extra term describes a process where both the negative frequency part and the positive frequency part of the displaced electric field interacts with the same atom. This extra term comes from the following contribution to the Stokes generator



The diagram shows a Feynman diagram on the left representing the Stokes generator. It consists of two wavy lines (representing negative frequency components) and two straight lines with arrows (representing positive frequency components) meeting at a central vertex. This is followed by an equals sign and an ellipsis, then a similar diagram where the two wavy lines and two straight lines are connected to a central vertex by four separate lines, with an ellipsis and a plus sign following.

$$\text{Diagram} = \dots + \text{Diagram} + \dots \quad (6.3.5)$$

When taking the spatial average of this term we again generate a term representing that the interaction happens at the same point. This particular term would not have been there if we only considered the spatial average of the displaced electric field. The generated term we will illustrate as



The diagram shows a Feynman diagram on the left with two wavy lines and two straight lines meeting at a central vertex. An arrow labeled 's.a.' points to the right, where the diagram is shown as a sum of two terms. The top term is the original diagram with a gray circle around the central vertex. The bottom term is a diagram where the central vertex is a gray circle, and the four lines (two wavy and two straight) are connected to it by separate lines.

$$\text{Diagram} \xrightarrow{\text{s.a.}} \text{Diagram} + \text{Diagram} \quad (6.3.6)$$

We constructed the interaction represented in the Feynman diagram as a gray circle, such that when taking the quantum mechanical average the term vanish. The new term gen-

erated when taking the spatial average, given as the lower right diagram of Eq. (6.3.6), describe the square of the fluctuations which is not vanishing. This was also the case for the terms containing the infinitely short propagator. The new term however differs from the second order terms containing the infinitely short propagators because here we need to use the full macroscopic propagator. To calculate the effect of this term in detail, we therefore need to have an expression for the spatial modes describing the system. We will consider this term for a simplified system in Sec 6.4.

To describe the experiments in Ref. [12] it is convenient to define a set of polarization dependent photon counting operators denoted as Stokes operators. These are defined in accordance with Eq. (6.3.4) as

$$\hat{s}_1^{\mathbf{q},\mathbf{q}'} = \frac{K}{2} \left[\langle\langle \tilde{\mathbf{f}}_{\mathbf{q}}^* | \bar{\mathbf{S}} | \tilde{\mathbf{f}}_{\mathbf{q}}^* \rangle\rangle - \langle\langle \tilde{\mathbf{f}}_{\mathbf{q}'}^* | \bar{\mathbf{S}} | \tilde{\mathbf{f}}_{\mathbf{q}'}^* \rangle\rangle \right] \quad (6.3.7a)$$

$$\hat{s}_2^{\mathbf{q},\mathbf{q}'} = \frac{K}{2} \left[\langle\langle \tilde{\mathbf{f}}_{\mathbf{q}}^* | \bar{\mathbf{S}} | \tilde{\mathbf{f}}_{\mathbf{q}'}^* \rangle\rangle + \langle\langle \tilde{\mathbf{f}}_{\mathbf{q}'}^* | \bar{\mathbf{S}} | \tilde{\mathbf{f}}_{\mathbf{q}}^* \rangle\rangle \right] \quad (6.3.7b)$$

$$\hat{s}_3^{\mathbf{q},\mathbf{q}'} = \frac{K}{2i} \left[\langle\langle \tilde{\mathbf{f}}_{\mathbf{q}}^* | \bar{\mathbf{S}} | \tilde{\mathbf{f}}_{\mathbf{q}'}^* \rangle\rangle - \langle\langle \tilde{\mathbf{f}}_{\mathbf{q}'}^* | \bar{\mathbf{S}} | \tilde{\mathbf{f}}_{\mathbf{q}}^* \rangle\rangle \right], \quad (6.3.7c)$$

where $K = \frac{2c^2}{\hbar\epsilon_0\omega_L}$. Using commutation relations for the creation and annihilation operators these Stokes operators are seen to have the commutation relations for angular momentum operators.

$$[\hat{s}_n^{\mathbf{q},\mathbf{q}'}; \hat{s}_m^{\mathbf{q},\mathbf{q}'}] = i \epsilon_{nml} \hat{s}_l^{\mathbf{q},\mathbf{q}'}, \quad (6.3.8)$$

We will calculate and discuss these Stokes operators to second order in the coupling coefficient β in the following.

6.4 Calculation of Stokes operators

In this section we shall calculate the Stokes operators to second order. In the experiments in Ref. [10–12] the Stokes operators are measured by sending the light onto polarizing beamsplitters followed by a measurement of the difference in the intensity of the two outputs. For instance if we take the indices \mathbf{q} and \mathbf{q}' to refer to the x and y polarizations of the light, the operator $\hat{s}_1^{x,y}$ in Eq. (6.3.7) can be measured by measuring the difference in the intensity of the x and y polarizations. The remaining operators $\hat{s}_2^{x,y}$ and $\hat{s}_3^{x,y}$ can

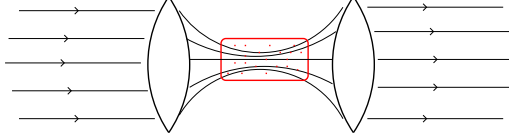


Figure 6.1: Schematic setup. We assume that away from the ensemble, the light-mode resembles a plane-wave with some transverse profile. A set of lenses focus the beam down into the ensemble.

respectively be related to the difference intensity with the polarizing beam splitter rotated by 45° and the difference intensity between the two circular polarizations. For a general light beam, however, diffraction will cause the polarization of the light to depend on the spatial position and there is no well defined polarization. The simple measurement scheme is thus only applicable in the paraxial approximation, where we can separate out a position independent polarization vector. Far away from the ensemble we will therefore assume a paraxial approximation. That is, the mode-functions $\tilde{\mathbf{f}}_{\mathbf{q}}(\mathbf{r}, t)$ and $\tilde{\mathbf{f}}_{\mathbf{q}'}(\mathbf{r}, t)$ describing the Stokes operators far away from the atomic ensemble resemble plane waves with transverse profiles that change slowly compared to the wavelength. The detector plane is placed far away from the atomic ensemble, and at this plane we will assume that the general set of basis-functions $\{\mathbf{f}_{\mathbf{q}}\}$ can be approximated as

$$\mathbf{f}_{\mathbf{q}}(\mathbf{r}) = \frac{1}{\sqrt{2\pi}} U_n(\mathbf{r}_\perp) \mathbf{e}_j e^{ikz}. \quad (6.4.1)$$

We have here set the direction of propagation to be along the z -axis. The index \mathbf{q} are now given as the set $\mathbf{q} = (k, n, j)$, where k is some wavenumber, n is an index referring to the transverse shape of the mode described by the scalar-field $U_n(\mathbf{r})$, and j describes the polarization of this mode, that can be either x - or y -polarized. The completeness relation Eq. (3.3.8), and orthonormality condition in this approximation thus gives

$$\sum_n U_n^*(\mathbf{r}_\perp) U_n(\mathbf{r}'_\perp) = \delta(\mathbf{r}_\perp - \mathbf{r}'_\perp), \quad (6.4.2a)$$

$$\int d^2 r_\perp U_n^*(\mathbf{r}_\perp) U_{n'}(\mathbf{r}_\perp) = \delta_{nn'}, \quad (6.4.2b)$$

and the dispersion relation Eq. (3.2.9a) at the detector plane is $\omega_{\mathbf{q}}^2 = c^2 k^2$.

The paraxial approximation above is convenient for expressing the measured observable in terms of the polarization of the field, but may not be sufficient to accurately de-

scribe experiments, where tightly focused beams are used. We shall therefore only assume this approximation to be applicable far away from the sample, and not necessarily inside the ensemble. Physically this could correspond to a situation, where an initially paraxial beam is focused onto the ensemble with a lens and converted back into a paraxial beam after the interaction by another lens, as shown in Fig. 6.1. A similar treatment was used in Ref. [31].

Inside the ensemble we make the much weaker approximation that the set of spatial mode functions $U_{nq}(\mathbf{r})$ is independent of the polarization of the field, so that the set $\mathbf{f}_q(\mathbf{r})$ is given by

$$\mathbf{f}_q(\mathbf{r}) = \frac{1}{\sqrt{2\pi}} U_{nq}(\mathbf{r}) \mathbf{e}_j(\mathbf{r}). \quad (6.4.3)$$

The mode $U_{nq}(\mathbf{r})$ now takes into account that the spatial shape of the beam may change through the ensemble, and likewise the polarization vector $\mathbf{e}_j(\mathbf{r})$, which we shall assume to be real-valued. The index j will still be either x or y , corresponding to the polarization of the mode far away from the sample, but the vector $\mathbf{e}_j(\mathbf{r})$ will not necessarily be parallel to the x or the y axis. A more general description of the mode-functions would include a dependence of the polarization vector \mathbf{e}_j on the polarization state $U_{mq}(\mathbf{r})$, i.e., $\mathbf{e}_{mj}(\mathbf{r})$. The correction this generalization gives to the Stokes operators, is presented in Appendix A.8, in relation to Sec. 7.3. When we make the relevant calculations to describe the Stokes operators defined in Eq. (6.3.7), we will chose to consider modes corresponding to the index $\mathbf{q} = (k, m, x)$ and $\mathbf{q}' = (k, m', y)$. We note that the set $\{\mathbf{f}_q\}$ defined in this way is in general not complete, since, e.g, the assumption that the polarization vector is independent of the transverse mode number applies in the paraxial approximation but does not apply in general. When calculating the effect on the forward scattered field to first order we only get contributions from the near paraxial modes in the forward direction. When we go to second order there will, however, be effects of all the transverse modes, and in this case a correct treatment requires a more accurate treatment of the complete set of modes. Above we have already employed such a more general set of modes, when we discussed the effect of spontaneous emission, which involve all the transverse modes. In addition to this, a more accurate set of modes is also required for describing the effect of dipole-dipole interactions, which also involves all the transverse mode.

We will in the following calculate the Stokes operators in the limit described above.

Diagrams containing a loop, we will not discuss, since these only leads to a decay of the light which we have discussed earlier. After taking spatial average the diagrams in consideration are

$$(6.4.4)$$

Let us begin our discussion of this perturbation series by considering the first term on the right hand side of equation (6.4.4). This term is the zeroth-order term of the Stokes generator $\bar{\mathcal{S}}^{(0)}$. In the far-field limit $z \rightarrow \infty$ the matrix-element we need to calculate is

$$\begin{aligned} \langle\langle \tilde{\mathbf{f}}_{kmj}^*(\mathbf{r}, t) | \tilde{\mathcal{D}}_0^{(-)}(\mathbf{r}, t) \rangle\rangle &= \\ \iint_{-\infty}^{\infty} dt d^2 r_{\perp} \frac{1}{\sqrt{2\pi}} U_m(\mathbf{r}_{\perp}) e_j e^{ikz - i(\omega_k - \omega_L)t} \sum_{qnl} \sqrt{\frac{\hbar \epsilon_0 \omega_L}{4\pi}} U_n^*(\mathbf{r}_{\perp}) e_l e^{-iqz - i(\omega_q - \omega_L)t} \hat{a}_{qnl}^{\dagger} \\ &= \sqrt{\frac{\hbar \epsilon_0 \omega_L}{2c^2}} \hat{a}_{kmj}^{\dagger} \end{aligned} \quad (6.4.5)$$

and $\bar{\mathcal{S}}^{(0)}$ thus gives us

$$K \langle\langle \tilde{\mathbf{f}}_{kmj}^*(\mathbf{r}, t) | \bar{\mathcal{S}}^{(0)} | \tilde{\mathbf{f}}_{km'j'}^*(\mathbf{r}, t) \rangle\rangle = \hat{a}_{kmj}^{\dagger} \hat{a}_{km'j'}. \quad (6.4.6)$$

The zeroth order Stokes operator $\hat{s}_1^{\mathbf{q}\mathbf{q}'}$ for $\mathbf{q} = (k, m, x)$ and $\mathbf{q}' = (k, m', y)$ gives

$$\hat{s}_1^{\mathbf{q}\mathbf{q}'} \equiv \hat{s}_1^{mm'} = \frac{1}{2} (\hat{a}_{kmx}^{\dagger} \hat{a}_{kmx} - \hat{a}_{km'y}^{\dagger} \hat{a}_{km'y}). \quad (6.4.7a)$$

The two remaining zeroth order Stokes operators are found accordingly,

$$\hat{S}_2^{mm'} = \frac{1}{2}(\hat{a}_{kmx}^\dagger \hat{a}_{km'y} + \hat{a}_{km'y}^\dagger \hat{a}_{kmx}), \quad (6.4.7b)$$

$$\hat{S}_3^{mm'} = \frac{1}{2i}(\hat{a}_{kmx}^\dagger \hat{a}_{km'y} - \hat{a}_{km'y}^\dagger \hat{a}_{kmx}). \quad (6.4.7c)$$

In the following we will calculate the first-order components of the Stokes operators. We assume the quantum mechanical average of the atomic spin \mathbf{J} to be parallel the x -axis. The relevant interaction matrix can in this case be written

$$\bar{m}[\hat{\mathbf{J}}] = ic_1\beta \begin{bmatrix} 0 & \hat{J}_z(\mathbf{r}) & -\hat{J}_y(\mathbf{r}) \\ -\hat{J}_z(\mathbf{r}) & 0 & 0 \\ \hat{J}_y(\mathbf{r}) & 0 & 0 \end{bmatrix}, \quad (6.4.8)$$

and after spatial averaging we simply write

$$\langle \bar{m}[\hat{\mathbf{J}}] \rangle_{\text{sa}} \equiv \bar{\mathcal{M}}[\bar{\mathbf{J}}] = -ic_1\beta\rho(\mathbf{r}) \begin{pmatrix} 0 \\ \bar{J}_y(\mathbf{r}) \\ \bar{J}_z(\mathbf{r}) \end{pmatrix} \times. \quad (6.4.9)$$

The second and the third term on the right hand side of Eq. (6.4.4) are the first order terms of the Stokes generator, $\bar{\mathcal{S}}^{(1)}$. To calculate the contribution to the Stokes operators from these terms we have to evaluate the expression

$$\langle \langle \tilde{\mathbf{f}}_{kmj}^*(\mathbf{r}, t) | c^2 \iint_{t_0}^t dt d^3r' \bar{P}^{(-)}(\mathbf{r}, t | \mathbf{r}', t') \bar{\mathcal{M}}^t[\bar{\mathbf{J}}] \tilde{\mathcal{D}}_0^{(-)}(\mathbf{r}', t') \rangle \rangle. \quad (6.4.10)$$

The initial time t_0 we will set to $-\infty$, and because we assume our detector plane to be infinitely far away from the atomic ensemble, we can take $t \rightarrow \infty$. Using the expression for the set $\{\mathbf{f}_q\}$ given by Eq. (6.4.1) for the detector plane and Eq. (6.4.3) inside the ensemble, Eq. (6.4.10) reduces to

$$\left(-i \sqrt{\frac{\hbar\omega_L\epsilon_0}{2c^2}} \right) \frac{k_L c_1 \beta}{2} \int d^3r' \sum_{nl} \rho(\mathbf{r}') \Theta_{jl}^{mn}(\mathbf{r}')^* \hat{a}_{knl}^\dagger, \quad (6.4.11)$$

where

$$\begin{aligned}\Theta_{jl}^{mn}(\mathbf{r}') &\equiv U_{km}(\mathbf{r}')^* U_{kn}(\mathbf{r}') \mathbf{e}_j(\mathbf{r}') \cdot \left[\begin{pmatrix} 0 \\ \bar{J}_y(\mathbf{r}') \\ \bar{J}_z(\mathbf{r}') \end{pmatrix} \times \mathbf{e}_l(\mathbf{r}') \right] \\ &= \Psi_k^{mn}(\mathbf{r}') [\delta_{lx} \delta_{jy} - \delta_{jx} \delta_{ly}] \left[\begin{pmatrix} 0 \\ \bar{J}_y(\mathbf{r}') \\ \bar{J}_z(\mathbf{r}') \end{pmatrix} \cdot \mathbf{e}_z(\mathbf{r}') \right],\end{aligned}\quad (6.4.12)$$

with

$$\Psi_k^{mn}(\mathbf{r}') = U_{km}(\mathbf{r}')^* U_{kn}(\mathbf{r}'). \quad (6.4.13)$$

In the final equality we have introduced the local basis vector $\mathbf{e}_z(\mathbf{r}) = \mathbf{e}_x(\mathbf{r}) \times \mathbf{e}_y(\mathbf{r})$. The effect of the first-order term of the Stokes generator $\bar{\mathcal{S}}^{(1)}$ to the Stokes operators thus reads

$$\begin{aligned}K \langle\langle \tilde{\mathbf{f}}_{kmj}^*(\mathbf{r}, t) | \bar{\mathcal{S}}^{(1)} | \tilde{\mathbf{f}}_{km'j'}^*(\mathbf{r}, t) \rangle\rangle = \\ k_L c_1 \beta \int d^3 r' \sum_{nl} \rho(\mathbf{r}') \frac{1}{2} \{ \Theta_{jl}^{mn}(\mathbf{r}')^* \hat{a}_{knl}^\dagger \hat{a}_{km'j'} + \Theta_{j'l}^{m'n}(\mathbf{r}') \hat{a}_{kml}^\dagger \hat{a}_{knl} \}.\end{aligned}\quad (6.4.14)$$

The remaining terms of the right hand side of Eq. (6.4.4), that is the second-order terms, can be calculated in a similar way. The results may be found in Appendix A.5. The calculations given in Eq. (6.4.14), (A.5.1), (A.5.2) and (A.5.5) is the starting-point for a discussion of the dynamics of the system subject to a general light field of many modes.

The description that we have used here, where we define the Stokes operators in term of expectation value between different orthogonal modes, is very convenient for a theoretical description of the process. It does, however, not directly correspond to the experimentally measured observables unless one, e.g., separates out particular modes with single mode optical fibers. We shall therefore defer the discussion of the consequences of these results to the next section, where we use these result to calculate the evolution of observables more relevant to experiments.

We will now give the equation for the atomic spin. The incoherent terms describing decay due to spontaneous emission have already been discussed. Here we will consider the coherent interaction up to second order in the perturbation series. Below we show the

Experimental application and validity

In this section we shall consider different limits where we can reduce our general theory to a theory resembling the simple description obtained in one dimensional theories [2,29]. Furthermore we discuss the validity of the approximations made to arrive at these simple limits as well as the validity of our perturbative treatment of the interaction.

7.1 Measurement procedure

In the previous section we discussed how our theory could be used to calculate Stokes operators corresponding to specific transverse modes of the field. While such a treatment is appealing from a theoretically perspective, it is less desirable experimentally, since the isolation of single transverse modes is complicated (although it could be done by passing the light through single mode optical fibers). Here we shall therefore express our result in terms of a simpler experimental procedure. Suppose that the detections is performed by sending the light onto a polarizing beamsplitter and recording the intensity of the two output port with two cameras. The difference between the intensities can now be used to define position dependent Stokes operators $\hat{s}_i(\mathbf{r}_\perp)$, i.e., $\hat{s}_1(\mathbf{r}_\perp)$ corresponds to the difference in intensity between x and y polarization at position \mathbf{r}_\perp in the detector plane. Similarly $\hat{s}_2(\mathbf{r}_\perp)$ and $\hat{s}_3(\mathbf{r}_\perp)$ can, respectively, be related to the difference intensity with the polarizer

rotated by 45° and the difference intensity between the two circular polarizations. These operators may in general be determined by

$$\hat{s}_1(\mathbf{r}_\perp) = \sum_{kmm'} \frac{1}{2} \left(U_m^*(\mathbf{r}_\perp) \hat{a}_{kmx}^\dagger \hat{a}_{km'x} U_{m'}(\mathbf{r}_\perp) - U_m^*(\mathbf{r}_\perp) \hat{a}_{kmy}^\dagger \hat{a}_{km'y} U_{m'}(\mathbf{r}_\perp) \right) \quad (7.1.1a)$$

$$\hat{s}_2(\mathbf{r}_\perp) = \sum_{kmm'} \frac{1}{2} \left(U_m^*(\mathbf{r}_\perp) \hat{a}_{kmx}^\dagger \hat{a}_{km'y} U_{m'}(\mathbf{r}_\perp) + U_m^*(\mathbf{r}_\perp) \hat{a}_{kmy}^\dagger \hat{a}_{km'x} U_{m'}(\mathbf{r}_\perp) \right) \quad (7.1.1b)$$

$$\hat{s}_3(\mathbf{r}_\perp) = \sum_{kmm'} \frac{1}{2i} \left(U_m^*(\mathbf{r}_\perp) \hat{a}_{kmx}^\dagger \hat{a}_{km'y} U_{m'}(\mathbf{r}_\perp) - U_m^*(\mathbf{r}_\perp) \hat{a}_{kmy}^\dagger \hat{a}_{km'x} U_{m'}(\mathbf{r}_\perp) \right). \quad (7.1.1c)$$

Below we shall derive expressions for the operators (7.1.1) and discuss how to implement a light-matter quantum interface based on these operators. In subsec. 7.2 we for simplicity first consider an extreme paraxial limit, where we assume that essentially no diffraction occurs during the propagation. In this limit the dynamics becomes extremely simple. In subsec. 7.3 we consider a more interesting limit, where we may have multiple modes which may experience diffraction. Here we show that measurement of the operators $\hat{s}_i(\mathbf{r}_\perp)$ still allows us to simplify the dynamics of the system. In a suitable limit we find a simple two mode transformation between transverse modes of the light field and single modes of the atomic ensembles.

7.2 Extreme paraxial approximation

In the extreme paraxial approximation, we completely ignore any dynamics transverse to the propagation direction of the light modes and approximate the set of modes $\{\mathbf{f}_\mathbf{q}\}$ with Eq. (6.4.1) throughout the ensemble. Since the typical distance for diffraction is given by $l_d \sim A/\lambda$, the condition for the validity of this approximation is $L \ll l_d$, or expressed in terms of the Fresnel number $\mathcal{F} \gg 1$.

The full expressions for the Stokes operators are quite involved, and we therefore leave the incoherent part of the evolution to Appendix A.7. Keeping only the coherent part of the interaction, we find the Stokes operators to second order in the interaction to

be

$$\begin{aligned} \hat{s}_{1,out}(\mathbf{r}_\perp) = & \hat{s}_{1,in}(\mathbf{r}_\perp) - k_L c_1 \beta \int dz' \rho(z', \mathbf{r}_\perp) \bar{J}_z(z', \mathbf{r}_\perp) \hat{s}_{2,in}(\mathbf{r}_\perp) \\ & - \frac{1}{2} (k_L \beta c_1)^2 \iint dz' dz'' \rho(z', \mathbf{r}_\perp) \rho(z'', \mathbf{r}_\perp) \bar{J}_z(z', \mathbf{r}_\perp) \bar{J}_z(z'', \mathbf{r}_\perp) \hat{s}_{1,in}(\mathbf{r}_\perp), \end{aligned} \quad (7.2.1a)$$

$$\begin{aligned} \hat{s}_{2,out}(\mathbf{r}_\perp) = & \hat{s}_{2,in}(\mathbf{r}_\perp) + k_L c_1 \beta \int dz' \rho(z', \mathbf{r}_\perp) \bar{J}_z(z', \mathbf{r}_\perp) \hat{s}_{1,in}(\mathbf{r}_\perp) \\ & - \frac{1}{2} (k_L \beta c_1)^2 \iint dz' dz'' \rho(z', \mathbf{r}_\perp) \rho(z'', \mathbf{r}_\perp) \bar{J}_z(z', \mathbf{r}_\perp) \bar{J}_z(z'', \mathbf{r}_\perp) \hat{s}_{2,in}(\mathbf{r}_\perp), \end{aligned} \quad (7.2.1b)$$

$$\hat{s}_{3,out}(\mathbf{r}_\perp) = \hat{s}_{3,in}(\mathbf{r}_\perp). \quad (7.2.1c)$$

In this limit we see that the Stokes operator \hat{s}_3 is decoupled from the coherent dynamics of the system, and only evolves due to spontaneous emission [derived in Eq. (A.7.2)].

Similarly we may find the coherent dynamics of the atomic spin. Leaving again the incoherent part to Appendix A.7, we find

$$\bar{J}_{x,out}(\mathbf{r}) = \bar{J}_{x,in}(\mathbf{r}) - \beta c_1 k_L \sum_k \bar{J}_{y,in}(\mathbf{r}) \hat{s}_{3,in}^k(\mathbf{r}_\perp) - \frac{1}{2} (\beta c_1 k_L)^2 \sum_{kk'} \bar{J}_{x,in}(\mathbf{r}) \hat{s}_{3,in}^k(\mathbf{r}_\perp) \hat{s}_{3,in}^{k'}(\mathbf{r}_\perp) \quad (7.2.2a)$$

$$\bar{J}_{y,out}(\mathbf{r}) = \bar{J}_{y,in}(\mathbf{r}) + \beta c_1 k_L \sum_k \bar{J}_{x,in}(\mathbf{r}) \hat{s}_{3,in}^k(\mathbf{r}_\perp) - \frac{1}{2} (\beta c_1 k_L)^2 \sum_{kk'} \bar{J}_{y,in}(\mathbf{r}) \hat{s}_{3,in}^k(\mathbf{r}_\perp) \hat{s}_{3,in}^{k'}(\mathbf{r}_\perp) \quad (7.2.2b)$$

$$\bar{J}_{z,out}(\mathbf{r}) = \bar{J}_{z,in}(\mathbf{r}). \quad (7.2.2c)$$

Analogous to what we found for \hat{s}_3 , we see that the operator \bar{J}_z is decoupled from the coherent dynamics of the system. This result can directly be associated to the conservation of angular momentum along the z -axis. In the extreme paraxial approximation this is true to all orders in the coherent interaction.

The results in Eq. (7.2.1) and (7.2.2) is essentially equivalent to the simplified one-dimensional description of the system given in Refs. [2,29]. The only difference is that the expressions derived here now apply for each value of \mathbf{r}_\perp , whereas the previous treatments assumed the system was transversely homogeneous and only considered the variables integrated over \mathbf{r}_\perp .

A further simplification of Eq. (7.2.2) can be obtained if we introduce the rotation

vector

$$\Omega = \beta c_1 k_L \sum_k \hat{s}_{3,in}^k(\mathbf{r}_\perp) \mathbf{e}_z. \quad (7.2.3)$$

With this definition we find that Eq. (7.2.2) describes nothing but a rotation of the spin around the \mathbf{e}_z -axis

$$\bar{\mathbf{J}}_{out} = \bar{\mathbf{J}}_{in} + \bar{\mathbf{J}}_{in} \times \Omega + \frac{1}{2}(\bar{\mathbf{J}}_{in} \times \Omega) \times \Omega. \quad (7.2.4)$$

7.3 Multi-mode coupling

In the previous subsection we basically ignored all the dynamics transverse to the propagation direction. Now we turn to a more interesting situation, where we may describe effects associated with diffraction of the light beams. Our goal in this section is to find a set of conditions under which we can have a simple dynamics, where the individual transverse modes of the light field talks to a single mode of the atomic ensemble. Such an interaction would enable the storage of information from several light modes into spatial modes of the ensemble, e.g., using the protocol in [11]. The realization of this interaction would thus expand the information storage capacity of the atomic ensembles. A similar problem is considered in Ref. [32]. In related work such storage of multimode memory has recently been achieved in atomic ensembles using electromagnetically induced transparency [33].

To achieve simple results in the end, we will here consider a situation, where we have a strong classical beam polarized in the x -direction in a single transverse mode $U_{ok}(\mathbf{r})$ (denoted by the index o). For the y -polarization we, however, include a complete set of modes, which may or may not include a term identical to the mode of the x -polarization. For the strong mode we will approximate $\hat{a}_{kox}^\dagger = \hat{a}_{kox} = \sqrt{N_x^o} \gg 1$ where N_x^o is the number of photons in this particular mode. Since the Stokes operators are dominated by the terms involving the classical component, the only important contributions in the Stokes operator (7.1.1) are the terms containing the strong classical mode. Eq. (7.1.1) are

thus approximated by

$$\hat{s}_1^{(in)}(\mathbf{r}_\perp) \approx \frac{1}{2} |U_{ok_L}(\mathbf{r}_\perp)|^2 N_x^o, \quad (7.3.1a)$$

$$\hat{s}_2^{(in)}(\mathbf{r}_\perp) \approx \frac{\sqrt{N_x^o}}{2} \sum_{km} \left(\text{Re}[U_{ok}^*(\mathbf{r}_\perp) U_{mk}(\mathbf{r}_\perp)] \hat{X}_P^m - \text{Im}[U_{ok}^*(\mathbf{r}_\perp) U_{mk}(\mathbf{r}_\perp)] \hat{P}_P^m \right), \quad (7.3.1b)$$

$$\hat{s}_3^{(in)}(\mathbf{r}_\perp) \approx \frac{\sqrt{N_x^o}}{2} \sum_{km} \left(\text{Re}[U_{ok}^*(\mathbf{r}_\perp) U_{mk}(\mathbf{r}_\perp)] \hat{P}_P^m + \text{Im}[U_{ok}^*(\mathbf{r}_\perp) U_{mk}(\mathbf{r}_\perp)] \hat{X}_P^m \right), \quad (7.3.1c)$$

where

$$\hat{X}_P^m = \frac{1}{\sqrt{2}} (\hat{a}_{kmy}^\dagger + \hat{a}_{kmy}), \quad (7.3.2a)$$

$$\hat{P}_P^m = \frac{1}{i\sqrt{2}} (\hat{a}_{kmy}^\dagger - \hat{a}_{kmy}). \quad (7.3.2b)$$

In order to obtain simple result in the measurement process, let us assume that we can choose the mode functions $U_{mk}(\mathbf{r})$ to be real in the detection plane. This could, e.g., be achieved by sending the light through a lens which converts the incoming modes into extreme paraxial beams as shown in Fig. 6.1 (note that since we only make this assumption in the detection plane, this assumption does not restrict the shape inside the ensemble). Experimentally the operators \hat{X}_P^m and \hat{P}_P^m defined here can then be measured by simply integrating the measured $\hat{s}_i(\mathbf{r}_\perp)$ with a suitable weight function, e.g.,

$$\sqrt{\frac{2}{N_x^o}} \int d\mathbf{r}_\perp \frac{U_m(\mathbf{r}_\perp)}{U_o(\mathbf{r}_\perp)} \hat{s}_2(\mathbf{r}_\perp) = \hat{X}_P^m, \quad (7.3.3)$$

where we have used the expansion in (7.1.1) as well as the orthogonality relation of the transverse mode functions (6.4.2b).

In our equations of motions we for simplicity only keep terms to first order in β and $\sqrt{N_x^o}$, and neglect all other terms. The equations of motion for the Stokes operators give

in this limit

$$\hat{X}_{out}^m = \hat{X}_{in}^m + k_L \beta c_1 \sqrt{\frac{N_x^o}{2}} \int d^3 r' \rho(\mathbf{r}') \begin{pmatrix} 0 \\ \bar{J}_y(\mathbf{r}) \\ \bar{J}_z(\mathbf{r}) \end{pmatrix} \cdot \mathbf{e}_z(\mathbf{r}) \text{Re}[\Psi_k^{mo}(\mathbf{r})] \quad (7.3.4a)$$

$$\hat{P}_{out}^m = \hat{P}_{in}^m + k_L \beta c_1 \sqrt{\frac{N_x^o}{2}} \int d^3 r' \rho(\mathbf{r}') \begin{pmatrix} 0 \\ \bar{J}_y(\mathbf{r}) \\ \bar{J}_z(\mathbf{r}) \end{pmatrix} \cdot \mathbf{e}_z(\mathbf{r}) \text{Im}[\Psi_k^{mo}(\mathbf{r})], \quad (7.3.4b)$$

where Ψ^{mo} is defined in terms of the mode functions U_m in Eq. (6.4.13). Employing the same set of approximations for the spin equation we find

$$\bar{\mathbf{J}}_{out}(\mathbf{r}) \approx \bar{\mathbf{J}}_{in}(\mathbf{r}) + k_L \beta c_1 \sqrt{\frac{N_x^o}{2}} \sum_n \left[\text{Re}[\Psi_k^{no}(\mathbf{r})] \hat{P}_{in}^n - \text{Im}[\Psi_k^{no}(\mathbf{r})] \hat{X}_{in}^n \right] (\bar{\mathbf{J}}_{in}(\mathbf{r}) \times \mathbf{e}_z(\mathbf{r})). \quad (7.3.5)$$

Note, that the expressions we have derived here, allow for a general set of transverse modes which may experience diffraction, and thus go beyond the extreme paraxial approximation made in the previous section. In the expressions above we do, however, still use the paraxial approximation in Eq. (6.4.3), where we ignore the dependence of the polarization vector on the mode number. In Appendix A.8 we relax this approximation.

The expressions in Eqs. (7.3.4) and (7.3.5) differ from the simple results of the last section because of the extra terms proportional to $\text{Im}[\Psi_k^{no}(\mathbf{r})]$. These terms complicate the dynamics and, e.g., means that one cannot use the protocol in Ref. [11] to store information in the ensemble. There are, however, certain limits where the extra terms in Eq. (7.3.5) disappear. One situation is when the mode we are considering in the y -polarization is identical to the classical mode in the x -polarization (except from the different orientation of the polarization). This situation corresponds to the experimental situation, where the weight factor U_n/U_o in Eq. (7.3.3) is unity, such that the final result is obtained by integrating the intensity over the transverse plane. This case therefore corresponds the experimental situation where the light is detected by photo detectors instead of cameras. In this case $\text{Im}[\Psi_k^{no}(\mathbf{r})]$ vanish identically and the evolution of the light operators again resemble the result of the last section, where, e.g., the \hat{s}_3 component was conserved, which translates into $\hat{P}_{out}^n = \hat{P}_{in}^n$. Note, however, that unlike the situation considered below, the atomic operators in this situation gets an admixture of several different input light modes, and will not in general reduce to the dynamics considered in Ref. [11].

Let us now consider a different limit ideally suited for a multi-mode memory. We assume that we are in the paraxial approximation, where we can ignore the spatial dependence of the polarization vectors. For simplicity we also assume that the classical mode $U_o(\mathbf{r})$ has a uniform intensity and that the density is constant over the region, where U_m is non-zero in the atomic ensemble. We furthermore assume that the macroscopic polarization is constant and along the x -axis, \bar{J}_x , and finally we assume that Ψ^{mo} is real (for a discussion of the validity of this approximation we refer to the next subsection). In the spin equation (7.3.5) we will only keep terms proportional to the macroscopic spin component \bar{J}_x . In this situation the relevant equations reads

$$\hat{X}_{P,out}^m = \hat{X}_{P,in}^m + k_1 \beta c_1 U_o \sqrt{\frac{N_x^o}{2}} \rho \int d^3 r' \bar{J}_z(\mathbf{r}) U_m(\mathbf{r}) e^{-ikz} \quad (7.3.6a)$$

$$\hat{P}_{P,out}^m = \hat{P}_{P,in}^m \quad (7.3.6b)$$

$$\bar{J}_{y,out}(\mathbf{r}) = \bar{J}_{y,in}(\mathbf{r}) + k_1 \beta c_1 U_o \sqrt{\frac{N_x^o}{2}} \sum_n U_n(\mathbf{r}) e^{-ikz} \hat{P}_{in}^n \bar{J}_{x,in} \quad (7.3.6c)$$

$$\bar{J}_{z,out}(\mathbf{r}) = \bar{J}_{z,in}(\mathbf{r}). \quad (7.3.6d)$$

Here the factor $\exp(-ikz)$ comes from the classical field and cancels the $\exp(ikz)$ dependence of the mode function U_m , since $U_m \exp(-ikz)$ should be real according to the assumption of Ψ being real. This set of equations can be symmetrized and simplified by introducing a set of collective operators

$$\tilde{X}_A^m = \sqrt{\frac{\rho}{J_x L}} \int d^3 r \bar{J}_y(\mathbf{r}) U_m(\mathbf{r}) e^{-ikz}, \quad (7.3.7a)$$

$$\tilde{P}_A^m = \sqrt{\frac{\rho}{J_x L}} \int d^3 r \bar{J}_z(\mathbf{r}) U_m(\mathbf{r}) e^{-ikz}, \quad (7.3.7b)$$

where L is the length of the ensemble. The coefficients here are chosen such that the operators \tilde{X}_A^m and \tilde{P}_A^m fulfil the standard commutation relation for position and momentum

$$[\tilde{X}_A^m, \tilde{P}_A^{m'}] = i \delta_{mm'}. \quad (7.3.8)$$

With these definitions Eqs. (7.3.6) reduce to

$$\tilde{X}_{P,out}^m = \tilde{X}_{P,in}^m + \kappa \tilde{P}_{A,in}^m, \quad (7.3.9a)$$

$$\tilde{P}_{P,out}^m = \tilde{P}_{P,in}^m, \quad (7.3.9b)$$

$$\tilde{X}_{A,out}^m = \tilde{X}_{A,in}^m + \kappa \tilde{P}_{P,in}^m, \quad (7.3.9c)$$

$$\tilde{P}_{A,out}^m = \tilde{P}_{A,in}^m, \quad (7.3.9d)$$

where

$$\kappa = k_1 \beta c_1 U_o \sqrt{\frac{N_x^o \rho \bar{J}_x L}{2}}. \quad (7.3.9e)$$

These equations describe a system where one transverse light-mode couples to a single mode of the atomic ensemble, which in turn couple back to the same light mode. This two-mode mode dynamics is exactly identical to the dynamics derived in Ref. [2] for a single transverse mode. The dynamics can thus, e.g., be used to realize a multi-mode version of the memory protocol implemented Ref. [11]. In this protocol $\hat{P}_{P,in}^m$ is stored in the atomic mode $\hat{X}_{a,out}^m$, while at the same time the atomic mode $\hat{P}_{A,in}^m$ is transferred to the light-mode $\hat{X}_{P,out}^m$, as described by Eq. (7.3.9). After detection of the light operator $\hat{X}_{P,out}^m$ one can then realize a quantum memory by feeding back the measurement result to the atoms as it was shown in Ref. [11].

7.4 Validity

7.4.1 Validity of the simple multi-mode dynamics

In the previous subsection we derived a simple multi-mode dynamics useful for making a multi-mode light matter quantum interface. For experimental implementation of these ideas an important question is the validity of the approximations leading to Eq. (7.3.9). First of all we need that the imaginary part of $\Psi^{om}(\mathbf{r})$ in Eq. (7.3.4) should vanish. Furthermore, in order to define orthogonal spin-modes that do not couple different transverse modes, we need $|U_o(\mathbf{r})|$ to be uniform. Taking the classical mode to be given by $U_o(\mathbf{r}) = U_o e^{ikz}$, where U_o is real, we also need the quantum mode $U_m(\mathbf{r})$ to be real-valued

apart from the e^{ikz} dependence. Let us now take the modes $U_m(\mathbf{r})$ to be Hermite-Gaussian beams [34]. Such modes can be represented by

$$\begin{aligned}
 U_{mn}(\mathbf{r}) = & \frac{Bw_0}{w(z)} H_m \left(\sqrt{2} \frac{x}{w(z)} \right) H_n \left(\sqrt{2} \frac{y}{w(z)} \right) \\
 & \times e^{i[kz - (m+n+1) \tanh z/z_0]} \\
 & \times e^{ik(x^2+y^2)/2R(z)} e^{-(x^2+y^2)/w^2(z)},
 \end{aligned} \tag{7.4.1a}$$

where

$$w(z) = w_0 \sqrt{1 + z^2/z_0^2}, \tag{7.4.1b}$$

$$R(z) = z + \frac{z_0^2}{z}, \tag{7.4.1c}$$

$$z_0 = \frac{\pi w_0^2}{\lambda}. \tag{7.4.1d}$$

Here w_0 is the minimum waist of the beam, k is the wave-number, λ is the wavelength, $B \in \mathbb{R}$ is a normalization coefficient, and H_n is the set of Hermite polynomials. The condition that $U_{mn}(\mathbf{r})$ must be real-valued gives the conditions

$$\lambda R(z) \gg w^2(z) \quad |(1+m+n) \frac{z}{z_0}| \ll 1 \tag{7.4.2}$$

These are in fact equivalent conditions, and introducing the Fresnel number $\mathcal{F} \equiv w^2(z)/\lambda L$ we find the condition

$$\mathcal{F} \gg 1 + m + n. \tag{7.4.3}$$

7.4.2 Validity of perturbation theory

The theory we have developed in this paper is based on perturbation theory in the interaction between light and atoms. In this subsection we discuss the limits of validity of this perturbative treatment. We will be considering worst case scenarios to find the limit, where our perturbation series Eq. (6.4.4) and (6.4.15) converge. An important parameter for these estimates will be the effective coupling constant for the collective operators κ defined in Eq. (7.3.9). For applications to light-matter quantum interfaces this parameter

should be of order unity. As we shall see below, this is still possible without violating the applicability of perturbation theory. Another important parameter is the optical depth, OD , defined by $OD \sim \rho \lambda^2 L$. The optical depth plays an important factor when describing the effect of the incoherent interaction, e.g., the spontaneous emission.

Throughout this work, we have assumed that the atomic ensemble is polarized along the x -axis, so that the atomic spin components $\rho \bar{J}_y, \rho \bar{J}_z$ only carries quantum noise. Also we have assumed that the classical component of the light is linearly polarized so that, e.g., circular components are governed by quantum noise. These assumptions will be important for estimating the terms below.

We first consider the expansion of the light field (6.4.4), and in particular the coherent part of the interaction. The effective perturbation coefficient for the first order term is found to scale at most as $(\beta k_L \sqrt{N_A})/A \sim \kappa / \sqrt{N_P}$ (may be found by estimating Eq. (6.4.14)). Here A is the transverse area of the atomic ensemble, and N_P is the total number of photons in a pulse. Going to second order an important term is described in Eq. (A.5.3). Since we are not including the the time evolution of the macroscopic polarization in the average interaction, this term has a potential scaling as large as κ^2 . We showed, however, that in the paraxial approximation the term vanish. Going beyond the paraxial approximation as done in Appendix A.8, we find that for linearly polarized light the scaling is $\kappa^2 / \sqrt{N_P}$. The last contribution to Eq. (6.4.4) is the incoherent interaction considered in Appendix A.7. The scaling of this effect $\kappa^2 \cdot (N_A/N_P)/OD$.

Now we consider the spin series (6.4.15) for a single atom. The incoherent part of the evolution of the spin is described in Eq. (6.1.9), and scales as κ^2/OD , it can be ignored for sufficiently large OD . The first order term scale as $\kappa / \sqrt{N_A}$ for linearly polarized light. To increase this coefficient we need circularly polarized light, which makes it interesting to examine the second order term describing the change of the polarization of the due to the interactions with atoms. This process is described in Eq. (A.6.1), which represent the optically induced dipole-dipole interaction. This particular term vanish when we take quantum mechanical averages, because we have subtracted the only non-vanishing component, but we can still calculate the root mean square contribution. The effect can then be separated into a short-range contribution and a long-range contribution. The long range contribution can be estimated to give a contribution of order $\kappa^2 \sqrt{d/(L \cdot OD)}$, where d is the smallest dimension of the setup, i.e., the smaller of the length and the transverse sizes of the beam and the ensemble. The short range part actually diverges within our present

approximations. If, however, we regularize the integral by excluding the volume, where the dipole-dipole interaction of an excited and a ground state atom $V \sim \gamma\lambda^3/r^3$ is of the same order as the detuning Δ , we find a contribution $\kappa^2 \sqrt{\Delta/\gamma} \sqrt{\lambda/(L \cdot OD)}$. The justification for this regularization is that when we made the adiabatic elimination we assumed a constant detuning Δ . This approximation breaks down when two atoms are sufficiently close that the dipole-dipole interaction is the strongest effect in the problem, in which case it is more appropriate to describe the atoms in terms of molecular states. Both the short and long range part of the interaction are thus small for sufficiently large optical depth OD and for sufficiently long ensembles (large L). It should, however, be noted that here we have only performed a very rough treatment of the dipole-dipole interaction, and it would be desirable to make a more accurate treatment of the effects of these terms. Also it should be noted that the estimates we have performed here apply to non-moving atoms, i.e., cold atoms. If we include the motion of the atoms, i.e., warm atoms as in Refs. [10–12], there will be a reduction of these terms because the sign of the interaction will change in time.

In summary, sufficient requirements for the convergence of the series for the light fields are

$$\frac{\kappa}{\sqrt{N_P}} \ll 1, \quad \frac{\kappa^2}{\sqrt{N_P}} \ll 1, \quad \frac{\kappa^2}{OD} \cdot \frac{N_A}{N_P} \ll 1, \quad (7.4.4)$$

and for the spin equation sufficient requirements are

$$\begin{aligned} \frac{\kappa}{\sqrt{N_A}} \ll 1, \quad \frac{\kappa^2}{OD} \ll 1, \quad \kappa^2 \sqrt{\frac{d}{L \cdot OD}} \ll 1, \\ \kappa^2 \sqrt{\frac{\Delta}{\gamma}} \sqrt{\frac{\lambda}{L \cdot OD}} \ll 1. \end{aligned} \quad (7.4.5)$$

By having many atoms and photons as well as a large optical depth, it is thus possible to achieve $\kappa \sim 1$ without violating the applicability of perturbation theory.

The main idea in this work is to develop a perturbation series, where we explicitly take into account the reshaping of the light modes caused by the mean effect of the interaction. Let us for comparison compare with the series, if the mean effect of the interaction had not been subtracted. For the Stokes operators the perturbative series is given in Eq. (6.4.4). If we do not subtract the average effect of the interaction, the scalar part of the interaction [the c_0 component in Eq. (3.1.4)] will give first order corrections to the field of order $\kappa \sqrt{N_A/N_P}$ times the incoming field. With $N_A \sim N_P$ as it is suggested in Ref. [2], this term

will give a factor of order unity for $\kappa \sim 1$, and this therefore cannot be considered a small term. For the calculation of the Stokes operators, however, the two large components in the first order terms in Eq. (6.4.4) cancel out. The calculation may thus yield reasonable result even without performing the more involved procedures described in this article, but the validity of the procedure would be questionable. (Some experiments actually uses $N_p \gg N_A$ [10], where this problem may be of minor concern). Furthermore, one of the major limiting factors identified above, is the dipole-dipole interactions. The effect of this term is much more complicated to evaluate if we had not subtracted the average interaction, but the term certainly will be larger, because the interactions in Eq. (A.6.1) would include a non-vanishing term, and not just the quantum fluctuations. Again this term would thus seriously question the applicability of perturbation theory. In contrast the present approach allows us to rigorously apply perturbation theory in experimentally relevant regimes.

Conclusion

In quantum optics the propagation of light through an atomic medium is often described in a one-dimensional approximation, where one completely ignores the transverse structure of the beam and only considers the longitudinal propagation. In this paper we have investigated the validity of this approximation by developing a full three-dimensional theory describing the interaction. The challenge in this work has been to develop a theory capable of describing the microscopic interaction with a single atoms as well as macroscopic effects such as the diffraction of the laser beam caused by the refractive index of the gas. In essence the theory we have developed here includes both the micro- and macroscopic effect by separating the interaction into an average part and the fluctuation from the average. In this formulation macroscopic effects such as diffraction are naturally associated with the average part whereas the microscopic fluctuations describe processes such as the mapping of quantum fluctuations between light and atoms. Furthermore we have shown that spontaneous emission from the atoms naturally appear as an effect caused by the fluctuations associated with the point particle nature and the random positions of the atoms.

Based on our separation into the average and the fluctuations we have developed a perturbative expansion in the fluctuations. The advantage of this procedure is that it has a wider region of applicability than a direct perturbative treatment. For instance in an experimental setup an index of refraction of the gas just change of the beam profile which

often only has a minor effect on the experiment. On the other hand, such 'trivial' effects may have a large influence on the theoretical calculation. If one considers perturbation theory based on the vacuum solutions to the wave equation, the perturbative expansion will include all the terms responsible for the reshaping of the beam, and this may break the validity of perturbation theory. On the other hand our theory performs perturbation theory on modes which are solutions to the wave equation including the index of refraction of the gas. Our theory is thus applicable even for situations where the beam is considerably distorted by the refractive index of the gas.

A major motivation for this work has been to investigate the validity of the one-dimensional approximation in the description of the experiments in Refs. [10–13]. In Chap. 7 we explicitly considered some situations where we could reduce our general theory to a theory resembling the one used to describe these experiments in the one dimensional approximation [2,29]. To achieve a simple description resembling the previous theories, an essential requirement is that we are in the paraxial approximation. If we are not in this limit, the polarization of the light change as its propagate through the ensemble, which complicates the interaction with the atoms. Furthermore, for the particular interaction considered here, we also find it to be desirable to be in a regime where the Fresnel number is much larger than unity $\mathcal{F} \gg 1$. In these limits our theory essentially reproduce the results of the simple theory. The only difference is that instead of the vacuum mode functions, the mode functions appearing in the theory should represent the modes, which are solutions to the diffraction problem including the index of refraction of the gas.

In the present work we have mainly focused on developing the theory and deriving how the usual approximations arise from our more complicated approach. The theory is, however, fully consistent and thus capable of including any higher order corrections not previously included in the theoretical description. In particular it could be interesting to study the effect of light induced dipole-dipole interactions. While such processes may not be relevant for understanding the current experiments, they may play an important role in future experiments, e.g., with Bose-Einstein condensates, where the density may be fairly high. Another interesting extension of our theory could be to study different types of interactions such as for instance electromagnetically induced transparency [21].

Part III

Three-dimensional theory for Superradiance

Introduction

The field of quantum information and quantum computation is a rapidly growing research area. Along with elaborate schemes and ideas for realizing quantum systems, follows the need for understanding the details of such systems. This paper is motivated by a proposal [35] to use an ensemble of Bose Einstein condensed atoms (BEC) as a generator of a beam of stimulated Raman scattering (SRS), or superradiation entangled with atoms in the BEC. The idea is to utilize entanglement properties of such superradiation and momentum classes of atoms in the condensate. While this system shows promising properties, its full potential can not be estimated without a detailed description of the full three-dimensional structure of the superradiated beam. The experimental history of SRS goes back to 1962 where the effect was first observed [36]. A theoretical explanation in terms of a photon rate equation was given in Ref. [37]. Much work has been made on the theory of superradiance e.g. [38–40]. Later Raymer and Mostowski [3] developed a microscopic quantum mechanical theory of SRS. The important step was to identify the mathematical description of the spontaneously initiated scattering process, as it involves the coupling of a radiation field to internal energy transitions in the gain medium. In 1985 Raymer and co-workers [41] generalized the theory to also include certain three-dimensional properties of the propagation of light in the gain medium. Common for these theories is that they are developed under the basic assumption that the region in which this SRS process happens is defined by the properties of the laser both in time and space. Thus

figures of merits are the width and temporal shape of the laser which is driving the SRS process. The experiments exploring the SRS process have changed since then [42–44], and much more attention is given to systems where the temporal and spatial shape of the laser have long surpassed the spatial geometries and temporal properties of the gain medium. Here we develop the theoretical framework that enables us to address questions such as how the Fresnel number and the optical depth of the gain medium effects the temporal behavior and spatial shape of the generated super-radiation? What is the threshold for this stimulated process, and when can we say that the scattered radiation is dominated by a coherent beam of light? The last question refers to the applicability of a BEC for realizing and utilizing entanglement properties of the SRS beam, and momentum classes of the BEC. Some progress have been made on such questions mainly however on a numerical basis [45,46]. One of the common strategies used to describe SRS is to look at the dipole interactions between typically some thousand atoms and rephrase the interaction problem into a linear differential matrix equation which can be handled numerically. The computational power therefore sets a limit to the number of atoms that can be included in the simulation. This on the other hand means that the spatial scalability of the atomic ensemble is limited. Based on these theories there is a theoretical understanding of the SRS process in the limit of very large gain medium as well as the opposite limit of a very small gain medium. In this paper we will look at the intermediate case, based on a generalization of the methods used in [3].

Equations of motion

In the electric dipole approximation the Hamiltonian describing the system that we want to analyze is given by

$$\mathcal{H} = \int \{\mathcal{H}_F + \mathcal{H}_I\} d^3 r + \mathcal{H}_A, \quad (10.0.1)$$

$$\mathcal{H}_F = \frac{\mathbf{D}^2}{2\epsilon_0} + \frac{\mathbf{B}^2}{2\mu_0} \quad (10.0.2)$$

$$\mathcal{H}_I = -\frac{1}{\epsilon_0} \mathbf{D}(\mathbf{r}, t) \cdot \mathbf{P}(\mathbf{r}, t) \quad (10.0.3)$$

$$\mathcal{H}_A = \sum_j \sum_n^{Atom} E_n^j \sigma_{nm}^j, \quad (10.0.4)$$

where \mathbf{D} is the displaced electric field, \mathbf{B} is the magnetic field and \mathbf{P} is the atomic polarization. The operator $\sigma_{nm}^j = |n\rangle\langle n|$ is a projection operator for the j 'th operator, and E_n^j is the energy corresponding to the state $|n\rangle$. We choose to use the displaced electric field and not the electric field for reasons discussed Chap. 3. This choice however does not influence the result of the analysis. Here we have ignored any direct interaction between the atoms, e.g. atomic collisions. As we shall often make reference to Ref. [3], we shall try and match the constants and the dynamics of our system to the system presented there. The Hamiltonian is also chosen such that results derived in Part II can be directly

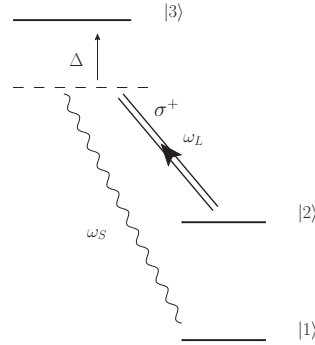


Figure 10.1: Atomic level structure. Two stable ground states $|1\rangle$ and $|2\rangle$ are coupled through an excited state $|3\rangle$. We assume a strong classical laser of σ^+ -polarized light, slightly detuned from resonance with atomic level $|2\rangle$ and $|3\rangle$ by Δ . The laser thereby effectively drives a transition from level $|2\rangle$ to $|1\rangle$. The radiation ω_S connected to the transition from $|3\rangle$ to $|1\rangle$ describes the Stokes field, that is analyzed here.

incorporated. In the following section we will focus on the dynamics of the atoms.

10.1 Atomic dynamics

The macroscopic description of the atomic ensemble is given by the polarization, $\mathbf{P}(\mathbf{r}, t)$ which again is the sum of the individual dipole moment of the atoms.

$$\mathbf{P}(\mathbf{r}, t) = \sum_j^{\text{Atoms}} \sum_{nm} \delta(\mathbf{r} - \mathbf{r}_j) \mathbf{d}_{nm} \sigma_{nm}^j(t), \quad (10.1.1)$$

where the time dependent operator $\sigma_{nm}^j(t)$ is the operator $|n\rangle\langle m|$ taking the j 'th atom from state $|m\rangle$ to state $|n\rangle$, and the dipole moment is $\mathbf{d}_{nm} = e\langle n|\mathbf{r}|m\rangle$. In addition we assume the atoms to be identical with an energy level structure shown in Fig. 10.1. We assume the two levels $|1\rangle$ and $|2\rangle$ to be stable ground states hence a transition between these is forbidden. For the chosen atomic system we assume that the transition from level $|1\rangle$ or $|2\rangle$ to $|3\rangle$ increases the atomic angular momentum by one unit of \hbar , and that there are no other states that the level $|3\rangle$ can decay to. This means that the only non-vanishing vector components of the dipole moments are $\mathbf{e}_+ = (\mathbf{e}_x + \mathbf{e}_y)/\sqrt{2}$ for positively oscillating terms and \mathbf{e}_+^* for negatively oscillating terms.

We employ the Rotating Wave Approximation (RWA) and adiabatically eliminate the excited level $|3\rangle$. In this process we split the radiation field \mathbf{D} into its positively and neg-

actively oscillating parts, and extract the strong classical field \mathcal{D}_{cl} oscillating with a frequency ω_L from the weak quantum mechanical stokes field $\hat{\mathbf{D}}$ oscillating with frequency ω_s . We will assume that the strong classical field is constant over the region of the atoms and can be written as a plane wave with a constant amplitude $\mathcal{D}_{cl}^{(+)} = |\mathcal{D}_{cl}|e^{-i\omega_s t}\mathbf{e}_+$. The presence of the strong classical field \mathcal{D}_{cl} induce a Stark shift of the atomic levels. The effective Stokes frequency ω_s is therefore given by

$$\omega'_s = \omega_s + \frac{|d_{31}|^2|\mathcal{D}_{cl}|^2}{\hbar^2\epsilon_0^2\Delta}. \quad (10.1.2)$$

We shall in general assume the shift to be absorbed in the definition of ω_s , the observable Stokes frequency. We define slowly oscillating operators both for the atomic operator σ_{21} and for the stokes field $\hat{\mathbf{D}}$

$$\tilde{\sigma}_{12}(t) = \sigma_{12}e^{i(\omega_s - \omega_L)t} \quad (10.1.3)$$

$$\tilde{\mathbf{D}}^{(+)} = \hat{\mathbf{D}}^{(+)}e^{i\omega_s t}. \quad (10.1.4)$$

For large detuning and weak fields we can adiabatically eliminate the excited state, and obtain an effective ground state equation of motion.

$$\frac{d}{dt}\sigma_{12}^j(t) = \frac{-ia}{\epsilon_0\hbar}(\sigma_{22}^j - \sigma_{11}^j)|\mathcal{D}_{cl}|\tilde{\mathbf{D}}_-^+(\mathbf{r}_j, t), \quad (10.1.5)$$

where the constant a is given by

$$a = \frac{d_{32}d_{31}^*}{\hbar\epsilon_0\Delta}. \quad (10.1.6)$$

The positively oscillating part of the polarization is in this approximation

$$\tilde{\mathbf{P}}^{(+)}(\mathbf{r}, t) = \sum_j a|\mathcal{D}_{cl}|\mathbf{e}_+\tilde{\sigma}_{12}^j(t)\delta(\mathbf{r} - \mathbf{r}_j). \quad (10.1.7)$$

The negatively oscillating part $\mathbf{P}^{(-)}(\mathbf{r}, t)$ is found by Hermitian conjugation.

10.2 Field equation

The equation of motion for the electric field $\mathbf{D}(\mathbf{r}, t)$ is given in general in Eq. (5.1.1), and reads for our simple system

$$\mathbf{D}^{(+)}(\mathbf{r}, t) = \mathbf{D}_0^+(\mathbf{r}, t) + \sum_j \int dt' \bar{P}^{(+)}(\mathbf{r}, t | \mathbf{r}_j, t') \cdot \mathbf{e}_+ a |\mathcal{D}_{cl}| \tilde{\sigma}_{12}^j(t'), \quad (10.2.1)$$

where \mathbf{D}_0 is the unperturbed field containing the vacuum Stokes field and the classical laser-field, and $\bar{P}^{(+)}$ is the propagator. The coupling between level $|2\rangle$ and $|3\rangle$ in principle give rise to an index of refraction. As shown in Part III, such an index of refraction should in principle be incorporated into the propagator $\bar{P}^{(\pm)}$. In the limit of large detuning Δ (but fixed $a|\mathcal{D}_{cl}|$), we can however neglect this, and will do so in the following. The propagator in the slowly varying approximation is in Fourier representation given by

$$\bar{P}^{(+)}(\mathbf{r}, \mathbf{r}') = k_s^3 \int d^3k \sum_{\mathbf{e} \perp \mathbf{k}} \frac{k^2 e^{i\mathbf{k} \cdot (\mathbf{r} - \mathbf{r}')}}{(2\pi)^3 (k^2 - 1)} \boldsymbol{\varepsilon} \boldsymbol{\varepsilon}^*, \quad (10.2.2)$$

where the \mathbf{k} -integral is understood to include only the contribution corresponding to the retarded Green function. Here and in the remainder of this work we will measure the spatial coordinates in units of k_s , which gives the factor of k_s^3 and a pole at 1 in Eq. (10.2.2).

Inserting Eq. (10.2.1) into Eq. (10.1.5) gives us an effective equation of motion for the atomic operators,

$$\frac{d}{dt} \tilde{\sigma}_{12}^j(t) = -\frac{\Gamma}{2} \tilde{\sigma}_{12}^j(t) + \sum_{j' \neq j} M_{jj'} \tilde{\sigma}_{12}^{j'}(t) + \hat{F}_j(t), \quad (10.2.3)$$

where

$$\Gamma = \frac{a^2 k_s^3 |\mathcal{D}_{cl}|^2}{3\pi \epsilon_0 \hbar}, \quad (10.2.4)$$

$$\hat{F}_j(t) = \frac{-ia}{\epsilon_0 \hbar} \mathbf{D}_0^{(+)}(\mathbf{r}_j, t) \cdot \mathbf{e}_- \mathcal{D}_{cl}^{(-)}(t), \quad (10.2.5)$$

$$M_{jj'} = \frac{-3\pi i \Gamma}{k_s^3} \mathbf{e}_- \cdot \bar{P}^{(+)}(\mathbf{r}_j, \mathbf{r}_{j'}) \cdot \mathbf{e}_+. \quad (10.2.6)$$

We have in addition made the approximation $\sigma_{22} - \sigma_{11} \approx 1$, where we assume that initially all atoms are in state $|2\rangle$ and that the experiment takes place on a timescale such that we may neglect depletion of this level. To derive the decay Γ we used the identity

$$\mathbf{e}_+^* \cdot \bar{\mathbf{P}}^{(+)}(\mathbf{r}_j, \mathbf{r}_j) \cdot \mathbf{e}_+ = \frac{ik_s^3}{6\pi}, \quad (10.2.7)$$

which is discussed in Part III as the infinitely short propagator. The effective equation of motion for the atoms, Eq. (10.2.3) is the starting point in many analyzes of superradiance, Ref. [3, 45, 46], but also in more general analyzes on the coupling between atomic spin-excitations and collective emission of light, Ref. [47]. In our analysis we neglect the effect of the source term \hat{F}_j in eq. (10.2.3), as we are eventually only interested in measuring $\langle D^{(-)} D^{(+)} \rangle$. It can be found from Eqs. (10.2.1) and (10.2.3) that the effect of the source term \hat{F}_j leads to a contribution $\langle D_0^{(-)} D_0^{(+)} \rangle$ to the measurement. This contribution vanishes as we assume that the Stokes field is unpopulated, i.e. it is in the vacuum state. We also assume that there is no classical noise in the laser field \mathcal{D}_{cl} . We shall also be interested in defining creation and annihilation operators for the atoms. This leads in general to nonlinear equations, but under the low excitation approximation, that is $\sigma_{22}^j - \sigma_{11}^j \approx 1$ we employ the Holstein-Primakoff approximation and simply use

$$\hat{b}_j^\dagger = \sigma_{12}, \quad \hat{b}_j = \sigma_{21}, \quad (10.2.8)$$

so that

$$[\hat{b}_j, \hat{b}_j^\dagger] = \delta_{jj}. \quad (10.2.9)$$

The effective equation of motion for the atoms is then given by

$$\frac{d}{dt} \hat{b}_j^\dagger(t) = -\frac{\Gamma}{2} \hat{b}_j^\dagger(t) + \sum_{j' \neq j} M_{jj'} \hat{b}_{j'}^\dagger(t), \quad (10.2.10)$$

and for the field Eq. (10.2.1) gives

$$\mathbf{D}^{(+)}(\mathbf{r}, t) = \mathbf{D}_0^+(\mathbf{r}, t) + \sum_j \int dt' \bar{\mathbf{P}}^{(+)}(\mathbf{r}, t | \mathbf{r}_j, t') \cdot \mathbf{e}_+ a | \mathcal{D}_{cl} | \hat{b}_j^\dagger(t). \quad (10.2.11)$$

Going from discrete to continuous system

Now we will be interested in treating Eq. (10.2.10) as a continuous equation. This follows the fact that for a atomic gas we do not know the individual positions of the atoms, thus an expectation value of a physical operator has to be accompanied by a spatial average of the individual atomic positions. We therefore define the density distribution $\check{\rho}(\mathbf{r})$,

$$\check{\rho}(\mathbf{r}) = \sum_j \delta(\mathbf{r} - \mathbf{r}_j). \quad (11.0.1)$$

After a spatial average of the position of the atoms in the ensemble the density distribution $\check{\rho}(\mathbf{r})$ can be described by a Gaussian function.

$$\langle \check{\rho}(\mathbf{r}) \rangle_{sa.} \equiv \rho(\mathbf{r}) = \rho_0 e^{-\frac{r^2}{2\sigma_{\perp}^2} - \frac{z^2}{2\sigma_{\parallel}^2}}. \quad (11.0.2)$$

We will assume that $1 \ll \sigma_{\perp} \ll \sigma_{\parallel}$ and also $\sigma_{\perp}^2 > \sigma_{\parallel}$ where spatial coordinates are measured in units of k_s . We then define the normalized continuous operator

$$\hat{b}(\mathbf{r}) = \frac{1}{\sqrt{\check{\rho}(\mathbf{r})}} \sum_j \delta(\mathbf{r} - \mathbf{r}_j) \hat{b}_j. \quad (11.0.3)$$

This definition leads to the standard commutation relations for such continuous operators,

$$[\hat{b}(\mathbf{r}), \hat{b}^\dagger(\mathbf{r}')] = \delta(\mathbf{r} - \mathbf{r}'). \quad (11.0.4)$$

From the definition of the continuous operators Eq. (10.2.10) can be written as

$$\begin{aligned} \frac{d}{dt} b^\dagger(\mathbf{r}, t) &= \int d^3 r' \sum_j \frac{\delta(\mathbf{r} - \mathbf{r}_j)}{\sqrt{\check{\rho}(\mathbf{r})}} M(\mathbf{r}, \mathbf{r}') \sqrt{\check{\rho}(\mathbf{r}')} b^\dagger(\mathbf{r}', t) \\ &= \int d^3 r' \frac{\rho(\mathbf{r})}{\sqrt{\check{\rho}(\mathbf{r})}} M(\mathbf{r}, \mathbf{r}') \sqrt{\check{\rho}(\mathbf{r}')} b^\dagger(\mathbf{r}', t) \\ &\quad + \int d^3 r' \sum_j \frac{\delta(\mathbf{r} - \mathbf{r}_j) - \rho(\mathbf{r})}{\sqrt{\check{\rho}(\mathbf{r})}} M(\mathbf{r}, \mathbf{r}') \sqrt{\check{\rho}(\mathbf{r}')} b^\dagger(\mathbf{r}', t), \end{aligned} \quad (11.0.5)$$

The lowest order spatial average is found simply by making a spatial average of Eq. (11.0.5). In Chap. 6 we considered higher order corrections coming from such a spatial average, and showed how fluctuations in position give rise to spontaneous emission and dipole-dipole effects. Here we ignore these effects. To lowest order in the spatial average, the first term in Eq. (11.0.5) describes the mean effect of the atoms interaction with each other, that is when averaged with respect to their individual positions. The second term gives then a decay described by Γ , which is independent of the interactions between atoms. Thus dressing the atomic operators with respect to the decay Γ , ignoring the source term \hat{F} and the point-particle corrections, the effective differential equation describing the excitation of the atoms is after spatial average then given by

$$\frac{d}{dt} b^\dagger(\mathbf{r}, t) = \int d^3 r' \sqrt{\rho(\mathbf{r})} M(\mathbf{r}, \mathbf{r}') \sqrt{\rho(\mathbf{r}')} b^\dagger(\mathbf{r}', t). \quad (11.0.6)$$

Similarly the field equation (10.2.1) can be described in terms of the continuous operators, and one find

$$\mathbf{D}^{(+)}(\mathbf{r}, t) = \mathbf{D}_0^+(\mathbf{r}, t) + a|\mathcal{D}_{cl}| \int d^3 r' \bar{\mathbf{P}}^{(+)}(\mathbf{r}, \mathbf{r}') \sqrt{\rho(\mathbf{r}')} \cdot \mathbf{e}_+ \hat{b}^\dagger(\mathbf{r}', t) \quad (11.0.7)$$

In the following we will find approximate solutions to the above equations.

Diagonalizing the interaction matrix

The system in consideration is assumed cylindrically symmetric, with a density described by Eq. (11.0.2). We shall therefore use a cylindrically symmetric set of basis functions for our diagonalization: a combination of plane waves and Bessel functions. We denote the basis $\{f_{kmn}\}$ where

$$f_{kmn}(r, z, \phi) = \frac{\sqrt{2}}{2\pi a_c J_{m+1}(X_{mn})} e^{ikz+im\phi} J_m(X_{mn} \frac{r}{a_c}). \quad (12.0.1)$$

J_m is the Bessel function of first kind of order m , X_{mn} is the n 'th zero of the m 'th order Bessel function of first kind. The parameter a_c is a cut-off in the radial direction, meaning that our basis is complete on the interval $r \in [0, a_c]$. We work with a cut-off in the radial direction and not in the z -direction due to the assumption $\sigma_{\parallel} \gg \sigma_{\perp}$. The inner product defined for this basis is therefore given by,

$$\langle \theta | \psi \rangle = \int_0^{2\pi} d\phi \int_{-\infty}^{\infty} dz \int_0^{a_c} r dr \theta^*(r, z, \phi) \psi(r, z, \phi). \quad (12.0.2)$$

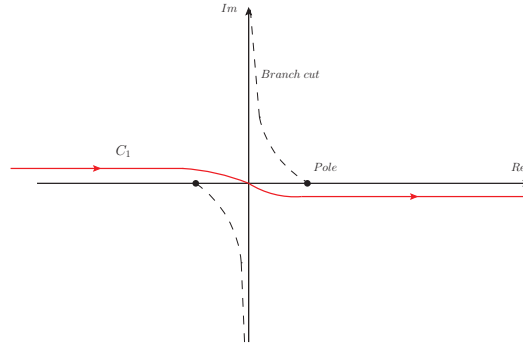


Figure 12.1: Sketch of the integration contour C_1 , in the integral representation (12.0.5) of the Green function.

For a discussion of this basis see e.g. Ref. [48]. The matrix, or in the continuous case the integral kernel, that we wish to diagonalize in the basis $\{f_{kmn}\}$ is now given by

$$M(\mathbf{r}, \mathbf{r}') = \frac{-3\pi i \Gamma}{k_s^3} \mathbf{e}_+^* \cdot \sqrt{\rho(\mathbf{r})} \bar{P}^{(+)}(\mathbf{r}, \mathbf{r}') \sqrt{\rho(\mathbf{r}')} \cdot \mathbf{e}_+. \quad (12.0.3)$$

The propagator $\bar{P}^{(+)}$ is found in a real space representation in Eq. (A.4.5). One may from the real space representation of the propagator show that

$$\mathbf{e}_+^* \cdot \bar{P}^{(+)}(\mathbf{r}, \mathbf{r}') \cdot \mathbf{e}_+ = \frac{-k_s^3}{8\pi} (\nabla^2 + \partial_z^2) \frac{e^{i|\mathbf{r}-\mathbf{r}'|}}{|\mathbf{r}-\mathbf{r}'|}. \quad (12.0.4)$$

The polarization effects are included in the differential operator $\nabla^2 + \partial_z^2$. In addition we use that the Green function can be written as [49]

$$\frac{e^{i|\mathbf{r}-\mathbf{r}'|}}{|\mathbf{r}-\mathbf{r}'|} = \frac{i}{2} \sum_m \int_{C_1} dh e^{im(\phi-\phi')+ih(z-z')} J_m(\sqrt{1-h^2}r_<) H_m^{(1)}(\sqrt{1-h^2}r_>), \quad (12.0.5)$$

where $r_<$ ($r_>$) is the minor (larger) of r and r' . C_1 is describing a curve essentially going from $-\infty$ to ∞ along the real axis but shifted to avoid the branch cut and pick out the retarded Green's function, as shown in Fig. 12.1. By introducing an integral, the non-trivial product of Bessel functions in Eq. (12.0.5), can be symmetrized [50]:

$$J_m(\sqrt{1-h^2}r_<) H_m^{(1)}(\sqrt{1-h^2}r_>) = \frac{2}{i\pi} \int x dx \frac{J_m(xr) J_m(xr')}{x^2 + h^2 - 1}. \quad (12.0.6)$$

The propagator is then given by

$$\mathbf{e}_- \cdot \bar{\mathbf{P}}^{(+)}(\mathbf{r}, \mathbf{r}') \cdot \mathbf{e}_+ = \frac{k_s^3}{8\pi^2} \sum_m \int_{C_1} dh \int x dx \frac{1+h^2}{x^2+h^2-1} e^{im(\phi-\phi') + ih(z-z')} J_m(xr) J_m(xr'). \quad (12.0.7)$$

In the basis $\{f_{kmn}\}$ the differential equation (11.0.6) can be written as

$$\frac{d}{dt} \hat{b}_{kmn}^\dagger(t) = \sum_{k'm'n'} M_{k'm'n'}^{kmn} \hat{b}_{k'm'n'}^\dagger \quad (12.0.8)$$

where

$$M_{k'm'n'}^{kmn} = \langle f_{kmn}(\mathbf{r}) | M(\mathbf{r}, \mathbf{r}') | f_{k'm'n'}(\mathbf{r}') \rangle, \quad (12.0.9)$$

and

$$b_{kmn}^\dagger(t) = \langle f_{kmn}(\mathbf{r}) | b^\dagger(\mathbf{r}, t) \rangle. \quad (12.0.10)$$

When calculating the matrix Eq. (12.0.9), we have to make integrals over r, z and ϕ . We can at this point simplify the radial integrals by extending the upper integral limit to infinity. This is correct since the cut-off a_c can be chosen arbitrarily and as we in the end will set it to infinity. The governing parameter is therefore the density function which has a finite width σ_\perp . The following results found in Ref. [50] is useful for making the radial integrals:

$$\int_0^\infty r dr e^{-\alpha r^2} I_m(\beta r) J_m(\gamma r) = \frac{1}{2\alpha} e^{\frac{\beta^2 - \gamma^2}{4\alpha}} J_m\left(\frac{\beta\gamma}{2\alpha}\right) \\ \text{Re}[\alpha] > 0, \text{Re}[m] > -\frac{1}{2} \quad (12.0.11)$$

and

$$\int_0^\infty r dr e^{-\alpha^2 r^2} J_m(\beta r) J_m(\gamma r) = \frac{1}{2\alpha^2} e^{-\frac{\beta^2 + \gamma^2}{4\alpha^2}} I_m\left(\frac{\beta\gamma}{2\alpha^2}\right) \\ |\arg[\alpha]| < \frac{\pi}{4}, \text{Re}[m] > -1, \beta > 0, \gamma > 0 \quad (12.0.12)$$

After making the spatial integrations the matrix M reduces to

$$M_{kmn}^{k'm'n'} = \delta_{mm'} \frac{\lambda_0}{i} \int_{C_1} dh \int x dx \eta(k-h)\eta(k'-h) \frac{1+h^2}{x^2+h^2-1} \frac{8\sigma_{\perp}^4 e^{-\sigma_{\perp}^2(\gamma_n^2+\gamma_{n'}^2)}}{a_c^2 J_{m+1}(X_{mn}) J_{m+1}(X_{mn'})} \times \\ e^{-2\sigma_{\perp}^2 x^2} I_m(2\sigma_{\perp}^2 \gamma_n x) I_m(2\sigma_{\perp}^2 \gamma_{n'} x) \quad (12.0.13)$$

where

$$\eta(k) = \frac{\sigma_{\parallel}}{\sqrt{\pi}} e^{-\sigma_{\parallel}^2 k^2}, \quad (12.0.14)$$

and where we have introduced the constant $\lambda_0 = \frac{3\pi\rho_0\Gamma}{2}$. We notice that both integrals over x and h is bounded by Gaussian functions, and since we assume $\sigma_{\perp} \gg 1$ we may make a series expansion in x and h of the function $1/(x^2 + h^2 - 1)$. We will be interested in a series expansion of the integrals over x and h only to the lowest order. Since we assume that $\sigma_{\parallel} \gg \sigma_{\perp}$, i.e. cigar-shape, our lowest order calculation will terminate after first order in $1/\sigma_{\perp}^2$. The integral over h can to this order be approximated by treating the function $\eta(k-h)$ as a delta function. We show in Appendix B.1 that the integral over x to lowest order in the variable $1/\sigma_{\perp}^2$ gives

$$M_{kmn}^{k'm'n'} = \delta_{mm'} \eta(k-k') \frac{\lambda_0}{i} \left\{ \Lambda_{mn'}^m \frac{1+k^2}{k^2-1} - \frac{\Lambda_{nn'}^{1m}}{\sqrt{8}\sigma_{\perp}^2} \frac{1+k^2}{(k^2-1)^2} \right\} + \mathcal{O}[\sigma_{\parallel}^{-2}, \sigma_{\perp}^{-4}], \quad (12.0.15)$$

where

$$\Lambda_{nn'}^m = \frac{2\sigma_{\perp}^2 e^{-\frac{\sigma_{\perp}^2}{2}(\gamma_n^2+\gamma_{n'}^2)} I_m(\sigma_{\perp}^2 \gamma_n \gamma_{n'})}{a_c^2 J_{m+1}(X_{nn}) J_{m+1}(X_{nn'})} \quad (12.0.16)$$

and

$$\Lambda_{nn'}^{1m} = \frac{4\sigma_{\perp}^2 e^{-\sigma_{\perp}^2(\gamma_n^2+\gamma_{n'}^2)} I_m(2\sigma_{\perp}^2 \gamma_n \gamma_{n'})}{a_c^2 J_{m+1}(X_{nn}) J_{m+1}(X_{nn'})}. \quad (12.0.17)$$

The matrices $\Lambda_{nn'}^m$ and $\Lambda_{nn'}^{1m}$ are normalized such that for $\sigma_{\perp} \rightarrow \infty$ they reduce to a delta-function $\delta(n-n')$.

We shall here and in the remainder of the article treat the function $\eta(k-k')$ as a delta function. This approximation enables us to solve the superradiance problem in certain limits, but it also imposes some limitations. In Appendix B.3 we explore the limitations

of the approximation, and show that when we look at the radiated light the approximation gets worse when moving to the far field region, as well as in the large time limit.

In the following we take a closer look at the matrix $\Lambda_{nn'}^m$ defined in Eq. (12.0.16). For simplicity we will not consider the correction $\Lambda_{nn'}^{1m}$, however the conclusions drawn in the following holds for the correction as well. The differential equation concerning our system with respect to the quantum number n, n' has got the form

$$\frac{d}{dt}a_n(t) = \sum_{n'} \omega \Lambda_{nn'}^m a_{n'}(t). \quad (12.0.18)$$

We wish to take the limit $a_c \rightarrow \infty$. To clarify what this means let us write the matrix Λ in the following way:

$$\Lambda_{nn'}^m = \Delta k_{nn'} \Xi_{nn'}^m \pi^2 \sigma_{\perp}^2 e^{-\frac{\pi^2 \sigma_{\perp}^2}{2}(k_{mn}^2 + k_{mn'}^2)} I_m(\pi^2 \sigma_{\perp}^2 k_{mn} k_{mn'}) \sqrt{k_{mn} k_{mn'}} \quad (12.0.19)$$

where

$$\Xi_{nn'}^m = \frac{2}{\pi} \frac{1}{\sqrt{X_{mn} X_{mn'}} J_{m+1}(X_{mn}) J_{m+1}(X_{mn'})} \quad (12.0.20a)$$

$$\approx (-1)^{n+n'} \quad \text{for } X_{mn}, X_{mn'} \rightarrow \infty$$

$$k_{mn} = \frac{X_{mn}}{\pi a_c} \quad (12.0.20b)$$

$$\Delta k_{nn'} = \frac{1}{a_c} \quad (12.0.20c)$$

We thus see that when letting $a_c \rightarrow \infty$, a transverse momentum naturally arises $k_{m\perp} = \lim_{a_c \rightarrow \infty} k_{mn}$, and the discrete matrix equation, Eq. (12.0.18) becomes an integral equation over the transverse momentum $k_{m\perp}$, using $\sum_{n'} \Delta k_{nn'} \rightarrow \int dk_{m\perp}$.

$$\frac{d}{dt}a(k_{m\perp}, t) = \int dk'_{m\perp} \omega \Lambda^m(k_{m\perp}, k'_{m\perp}) a(k'_{m\perp}, t) \quad (12.0.21)$$

It is evident that when using the limiting properties of the Bessel function $I_m(x)$ the integral kernel $\Lambda^m(k_{m\perp}, k'_{m\perp})$ becomes a delta function for $\sigma_{\perp} \rightarrow \infty$. We thus realize that the effective one-dimensional result obtained by Raymer and Mostowski [3] is exact for an infinitely large atomic ensemble.

Now we again include the correction $\Lambda_{nn'}^{1m}$ to the analysis. Both matrices $\Lambda_{nn'}^m$ and $\Lambda_{nn'}^{1m}$ are real and symmetric and thus can be diagonalized. In Appendix B.2 we show that the two matrices commute. We can therefore choose a common set of eigenfunctions, $\{F_{kmn}(r)\}$ for both matrices. We define the unitary matrix \bar{U} that transform our initial basis $\{f_{kmp}\}$ to the basis given by the eigenfunctions $\{F_{kmn}(r)\}$,

$$F_{kmn}(\mathbf{r}) = \sum_p U_{np} f_{kmp}(\mathbf{r}) \quad (12.0.22)$$

Finally we will define a corresponding set of eigenvalues,

$$\Lambda_{pp'}^m = \sum_n U_{np} \lambda_{mn} U_{np'} \quad (12.0.23)$$

and

$$\Lambda_{pp'}^{1m} = \sum_n U_{np} \lambda_{mn}^1 U_{np'} \quad (12.0.24)$$

It is convenient in the following to change to this basis, where $\Lambda_{nn'}^m$ and $\Lambda_{nn'}^{1m}$ are diagonal. We therefore write the Eq. (12.0.15) as

$$\sum_{pp'} U_{np} M_{kmp}^{k'm'p'} U_{n'p'} = \frac{\lambda_0}{i} \left\{ \lambda_{mn} \frac{1+k^2}{k^2-1} - \frac{\lambda_{mn}^1}{\sqrt{8}\sigma_{\perp}^2} \frac{1+k^2}{(k^2-1)^2} \right\} \delta_{mm'} \delta_{nn'} \eta(k-k') + O[\sigma_{\parallel}^{-2}, \sigma_{\perp}^{-4}] \quad (12.0.25)$$

Real space representation of the electric field

In the following section we will, based on the eigenvalue analysis of the atomic operators, derive the real-space behavior of the electric field. We shall divide the analysis into a regime of small times where the dominating effect is spontaneous emission, and a large time regime, where the dominating effect is the cooperatively emitted light, the superradiated beam. To keep things simple, we mainly consider the electric field at and around the symmetry axis. In this regime the scattered radiation field is sufficiently well described by the vector component $D_+^{(+)}$ and the Hermitian conjugate, which can be seen from Eq. (11.0.7) and the real space representation of the propagator Eq. (10.2.2).

Let us first determine the electric field at the symmetry axis at zero time, $t = 0$. In this case the electric field is given by:

$$D_+^{(+)}(\mathbf{r}_s, 0) = D_+^{(+)}(\mathbf{r}_s, 0)_0 + \int d^3 r' \frac{a|\mathcal{D}_{cl}|k_s^3}{4\pi} \frac{((z - z')^2 + \frac{1}{2}r'^2)e^{i\sqrt{(z-z')^2+r'^2}}}{(r'^2 + (z - z')^2)^{3/2}} \sqrt{\rho(\mathbf{r}')} \hat{b}^\dagger(\mathbf{r}', 0), \quad (13.0.1)$$

where the index s refers to being at the symmetry axis. To arrive at the above result we used the real space representation of the propagator \bar{P} Eq. (12.0.4) to leading order in one over distance. This approximation is done out of convenience but is not strictly

necessary. When making the calculations for the mode expansion of the electric field in the general modes F_{kmn} we shall check that the limit $t \rightarrow 0$ exist and are given by the expression, (13.0.1).

The analysis of the radiation field for $t \neq 0$ starts by inserting the unit,

$$\mathbb{1} = \int d^3 r' \int dk \sum_{mn} F_{kmn}(\mathbf{r}) F_{kmn}^*(\mathbf{r}') \quad (13.0.2)$$

into the field equation, Eq. (11.0.7). We then get the following expansion of the electric field.

$$D_+^{(+)}(\mathbf{r}, t) = D_+^{(+)}(\mathbf{r}, t)_0 + \int d^3 r' \int dk \sum_{mn} C_{kmn}(\mathbf{r}) e^{\lambda_{kmn} t} F_{kmn}^*(\mathbf{r}') \hat{b}^\dagger(\mathbf{r}', 0), \quad (13.0.3)$$

where

$$C_{kmn}(\mathbf{r}) = a |\mathcal{D}_{cl}| \int d^3 r' \mathbf{e}_+^* \cdot \bar{\mathbf{P}}^{(+)}(\mathbf{r}, \mathbf{r}') \cdot \mathbf{e}_+ \sqrt{\rho(\mathbf{r}')} F_{kmn}(\mathbf{r}'), \quad (13.0.4)$$

the functions F_{kmn} are the basis functions given in Eq. (12.0.22), and the eigenvalue λ_{kmn} is given in Eq. (12.0.25).

The calculation of the modefunctions C_{kmn} is initiated by integrating with respect to the spatial coordinate \mathbf{r}' . The integrals involving Bessel functions are found in e.g. [50] or (12.0.12), and one arrive at

$$C_{kmn}(\mathbf{r}) = \frac{a |\mathcal{D}_{cl}| k_s^3 \sqrt{\rho_0} (1 - \partial_z^2)}{4\pi} \int dy \int x dx \sum_p U_{np} \frac{e^{im\phi + i(k+y)z}}{x^2 + (k+y)^2 - 1} \frac{\sqrt{2} J_m(xr)}{a_c J_{m+1}(X_{mp})} \times \frac{2\sigma_\perp^2 \sigma_\parallel}{\sqrt{\pi}} e^{-\sigma_\parallel^2 y^2 - \sigma_\perp^2 (\gamma_p^2 + x^2)} I_m(2\sigma_\perp \gamma_p x). \quad (13.0.5)$$

The next step of the calculation is to include the mode summation. We will therefore define the propagator $P^{(+)}$ given by

$$P^{(+)}(\mathbf{r}, \mathbf{r}'; t) = \int dk \sum_{mn} C_{kmn}(\mathbf{r}) e^{\lambda_{kmn} t} F_{kmn}^*(\mathbf{r}'). \quad (13.0.6)$$

We notice that the variable y in Eq. (13.0.5) is small, as it is controlled by the Gaussian function of σ_\parallel . We shall therefore by a translation of the integral variable $k' = k + y$ move

the perturbation y to the eigenvalue λ_{kmn} , so that we use $\lambda_{k'-y,mn}$. This choice ensure that we will get the correct behavior of the integrals in the limit $t = 0$. This way we can in principle make the k' integral by using the series expansion of the function $e^{\lambda_{k'-y,mn}t}$, where the zeroth order term in the expansion in t is the limit given by Eq.(13.0.1). Though in principle the k' integral can be made using the series expansion of the exponential, we shall follow the path used by e.g. Ref. [3].

In the following we make a series expansion of the eigenvalue $\lambda_{k-y,mn}$ given in Eq. (12.0.25) with respect to the variable y .

$$\begin{aligned}\lambda_{k-y,mn} &\equiv \frac{1}{i} \left(\lambda_{mn} \frac{(k-y)^2 + 1}{(k-y)^2 - 1} - \frac{\lambda_{mn}^1}{\sqrt{8}\sigma_{\perp}^2} \frac{(k-y)^2 + 1}{((k-y)^2 - 1)^2} \right) \\ &\approx \frac{1}{i} \left(\lambda_{mn} \frac{k^2 + 1}{k^2 - 1} + 2\mu_{mn} \frac{k^2 + 1}{(k^2 - 1)^2} \right),\end{aligned}\quad (13.0.7)$$

The series expansion can be done since the y -integral is bound by a Gaussian function. To shorten notation we have substituted $k' \rightarrow k$, and introduced the coefficient $\mu_{mn} = \lambda_{mn}y - \frac{\lambda_{mn}^1}{\sqrt{8}\sigma_{\perp}^2}$.

In Eq. (13.0.6) the k -integral includes a pole

$$\frac{1}{k^2 + x^2 - 1} \rightarrow \frac{1}{2\sqrt{1-x^2}(k - \sqrt{1-x^2})},\quad (13.0.8)$$

where the arrow reflects the fact that we are only interested in the retarded Green function, which correspond to the pole $k = \sqrt{1-x^2}$. Since we are particularly interested in this pole, we shall in the k -integral in Eq. (13.0.6), make a translation of the eigenvalue $\lambda_{k-y,mn} \rightarrow \lambda_{k+y+\sqrt{1-x^2},mn}$, and then a series expansion similar to Eq. (13.0.7). We can make the calculation with two different situations in mind, one situation explains the spontaneous radiation originating from a sample of atoms of some geometrical shape. We are most interested in the other situation describing the collective emission or the superradiance occurring when the atoms co-radiate. As a check of our formalism we shall, however, also consider the short time-limit where there is just spontaneous emission. We expect that as time evolves the superradiating mode will become the dominating effect. Therefore we demonstrate where the superradiating effect is found and described in our mathematical treatment of the problem.

Let us first show how the important steps in the calculation of superradiance is done, before going into the full details. The integral appearing in the calculation are of the type

$$\mathcal{I}_k(t) = \frac{1}{2\pi} \int dk \frac{e^{\lambda_{k-y, mn} t + ik\Delta z}}{k^2 + x^2 - 1}, \quad (13.0.9)$$

where $\Delta z = z - z'$. For now we consider the lowest order correction for simplicity, that is we neglect μ_{mn} in Eq. (13.0.7). Including μ_{mn} to the eigenvalue is a trivial generalization. We focus on the pole in the integral at $k = \sqrt{1 - x^2}$, as this pole describes the energetically allowed scattering processes. We will here and in the following assume Δz is large, thus by introducing the variable $s = i\Delta z(k - \sqrt{1 - x^2})$ the integral \mathcal{I}_k^0 can be written as

$$\mathcal{I}_k^0(t) = i \frac{1}{2\pi i} \int_{-i\infty}^{i\infty} ds e^{\frac{s + i\Delta z \sqrt{1-x^2} + \frac{\lambda_{mn} t \Delta z}{s - i \frac{x^2 \Delta z}{2}}}{2 \sqrt{1-x^2} s}}, \quad (13.0.10)$$

where the superscript 0 indicates that this is a zeroth order calculation in the correction to the eigenvalue due to finite size. The superradiant contribution to Eq. (13.0.10) comes from the pole of the exponential. In order for this pole to contribute to the pole describing the propagated light, that is the zero point of the denominator, the term $\frac{x^2 \Delta z}{2}$ has to be small. For $\frac{x^2 \Delta z}{2} < 1$ we shall treat it as a perturbation. When this no longer apply, the pole in the exponent can be neglected, and we are thus left with the result for short times, i.e. spontaneous emission. The latter is analyzed in the following section, and we shall for now concern ourselves with the superradiant contribution. Since $\frac{x^2 \Delta z}{2} < 1$ we can make an expansion in this quantity and obtain

$$\mathcal{I}_k(t) = \frac{ie^{i\Delta z}}{2} \sum_{l=0}^{\infty} \sum_{q=0}^{\infty} \left(\frac{ix^2 \Delta z}{2} \right)^l \frac{(-2it\mu_{mn}\Delta z^2)^q}{q!} \frac{1}{2\pi i} \int_{-i\infty}^{i\infty} ds e^{s + \frac{\lambda_{mn} t \Delta z}{s}} s^{1+l+2q}. \quad (13.0.11)$$

The integral may be found in Ref. [51] and we find (Here we include the correction to the eigenvalue in Eq. (13.0.7).)

$$\mathcal{I}_k(t) = \frac{ie^{i\Delta z}}{2} \sum_{l=0}^{\infty} \sum_{q=0}^{\infty} \left(\frac{ix^2 \Delta z}{2} \right)^l \frac{(-2i\mu_{mn}\Delta z^2)^q}{q!} \frac{I_{l+2q}(2\sqrt{\lambda_{mn} t \Delta z})}{(\sqrt{\lambda_{mn} t \Delta z})^{l+2q}}. \quad (13.0.12)$$

13.1 Short time limit

In order to understand our calculation of superradiance, we first analyze it for $t = 0$, as we know how the propagator for $t = 0$ looks when measured at the symmetry axis. The $t = 0$ regime is also met for $\frac{x^2 \Delta z}{2} > 1$. We shall therefore also refer to this calculation as the short time limit. Here we find from a residue calculation Eq. (13.0.9) to give

$$\mathcal{I}_k(0) = \frac{ie^{i\sqrt{1-x^2}\Delta z}}{2\sqrt{1-x^2}}. \quad (13.1.1)$$

Let us therefore return to the k integral for $t = 0$ in eq. (13.1.1). By inserting this into the propagator in Eq. (13.0.6), the propagator may be written

$$P^{(+)}(\mathbf{r}, \mathbf{r}'; 0) = \sum_{mn} \frac{a|\mathcal{D}_{cl}|k_s^3 \sqrt{\rho_0}(1 - \partial_z^2)}{4\pi} \int x dx \sum_{pp'} U_{np} U_{np'} \frac{2i\sigma_{\perp}^2 e^{im\Delta\phi + i\sqrt{1-x^2}\Delta z}}{\sqrt{1-x^2}} \times \frac{J_m(xr)J_m(\gamma_{p'}r')I_m(2\sigma_{\perp}^2\gamma_p x)}{a_c^2 J_{m+1}(X_{mp})J_{m+1}(X_{mp'})} e^{-\sigma_{\perp}^2(\gamma_p^2 + x^2) - \frac{z'^2}{4\sigma_{\perp}^2}}. \quad (13.1.2)$$

The only dependence on the mode-index n is in the product of the two matrices $U_{np}U_{np'}$ and the sum over n reduces to a delta function $\delta_{pp'}$. We then make identification similar to Sec. 12, $\sum_p \frac{1}{a_c} \rightarrow \int \frac{d\gamma_p}{\pi}$ for $a_c \rightarrow \infty$. The variable γ_n is in this sense fixed, thus letting $a_c \rightarrow \infty$ has to be accompanied by $X_{mn} \rightarrow \infty$. Therefore we can use the large argument approximation for the Bessel functions,

$$J_m(X_{mn}) \approx \sqrt{\frac{2}{\pi X_{mn}}} \cos(X_{mn} - \frac{m\pi}{2} - \frac{\pi}{4}), \quad X_{mn} \gg 1. \quad (13.1.3)$$

Using this we can make the integrals over γ_p and $\gamma_{p'}$. The result of the mode summation, eq. (13.0.6) is then

$$P^{(+)}(\mathbf{r}, \mathbf{r}'; 0) = \frac{a|\mathcal{D}_{cl}|k_s^3 \sqrt{\rho(\mathbf{r}')}(1 - \partial_z^2)}{8\pi} \sum_m e^{im\Delta\phi} \int x dx \frac{ie^{i\sqrt{1-x^2}\Delta z}}{\sqrt{1-x^2}} J_m(xr)J_m(xr') \quad (13.1.4)$$

This is the main result of this section. To verify the validity of the approach taken so far, we shall now show that the propagator Eq. (13.1.4) reduces to the one used in Eq.

(13.0.1) on the symmetry axis. In order to show this we will use the summation theorem for Bessel functions, see e.g. [50],

$$\sum_m e^{im\Delta\phi} J_m(xr)J_m(xr') = J_0(xR), \quad (13.1.5)$$

where $R = \sqrt{r^2 + r'^2 - 2rr' \cos(\Delta\phi)}$. This way the propagator in Eq. (13.1.4) can be written

$$P^{(+)}(\mathbf{r}, \mathbf{r}', 0) = \frac{a|\mathcal{D}_{cl}|k_s^3 \sqrt{\rho(\mathbf{r}')} (1 - \partial_z^2)}{8\pi} \int x dx \frac{ie^{i\sqrt{1-x^2}\Delta z} J_0(xR)}{\sqrt{1-x^2}}. \quad (13.1.6)$$

The x -integral is known and may be found in Ref. [51], to give

$$P^{(+)}(\mathbf{r}, \mathbf{r}', 0) = \frac{-a|\mathcal{D}_{cl}|k_s^3 \sqrt{\rho(\mathbf{r}')} (1 - \partial_z^2)}{8\pi} \frac{e^{i\sqrt{R^2+\Delta z^2}}}{\sqrt{R^2 + \Delta z^2}}. \quad (13.1.7)$$

Finally the z differential give us the result we are looking for.

$$P^{(+)}(\mathbf{r}, \mathbf{r}', 0) = \frac{a|\mathcal{D}_{cl}|k_s^3 \sqrt{\rho(\mathbf{r}')}}{4\pi} \frac{e^{i\sqrt{R^2+\Delta z^2}}}{\sqrt{R^2 + \Delta z^2}} \frac{\frac{1}{2}R^2 + \Delta z^2}{R^2 + \Delta z^2}. \quad (13.1.8)$$

When we then look at the symmetry axis, the variable R reduce to r' and we are left with the result in Eq. (13.0.1). The result of this section can be written as

$$D_+^{(+)}(\mathbf{r}, 0) = D_+^{(+)}(\mathbf{r}, 0)_0 + \int d^3r' P^{(+)}(\mathbf{r}, \mathbf{r}'; 0) \hat{b}^\dagger(\mathbf{r}', 0). \quad (13.1.9)$$

13.2 Finite time, build up of superradiance

In the following we shall analyze the effect of the eigenvalues λ_{mn} and λ_{mn}^1 in the expression (13.0.12). When we introduce the eigenvalues in Sec. 12 we only concluded they could be found. We also know that physics connected to the eigenvalues can not depend on the cut-off a_c involved in the index n . In the following we show that indeed the physics is independent of the cut-off a_c . To find this result we shall in particular look at the sum $\sum_n U_{np} \mu_{mn}^M \lambda_{mn}^N U_{np'}$ where the powers N and M are zero or a some positive integer. [The powers N and M are connected to series expansions of functions involving the eigenvalue

λ_{mn} , e.g. Eq. (13.0.12)] The eigenvalues λ_{mn} and λ_{mn}^1 are related to the matrices $\Lambda_{pp'}^m$ and $\Lambda_{pp'}^1$ in Eqs. (12.0.23) and (12.0.24). This enables us to carry out the calculations in the limit $a_c \rightarrow \infty$. Let us generalize the matrices $\Lambda_{pp'}^m$ and $\Lambda_{pp'}^1$, defined in Eqs. (12.0.16) and (12.0.17) to

$$\Lambda_{pp'}^m\left(\frac{\sigma_{\perp}^2}{N}\right) = \frac{4\sigma_{\perp}^2 e^{-\frac{\sigma_{\perp}^2}{N}(\gamma_p^2 + \gamma_{p'}^2)} I_m\left(\frac{2\sigma_{\perp}^2}{N} \gamma_p \gamma_{p'}\right)}{N a_c^2 J_m(X_{mp}) J_m(X_{mp'})}, \quad (13.2.1)$$

i.e. (12.0.16) is the $N = 2$ limit and (12.0.17) the $N = 1$ limit. One can then show that

$$\sum_n U_{np} \mu_{mn}^M \lambda_{mn}^N U_{np'} = \sum_s \binom{M}{s} y^{M-s} (-4\sigma_{\perp}^2)^{-s} \Lambda_{pp'}^m\left(\frac{\sigma_{\perp}^2}{2(N+M-s)+s}\right) \quad (13.2.2)$$

This result along with the appropriate series expansion of functions involving the eigenvalues λ_{mn} and λ_{mn}^1 can be inserted into the result for the propagator Eq. (13.0.6), and the resulting sum over indices p and p' becomes of the form

$$\sum_{pp'} \frac{J_m(\gamma_{p'} r') I_m(2\sigma_{\perp}^2 \gamma_p x) e^{-\sigma_{\perp}^2(x^2 + \gamma_p^2)}}{a_c^2 J_{m+1}(X_{mp}) J_{m+1}(X_{mp'})} \Lambda_{pp'}^m\left(\frac{\sigma_{\perp}^2}{N}\right) = \frac{1}{4\sigma_{\perp}^2} e^{-\frac{r'^2}{4\sigma_{\perp}^2} - \frac{Nr'^2}{4\sigma_{\perp}^2}} J_m(xr'), \quad (13.2.3)$$

where N is an integer derived from Eq. (13.2.2) and the before mentioned series expansions. The propagator Eq. (13.0.6) can therefore be written as

$$\begin{aligned} P^{(+)}(\mathbf{r}, \mathbf{r}'; t) &= \sum_{mn} \frac{a |\mathcal{D}_{cl}| k_s^3 \sqrt{\rho_0} (1 - \partial_z^2)}{4\pi} \int x dx \int dy \frac{\sigma_{\parallel}}{\sqrt{\pi}} e^{-\sigma_{\parallel}^2 y^2 + iy z'} \sum_{pp'} U_{np} U_{np'} \times \\ &\quad 4\sigma_{\perp}^2 e^{im\Delta\phi} \mathcal{I}_k \frac{J_m(xr) J_m(\gamma_{p'} r') I_m(2\sigma_{\perp}^2 \gamma_p x)}{a_c^2 J_{m+1}(X_{mp}) J_{m+1}(X_{mp'})} e^{-\sigma_{\perp}^2(\gamma_p^2 + x^2) - \frac{r'^2}{4\sigma_{\perp}^2}} \\ &= \frac{ia |\mathcal{D}_{cl}| k_s^3}{4\pi} \sqrt{\rho(\mathbf{r})} \sum_m \int_0^{\sqrt{\frac{2}{kz}}} x dx e^{im\Delta\phi + i\Delta z} J_m(xr) J_m(xr') \times \\ &\quad \sum_{l=0}^{\infty} \sum_{q=0}^{\infty} \left(\frac{ix^2 \Delta z}{2}\right)^l \left(\frac{i\lambda_0 t \Delta z^2}{\sqrt{8}\sigma_{\perp}^2}\right)^q \Phi^q(r', z') \frac{I_{l+2q}\left(2\sqrt{e^{-\frac{r'^2}{2\sigma_{\perp}^2}} \lambda_0 t \Delta z}\right)}{\left(\sqrt{e^{-\frac{r'^2}{2\sigma_{\perp}^2}} \lambda_0 t \Delta z}\right)^{l+2q}}. \end{aligned} \quad (13.2.4)$$

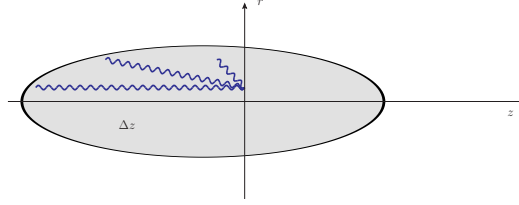


Figure 13.1: A sketch of the coherent build-up of radiation in an atomic cloud. In principle the build-up can happen along any direction, however for a cigar-shaped geometry such as this the most significant build-up happens along the cigar.

where

$$\Phi^q(r', z') = \sum_{n=0}^q \sum_{s=0}^{E(n/2)} \frac{e^{-\frac{r'^2}{4\sigma_{\perp}^2}(q+n)}}{(q-n)!(n-2s)!s!} \left(\frac{-4i\sigma_{\perp}^2}{\sigma_{\parallel}^2} \right)^n (-\sigma_{\parallel}^2)^s z'^{n-2s} \quad (13.2.5)$$

We notice since $(x^2\Delta z)/2 < 1$, that choosing the variable Δz large means that the sum over l will converge very fast. Choosing the variable Δz large can be done by placing the detector plane far away from the sample, in which case we will talk about a far-field calculation. Unfortunately the sum over q converges more slowly when Δz is larger, and as discussed in Appendix B.3 we can not quite rely on our initial approximations [$\eta(k - k') \approx \delta(k - k')$, see Sec. 12] for large Δz . We shall therefore consider the problem in the near field region. The limit $\sqrt{2/\Delta z}$ in the x -integral we shall on the other hand approximate with the value $\sqrt{2/L}$, where $L = \sqrt{2\pi}\sigma_{\parallel}$ is the effective length of the atomic ensemble. This approximation will become better at later times, since the coherent build-up is essentially described by the modified Bessel function $I_{l+2q}(2\sqrt{\lambda_0\Delta z}t)$ which in time will dominate for large values of Δz . In Fig. 13.1 we illustrate the physical significance of the integral over x , which represents an integral over transverse momentum. We see that as we include more light from deviating angles, this radiation has a shorter region over which it can build up, and as the build-up is exponential in the build-up length, the error made by the cut-off L becomes relatively small. From the propagator Eq. (13.2.4) the electric field can be written, similar to the spontaneously emitted radiation, Eq. (13.1.9), as

$$D_+^{(+)}(\mathbf{r}, t) = D_+^{(+)}(\mathbf{r}, t)_0 + \int d^3r' P^{(+)}(\mathbf{r}, \mathbf{r}'; t) \hat{b}^{\dagger}(\mathbf{r}', 0). \quad (13.2.6)$$

Intensity and the correlation function

In this section we consider the electric field, and assume that we place a detector in a plane at some position z_0 after the end of the atomic sample. Then we define the correlation function as a function of the radial coordinate r and of time t

$$C(r, r', t) = \frac{2}{\hbar\epsilon_0 k_s} \int d\phi \langle \hat{D}_+^{(-)}(z_0, r, \phi, t) \hat{D}_-^{(+)}(z_0, r', \phi, t) \rangle, \quad (14.0.1)$$

where $\langle \cdot \rangle$ is the quantum mechanical average. The normalization $\frac{2}{\hbar\epsilon_0 k_s}$ is chosen such that the number of photons in a pulse is given by

$$N_p = \int dA \int dt C(r, r, t) k_s^2. \quad (14.0.2)$$

Inserting the propagator in Eq. (13.2.4) allows us to describe superradiance, while the propagator Eq. (13.1.2) gives the spontaneous emission for short times. We shall be most interested in the super-radiated light, but will also for comparison examine the spontaneously emitted light. First we present the correlation function describing the superradiation, when measured in a plane at the end of the atomic sample. An important Parameter below will be the Fresnel number \mathcal{F} which we define by $\mathcal{F} = \frac{\sigma_s^2}{L}$. We shall in general assume the Fresnel number to be large, in particular $\mathcal{F} > 1$. In the integration over z' we

will use the following substitution

$$\int dz' e^{\frac{z'^2}{2\sigma_{\parallel}^2}} \rightarrow \int_0^L dz', \quad \text{where } L = \sqrt{2\pi}\sigma_{\parallel}. \quad (14.0.3)$$

This way the correlation function can be calculated to give

$$C(r, r', t) = \frac{k_s^2 \lambda_0 e^{-\Gamma t}}{4\mathcal{F}} \sum_m \sum_{\substack{lqk \\ l'q'k'}} \sum_{\substack{q,q' \\ n,n'}} \int_0^{2\mathcal{F}} dy \int_0^{2\mathcal{F}} dy' \left\{ \left(\frac{-iy}{2\mathcal{F}} \right)^l \left(\frac{iy'}{2\mathcal{F}} \right)^{l'} \left(\frac{-i}{\sqrt{8\mathcal{F}}} \right)^q \left(\frac{i}{\sqrt{8\mathcal{F}}} \right)^{q'} (8i\pi\mathcal{F})^n (-8i\pi\mathcal{F})^{n'} \times \right. \\ \left. J_m \left(\sqrt{y} \frac{r}{\sigma_{\perp}} \right) J_m \left(\sqrt{y'} \frac{r'}{\sigma_{\perp}} \right) e^{-\frac{y+y'}{2+2(k+k')+q+q'+n+n'}} I_m \left(\frac{2\sqrt{yy'}}{2+2(k+k')+q+q'+n+n'} \right) \times \right. \\ \left. \chi_{lqkn}^{l'q'k'n'} \frac{(\lambda_0 t L)^{k+k'+q+q'}}{k!k'!(l+2q+k)!(l+2q'+k')!} \right\}, \quad (14.0.4)$$

where

$$\chi_{lqkn}^{l'q'k'n'} = \sum_{s,s'} \frac{E(n/2, n-2s, E(n'/2) n'-2s')}{Q, Q'} 2 \left(\frac{(-1)^{Q+Q'+s+s'} (2\pi)^{-s-s'}}{(q-n)!(q'-n')!(n-2s-Q)!(n'-2s'-Q')!s!s'Q!Q'} \right). \quad (14.0.5)$$

This is the main result of this section. We notice that the only variables controlling the behavior of the correlation function is the Fresnel number, \mathcal{F} , the optical depth $\rho_0 L$ and time measured in units of the single atom scattering rate Γ . This follows since $\lambda_0 t L = \frac{3\pi}{2} \rho_0 L \Gamma t$. From the correlation function (14.0.4) we also expect fast convergence in the index q and l as the Fresnel number increases. In the remainder of the article we shall evaluate the correlation function numerically. Even though the correlation function involves a double integral beside the large number of sums, we see that as we increase the index k, k', q, q', n, n' , the y - and y' -integrals will simplify. This follows since the argument of the modified Bessel function decreases as the indices k, k', q, q', n, n' increases, we can therefore use the small argument limit. Similarly the Gaussian function can be approximated by unity. From Eq. (14.0.4) we see that the dominating term in the sum over k will have a higher k when time grows. This means that the radial behavior of the beam simplifies and is due to the small argument description of the modified Bessel function eventually dominated by the $m = 0$ mode.

In the following section we will examine the radiated light at the symmetry axis.

The purpose is to examine the timescale on which there is a crossover from spontaneous emission to superradiance.

14.1 Intensity on the symmetry axis

Placing the detector on the symmetry axis is a nice simplification especially for the spontaneous emission correlation function, since in that case we may use the result presented in Eqs. (13.1.9) and (13.1.8). Also the coherent emission correlation function simplifies since terms with $m \neq 0$ vanish at the symmetry axis. In the spontaneous emission limit $t \approx 0$ the intensity on the axis is given by

$$C_0(0, 0) = k_s^2 \lambda_0 \int_0^L d\Delta z \int r' dr' e^{-\frac{r'^2}{2\sigma_\perp^2}} \frac{(\frac{1}{2}r'^2 + \Delta z^2)^2}{(r'^2 + \Delta z^2)^3}, \quad (14.1.1)$$

where we use the substitution in Eq. (14.0.3), and assume that the detector is placed at the end of the atomic ensemble. The z -integral can be performed analytically and one finds

$$C_0(0, 0) = k_s^2 \lambda_0 L \int r dr \frac{e^{-\frac{r^2}{2\sigma_\perp^2}}}{32} \left\{ \frac{-13 - 11r^2}{(1 + r^2)^2} + \frac{19 \arctan(r^{-1})}{r} \right\}. \quad (14.1.2)$$

From Eq. (14.1.2) we find that the parameters controlling the intensity on the symmetry axis is here the optical depth, and the relation between the length and the width of the atomic ensemble. In Fig. 14.1 we show how this intensity varies as the relation between the length and the width of the sample is changed. Here and in the following we shall measure the correlation function in units of $k_s^2 \Gamma$. For short time the emitted light is dominated by spontaneous emission. We shall now investigate the time scale on which superradiance begins to dominate the radiation. In the time-domain where the radiation is dominated by spontaneous emission, we expect that the radiation is being emitted almost homogeneously in all directions. This statement is not completely true, as indicated in Fig. 14.1. We thus find that the figure of merit for the spontaneous emission is the density the length and the width of the atomic ensemble, and not as in the case of superradiance, only the Fresnel number and the optical depth. Thus in order to compare the two time domains, the spontaneous emission and the superradiance, we will in the future have to fix e.g. the length of the system. In Fig. 14.2 we show the coherent radiation build up as a func-

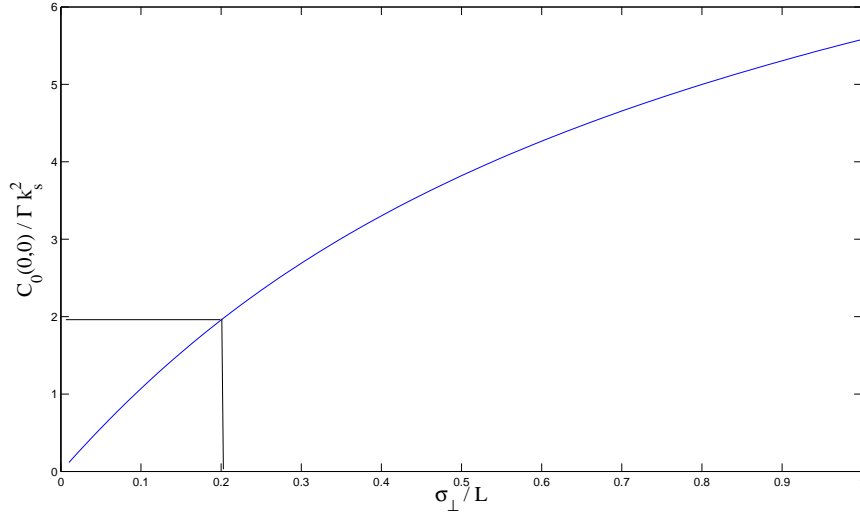


Figure 14.1: Plot of the spontaneous emission intensity, Eq. (14.1.2) on the symmetry axis for varying width of the atomic ensemble. The intensity is measured in units of number of photons times k_s^2 per Γt . In the graph we marked the point corresponding to a Fresnel number $\mathcal{F} = 4$, assuming we fix $L = 100$

tion of time. In the plot we also show the spontaneous emission where we have included the self-coupling of the atoms giving rise to the decay Γ described in Eq. (10.2.3). The superradiation is calculated for different values of the Fresnel number. Time is measured in units of Γ , and we have used a fixed value of the optical depth such that

$$\frac{\lambda_0 L}{\Gamma} = 10, \quad \text{or} \quad \rho_0 L = \frac{20}{3\pi} \approx 2.12. \quad (14.1.3)$$

To compare the superradiation with the spontaneous emission we have fixed the length $L = 100$. This parameter is only important when looking at the spontaneous emission. Fig. 14.2 shows how one may increase the coherent radiation dominance by increasing the width of the sample.

14.2 Intensity profile

In this section we shall look at the spatial shape of the radiation leaving the atomic ensemble. Before we present the numerical calculations for the coherent emission we will look at the correlation function in Eq. (14.0.4). The spatial shape of the function is mainly

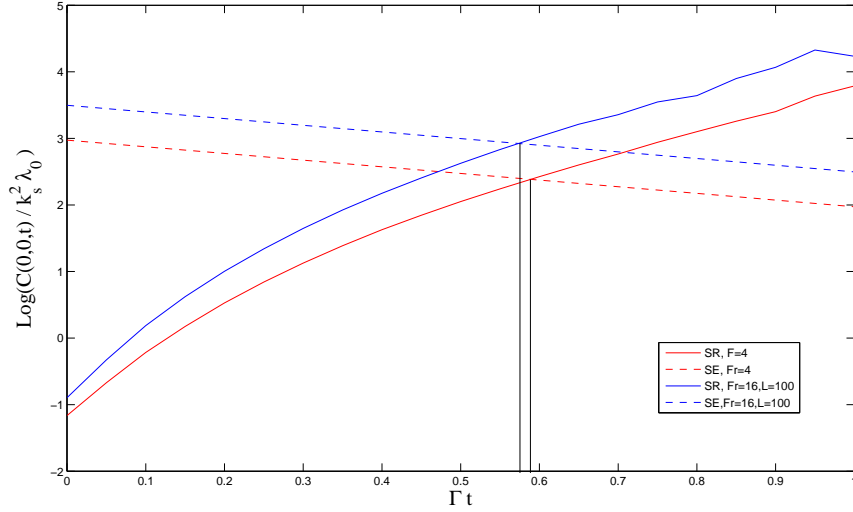


Figure 14.2: Plot of the time evolution of the logarithm of the intensity of coherent radiation as well as of spontaneous radiation when measured at the symmetry axis. We notice the effect of varying the width of the sample, in which case the time at which the coherent radiation dominates change.

given by

$$\int_0^{\mathcal{F}} dy \int_0^{\mathcal{F}} dy' J_m\left(\sqrt{y} \frac{r}{\sigma_{\perp}}\right) J_m\left(\sqrt{y'} \frac{r'}{\sigma_{\perp}}\right) e^{-\frac{y+y'}{2+2(k+k')+q+q'+n+n'}} I_m\left(\frac{2\sqrt{yy'}}{2+2(k+k')+q+q'+n+n'}\right) \quad (14.2.1)$$

With increasing values of k, k', q, q', n and n' , the exponential function can to a higher and higher precision be approximated by unity. The modified Bessel function of order m can for small arguments be approximated with a m 'th order polynomial

$$I_m(z) \approx \frac{(z/2)^m}{m!}. \quad (14.2.2)$$

From the argument of the modified Bessel function in Eq. (14.2.1) we find that region for which the approximation Eq. (14.2.2) is applicable is given both by the number $2 + 2 * (k + k') + q + q' + n + n'$ and by the integration range \mathcal{F} . Eq. (14.2.1) indicates that as time increases the dominant mode will be the $m = 0$ mode for a finite sized atomic ensemble. On the other hand we see that for an infinitely sized atomic ensemble all m -modes will contribute. This is essentially the limit considered in the one-dimensional theory [3]. This theory applies to an infinitely wide sample such that all modes experience the same dynamics. For a sample of finite width we see that the oscillating behavior of the Bessel functions J_m gives a cut in the width of the beam scaling with approximately

$r_c/\sigma_\perp \sim 1/\sqrt{\mathcal{F}}$. This cut r_c/σ_\perp will, due to the behavior of the Bessel function J_m , increase as m increases. We thus see that even though the width of the beam is mainly determined by the length of the atomic ensemble, the width of the atomic ensemble plays an important role as a wider ensemble supports higher order modes that are inherently wider, thus in effect a wider atomic ensemble will generate a wider beam. From the expansion Eq. (14.0.4) and the small argument limit of the modified Bessel function Eq. (14.2.2) along with Eq. (14.2.1) we see that as time increases the contributions to the intensity from modes $m \neq 0$ will diminish. In Fig. 14.3 we show a plot of the radiated power in three superradiating modes at time $t = 0$. In Fig. 14.4 we use an atomic ensemble with Fresnel number $\mathcal{F} = 4$, and in Fig. 14.3 we use $\mathcal{F} = 8$. The plot demonstrates how the relative importance between different modes are changed as the Fresnel number is changed. From the two plots in Figs. 14.4 and 14.3 that the larger the Fresnel number, the more modes corresponding to the number m can we fit in the system. In Fig. 14.4 we see a relative maximum of the first order mode $m = 1$ at about 15% of the principal mode $m = 0$, and the second order mode $m = 2$ the maximum is about 3.7% of the principal mode. When the Fresnel number is doubled in Fig. 14.3 these numbers reads for $m = 1$ approximately 20% and $m = 2$ approximately 7.4%. These numbers indicates that for an infinitely sized sample, all modes will contribute. However to conclude such behavior we have to look at the total number of photons in each mode. This is the topic of Sec. 14.3, and from the results derived there we indeed find that we can have relatively more photons in higher order modes as the Fresnel number is increased. E.g for $\mathcal{F} = 8$ the photon power in the $m = 1$ mode relative to the $m = 0$ mode is about 62% whereas for $\mathcal{F} = 4$ this number is reduced to 49%.

Next we consider how the time evolution of the superradiant modes corresponding to different m changes. From the earlier discussion of Eq. (14.2.1) we expect that the relative photon power carried by modes m different from the principal mode $m = 0$ will decrease compared to the principal mode as time is increased. In Figs. 14.6 and 14.5 we plot the radial distribution of the photon power at time $\Gamma t = 1$. We see that the radial shape of the modes have not changed compared with the initial time plots, 14.4 and 14.3, however the relative maximal photon power for modes $m \neq 0$ has decreased compared with the principal mode $m = 0$. Again we can look at the total photon power in each mode, discussed in Sec. 14.3, and find that for the case of Fresnel number $\mathcal{F} = 4$ the mode $m = 1$ now only contains 22% of the intensity carried in the $m = 0$ mode, and the $m = 2$ mode only 4.2%. A similar behavior is found for the $\mathcal{F} = 8$ case, though less pronounced, e.g

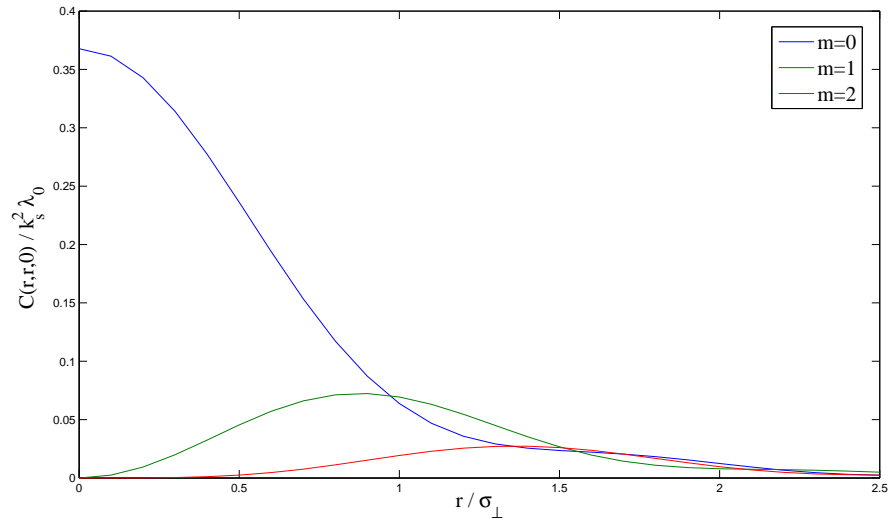


Figure 14.3: Plot of the radiated power for different modes $m = 0, 1, 2$ as a function of the detection coordinate r/σ_{\perp} . The plot is taken at the initial time, $\Gamma t = 0$, and demonstrates how the relative distribution of radiation in different modes m is changed as the Fresnel number \mathcal{F} is varied. In Fig. 14.4) we use $\mathcal{F} = 4$ and here we use $\mathcal{F} = 8$

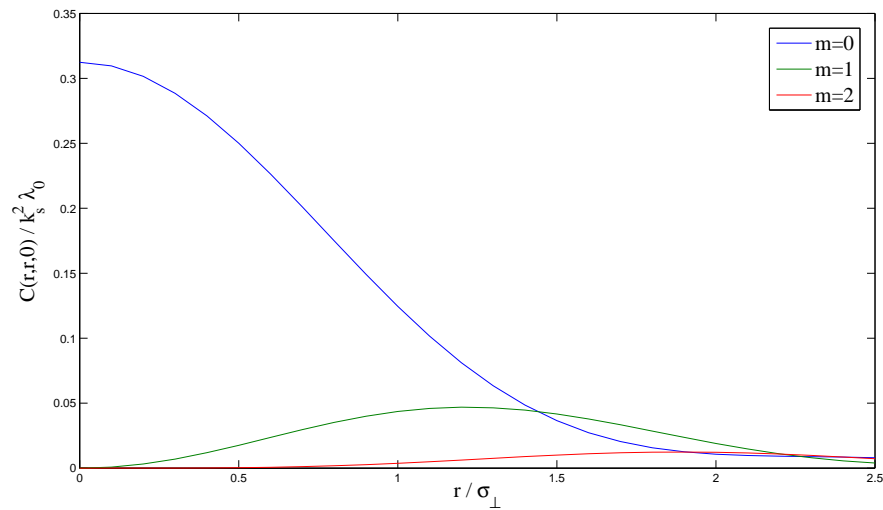


Figure 14.4: Same as Fig. 14.3 but with Fresnel number $\mathcal{F} = 4$

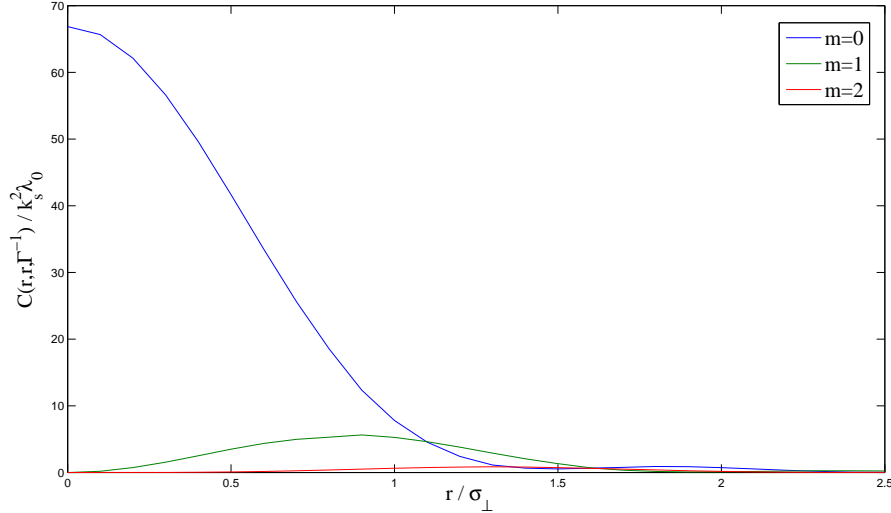
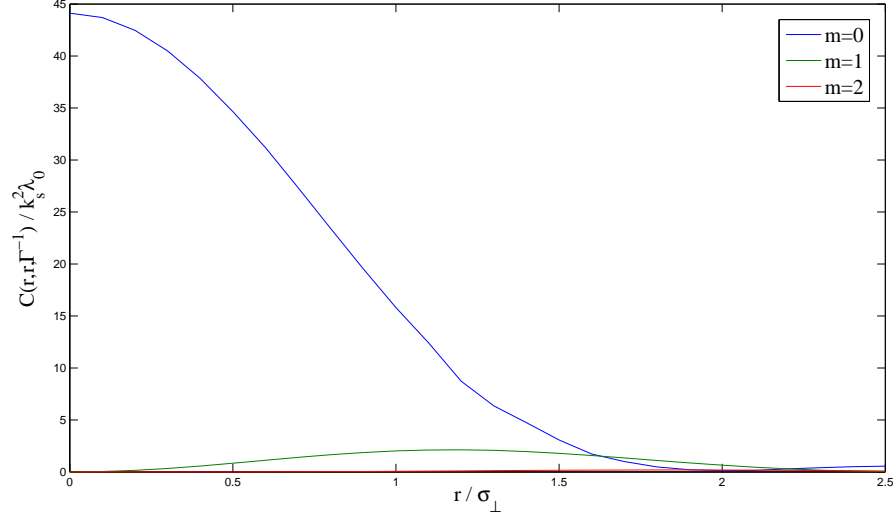


Figure 14.5: Plot of the radiated power for different modes $m = 0, 1, 2$ as a function of the detection coordinate r/σ_{\perp} . Here the plot is made at a time of $\Gamma t = 1$. The plot demonstrate how the relative distribution of radiation in different modes m is changed as the Fresnel number \mathcal{F} is varied. In Fig. 14.4) we use $\mathcal{F} = 4$ and here we use $\mathcal{F} = 8$. When these plots, 14.6 and 14.5 are compared with the initial time plots, Figs. 14.4 and 14.3 we indeed see that as time increases, the evolution of the principal superradiating mode, $m = 0$ is faster than the higher order modes.

the mode now $m = 1$ carries 35% of the photon power compared with the $m = 0$ mode, and the $m = 2$ mode it is 12%. Thus from the plots and the numbers presented here we see the expected behavior of the superradiating modes as time increases.

14.3 Total coherent radiation.

Finally we will examine the behavior of the total intensity of the coherently emitted radiation. We shall in this section not only show the effect of the analytical calculations made so far but also compare the result with an purely numerical treatment of the equations given in Eq. (10.2.10). The total intensity is normalized such that it gives the number of

Figure 14.6: Same as Fig. 14.5, but with Fresnel number $\mathcal{F} = 4$

photons per second coming through the detector-plane.

$$I_T(t) = \frac{2}{k_s \epsilon_0 \hbar} \int \frac{r dr}{k_L^2} \int d\phi \langle \hat{D}_+^{(-)}(z_0, r, \phi, t) \hat{D}_-^{(+)}(z_0, r', \phi, t) \rangle. \quad (14.3.1)$$

To find the total intensity we use the result Eq.(14.0.4) and make the radial integral. To do this we use the relation

$$\int_0^\infty r dr J_m(xr) J_m(x'r) = \frac{\delta(x - x')}{x}, \quad (14.3.2)$$

derived in Appendix B.4. The total radiation is then found to be

$$I_T(t) = \frac{\lambda_0 L e^{-\Gamma t}}{2} \sum_m \sum_{lqk}^{q, q'} \sum_{n, n'} \int_0^{\mathcal{F}} dy \left\{ \left(\frac{-iy}{2\mathcal{F}} \right)^l \left(\frac{iy}{2\mathcal{F}} \right)^l \left(\frac{-i}{\sqrt{8\mathcal{F}}} \right)^q \left(\frac{i}{\sqrt{8\mathcal{F}}} \right)^{q'} (8i\pi\mathcal{F})^n (-8i\pi\mathcal{F})^{n'} \times \right. \\ \left. \chi_{lqkn}^{l'q'k'n'} \frac{(\lambda_0 t L)^{k+k'+q+q'}}{k!k'!(l+2q+k)!(l+2q'+k')!} e^{-\frac{2y}{2+2(k+k')+q+q'+n+n'}} I_m \left(\frac{2y}{2+2(k+k')+q+q'+n+n'} \right) \right\}. \quad (14.3.3)$$

In Fig 14.7 we show a plot of the total radiated power, Eq. (14.3.3) for the parameters $\mathcal{F} = 4$ and $\frac{\lambda_0 L}{\Gamma} = 4$ which correspond to an optical depth of $\rho_0 L = \frac{8}{3\pi} \approx 0.85$. It is interesting to notice that indeed the intensity in modes $m \neq 0$ evolves slower in time than for the mode $m = 0$. This can be seen by looking at the slope of the curves as they are

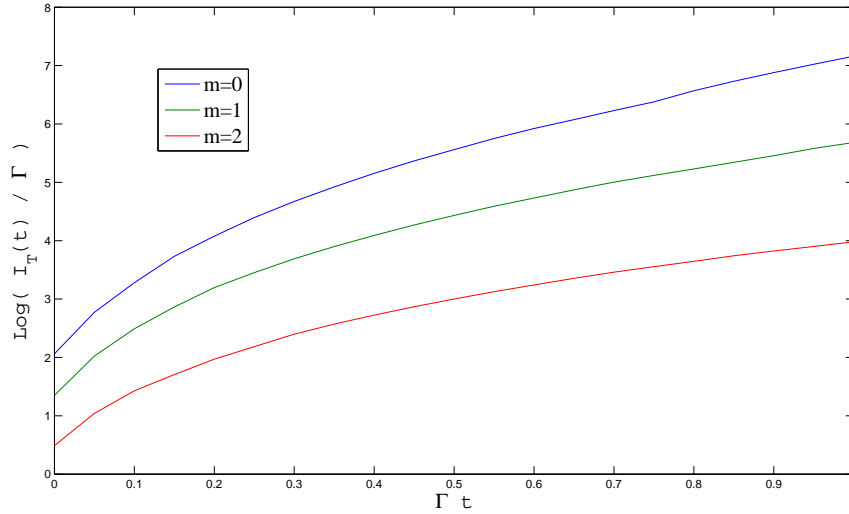


Figure 14.7: Plot of the total radiated power measured in number of photons, $\#N_p$ per decay time, Γt . We use a Fresnel number of $\mathcal{F} = 4$ and show three different m -modes. We see that the principal mode $m = 0$ has a slightly faster growth than higher order modes.

plotted on a logarithmic scale.

We now compare the result for the total radiated power with the effective one-dimensional calculation derived in Ref. [3]. The general assumption in the one-dimensional calculation is that the atomic ensemble is infinitely wide. This assumption makes the problem easy to solve in Fourier space, and when the transverse momentum in the propagator for the light is being neglected, the result for the total radiated power is that all modes corresponding to different transverse momentum gives equal contribution to the total radiated power. Thus the total radiated power measured in units of number of photons per time gives

$$I_T^{RM}(t) = \sum_{\mathbf{k}_\perp} \lambda_0 L e^{-\Gamma t} \left(I_0^2(2\sqrt{\lambda_0 L t}) - I_1^2(2\sqrt{\lambda_0 L t}) \right). \quad (14.3.4)$$

This result holds some complications since there is a priori no upper limit on the transverse momentum, thus taking all modes corresponding to all transverse momentum into account gives an infinite contribution. A derivation of such a mode description can be found in Ref. [52]. It is concluded in Ref. [41] that for a Fresnel number near unity the radiation is dominated by a single transverse mode, and thus the total radiation is finite. We can also make a simplification of our result Eq. (14.3.3) by neglecting all kinds of finite size effects in the eigenvalue matrix, $M_{k'm'n'}^{kmn}$. We know this will be an oversimpli-

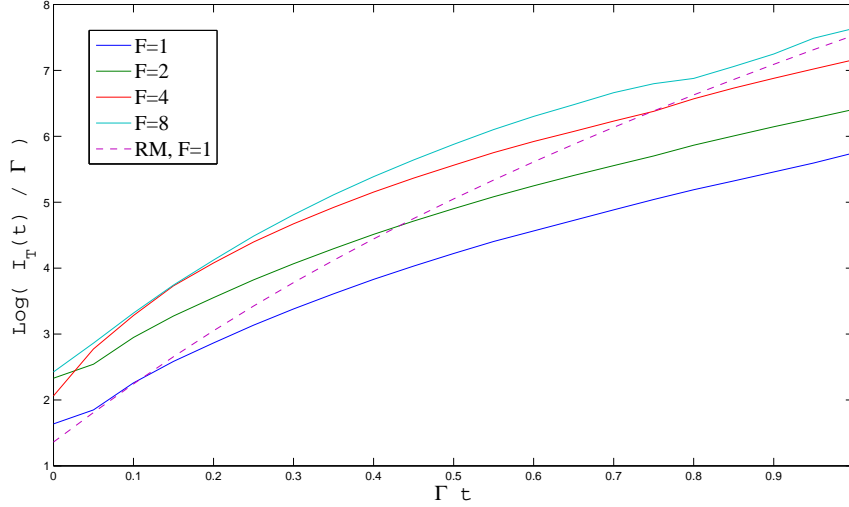


Figure 14.8: Plot of the total radiated power calculated for varying Fresnel numbers. The solid lines are calculated using the expression Eq. (14.3.3) for the principal mode $m = 0$, whereas the dashed line is the Raymer Mostowski result in Eq. (14.3.5). Apart from a complicated behavior initially in time we see that the total radiation for large times is linearly proportional to the Fresnel number. This can also be seen from Eq. (14.3.3).

fication, the approximation however serves well when discussing the results by Raymer and Mostowski in Ref. [3]. We also assume $\mathcal{F} \sim 1$, and use the approximation of the modified Bessel function in Eq. (14.2.2). In this limit we find the total radiated power to give

$$I_T(t) = \lambda_0 L e^{-\Gamma t} (1 - e^{-\frac{\mathcal{F}}{2}}) \left(I_0^2(2\sqrt{\lambda_0 L t}) - I_1^2(2\sqrt{\lambda_0 L t}) \right), \quad (14.3.5)$$

where we made the sum over m . We are thus led to conclude that for a Fresnel number near unity, the simple Raymer Mostowski result correspond to neglecting all spatial corrections to the dynamic of the atoms and also neglecting spatial corrections to the propagation of light out of the atomic ensemble. In Fig. 14.8 we compare the three-dimensional calculation of the total radiated power, Eq. (14.3.3) with the approximation in Eq. (14.3.5). We also analyze how the total radiation depends on the Fresnel number, and as can be seen for large times, the dependence is approximately linear in Fresnel number. This may also be concluded from Eq. (14.3.3). We also see that the Raymer Mostowski result is largely overestimating the time evolution of the total radiated power.

In Fig. 14.9 we analyze how the different corrections to the Raymer Mostowski calculation effects the total radiated power. We use an optical depth at $\rho_0 L = \frac{20}{3\pi}$, and fix

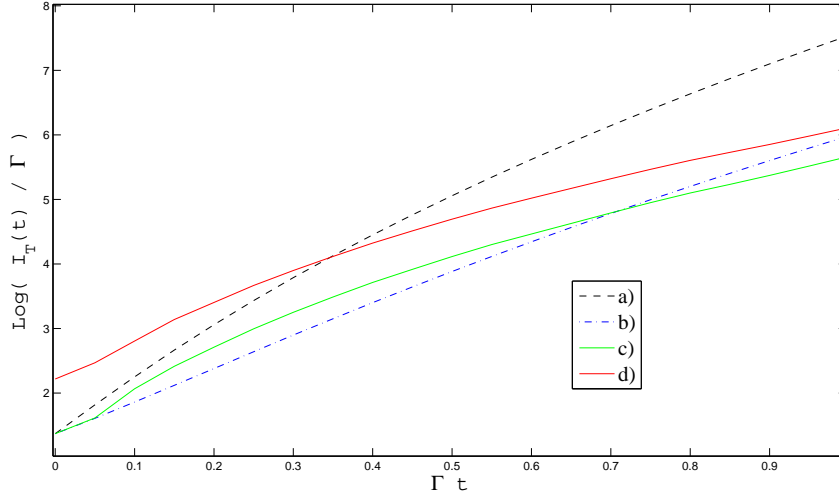


Figure 14.9: Plot of the total radiated power measured in number of photons, per decay time, I_T/Γ . Here we use $\mathcal{F} = 1$. To demonstrate the effects of finite sized atomic ensemble, we show four different plots. a) is the result completely neglecting geometrical effects on the eigenvalue $M_{k'm'n'}^{kmn}$, and the propagator $P^{(+)}$ as in Eq. (14.3.5). In b) we include the correction to the eigenvalue coming from the term $\Lambda_{nn'}^m$. In c) we also include corrections coming from the term $\Lambda_{nn'}^1$, and finally in d) we plot the total radiated power as given in (14.3.3).

the Fresnel number at $\mathcal{F} = 1$, as this is the limit where the Raymer Mostowski result is assumed to be valid. For $\mathcal{F} = 1$ we can also from Eq. (14.2.2) and the connected discussion, approximate the sum over modes m , as done in Eq. (14.3.3). The curve a) is the simple Raymer Mostowski result Eq. (14.3.5). In curve b) we add the lowest order finite size correction to the atomic time evolution described by the matrix $\Lambda_{nn'}^m$. We see that this does not change the initial radiation, however the build-up in time is much slower. In curve c) we add the second order finite size correction to the eigenvalue describing the time evolution of the atomic ensemble given by the matrix $\Lambda_{nn'}^1$. Finally in d) we include corrections coming from the propagator describing the light as it exits the atomic ensemble. These corrections describes the inclusion of modes having finite transverse momentum. We see from the graph that the total radiated power is indeed increased by this inclusion, but also that the correction is more significant for small times than for large times. This has to do with the fact that the most significant build-up of radiation happens along the atomic ensemble, where the transverse momentum is zero, as indicated in Fig. 13.1.

Finally we compare the result of Eq. (14.3.3) with a purely numerical calculation based on the point particle equations Eqs. (10.2.10) and (10.2.11). To make such a

comparison we need to connect the evolution of the atomic operators $\hat{b}_j(t)$ with the total intensity of the radiated field. Based on energy conservation argument, the evolution of the number of atoms in the ground state, is given exclusively by the number of photons exiting a boundary sphere enclosing the atomic ensemble. In Appendix B.5 we show that this is indeed the case, and that the conservation law is

$$\frac{2}{k_s \hbar \epsilon_0} \int d\Omega \mathbf{D}^{(-)}(\mathbf{r}, t) \cdot \mathbf{D}^{(+)}(\mathbf{r}, t) = \sum_{jj'} \left\{ \tilde{M}_{jj'} \hat{b}_j(t) \hat{b}_{j'}^\dagger(t) + H.c. \right\}, \quad (14.3.6)$$

where $\tilde{M}_{jj'}$ is given by $M_{jj'} + \Gamma \delta_{jj'}$, and $M_{jj'}$ is given in Eq. (10.2.6). When comparing the result of Eq. (14.3.3) to the atomic evolution we have to remember that we are only measuring half of the photons, since we only consider the emission at one end of the ensemble. Using that the evolution of the atomic operators are given by

$$\frac{d}{dt} b_j(t) = \sum_{j'} M_{jj'} b_{j'}(t) \quad (14.3.7)$$

the problem of calculating the atomic sum given in Eq. (14.3.6) reduce to finding eigenvalues of the matrix $M_{jj'}$. In Ref. [47] is a discussion of this method, where the implications of dealing with the non-Hermitian matrix $M_{jj'}$ is addressed. Let us denote the set of eigenvalues to the matrix $M_{jj'}$ by λ_n , we find after taking quantum average of the result in Eq. (14.3.6) that

$$\frac{2}{k_s \hbar \epsilon_0} \int d\Omega \langle \hat{D}_+^{(-)}(\mathbf{r}, t) \hat{D}_-^{(+)}(\mathbf{r}, t) \rangle = \sum_n \left\{ (\lambda_n + 1) e^{(\lambda_n + \lambda_n^*)t} + H.c. \right\}. \quad (14.3.8)$$

We then find the total intensity from the point particle model

$$I_T^{pp}(t) = \frac{1}{2} \sum_n \left\{ (\lambda_n + 1) e^{(\lambda_n + \lambda_n^*)t} + H.c. \right\}, \quad (14.3.9)$$

where we normalize with a factor 1/2 since we want to compare the result with the result in Eq. (14.3.3). The advantages of making these calculations, or indeed solving the problem of superradiance on a computer are clear. One avoids the problems of shifting from the point particle model to continuous model, not to mention the complications involving the basis transformations in the continuous case. Also the computer easily describes the total radiated field and not only the strongest super-radiating mode as we

have analyzed here. On the other hand the direct method is numerically heavy for a large number of atoms, and we are limited to $N \sim 3000$ atoms. To understand the behavior at larger number of atoms it is therefore important to have an analytical theory along the lines considered here.

To make the numerical simulation we have randomly distributed 3000 atoms with a distribution function given by Eq. (11.0.2). After that the matrix $M_{jj'}$ is calculated and processed in order to find the total number of Stokes photons Eq. (14.3.9). We can then by making a series of such realizations of the position of the atoms get some statistics on the inherent noise on the point particle model. In Fig. 14.10 we show the result of a numerical calculation using parameters $\sigma_{\perp} = 20$ and $L = \sqrt{2\pi}\sigma_{\parallel} = 100$, these values of ensemble geometry and particle number match a value of $\frac{\lambda_0 L}{\Gamma} = 45/8$, or an optical depth of $\rho_0 L = \frac{15}{4\pi i} \approx 1.19$. That the two methods gives very different results for small times is quite clear since initially the radiation is dominated by the spontaneous emission, which is not included in the analytical calculation. In the curve SR we have plotted the total radiated power where we have estimated the sum over modes m , using the same principles as for the $\mathcal{F} \sim 1$ case. This approximation gets better at increasing times, and should therefore be good when comparing the analytical result with the numerical. In curve RM we show the result in Eq. (14.3.4) for a single transverse mode, $\mathbf{k}_{\perp} = 0$. We show five realizations of the numerical simulation where we vary the number of particles but keep the Fresnel number and optical depth constant. We see that the slope of the analytically calculated curve agrees reasonable well with the numerically calculated curve, however quantitatively we still have a factor of about 7.5 to explain. We also see from the curve, that the conclusion that the superradiance only depend on Fresnel number and optical depth is still an approximation as the numerical calculation indicate, at least in the point particle model, this is not completely true.

We finally note that for the time-scale used here, the approximation of neglecting depletion is not completely justified, as the number of emitted photons exceeds the number of atoms already at the onset of superradiance. For the ongoing superradiance experiments using Bose-Einstein condensed atoms e.g. Ref. [53] the number of atoms used in the process is factors of thousands larger than what we are able to numerically simulate here, and then the approximation is much less severe.

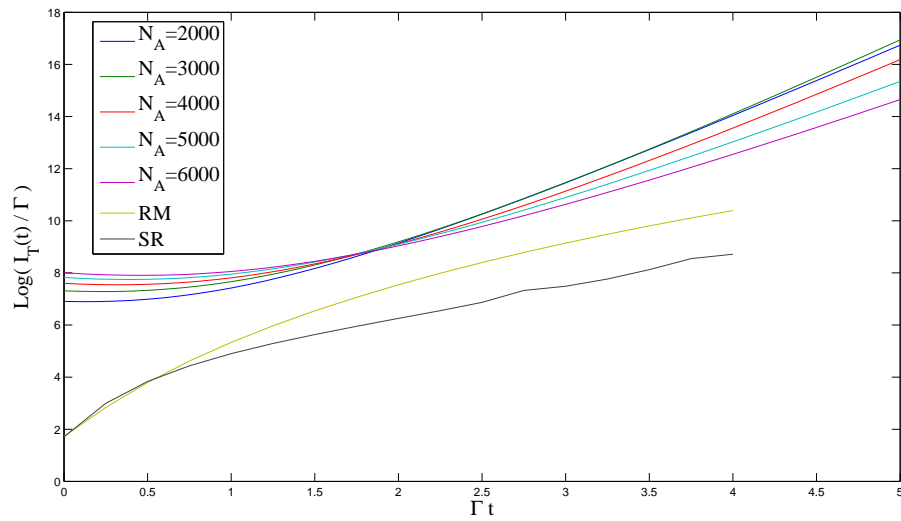


Figure 14.10: Here we compare the analytical result for the total radiated power in the superradiating mode Eq. (14.3.3), graph SR, with the total intensity of a single mode of the Raymer Mostwski result in Eq. (14.3.4), graph RM, and a numerical simulation of the total number of Stokes photons in the point particle model Eq. (14.3.9). To exploit the numerical model we fix the Fresnel number and the optical depth, but vary the number of atoms involved. As the plot shows there seems to be a dependence on the atomic density that are not included in the analytical theory.

Conclusion

In this paper we have developed a three-dimensional theory for superradiance. We have shown that parameters such as transverse momentum naturally arise when developing the theory, and that the properties of superradiant build-up gives a cut-off in the transverse momentum, thus giving a finite theory as it should. In the theory we take into account spatial effects both regarding the dipole-dipole interactions among atoms leading to superradiant radiation, but also the propagation of the light when leaving the atomic ensemble. We derive a correlation function that describes the superradiated light, and find that the only parameter controlling this function is the optical depth $\rho_0 L$ and the Fresnel number \mathcal{F} . From this one can in principle make a mode analysis of the electric field. Here we have considered the intensity of the superradiation. First in Chap. 14.1 we made an estimate of the timescale on which the superradiance begins to dominate the spontaneous emission, and found that increasing the Fresnel number has a positive effect. In Chap. 14.2 we calculated the radial distribution of radiated power in the superradiating modes. We learned that the Fresnel number \mathcal{F} defines how many m -modes that will contribute to the superradiance. For a larger Fresnel number more modes contribute. We also found that as time increases the finite size effects of the eigenvalues (12.0.25) means that the photon power in higher order modes $m \neq 0$ decreases relative to the principal mode $m = 0$. Again this decrease depends on the Fresnel number. In Chap. 14.3 we analyzed the total radiated power in the superradiating modes and found that under certain approximations the one

dimensional result derived in e.g. Ref. [3] agrees with the tree-dimensional calculation presented here for Fresnel number $F \sim 1$. We also showed that when including finite size effects in the eigenvalue Eq. (12.0.25) the one-dimensional calculation overestimates the total superradiated photon power. Finally we made a comparison between our analytical results and a numerical calculation of the total superradiated power. Though we are optimistic about the method used in the analytical calculation, the comparison showed that our analytical calculation only accounts for about 10% of the superradiated power found from the numerical calculation in the point particle model.

Part IV

Qubit protection in nuclear-spin quantum dot memories

*Qubit protection in nuclear-spin
quantum dot memories*

An essential ingredient for quantum computation and long-distance quantum communication is a reliable quantum memory. Nuclear spins in semiconductor nanostructures are excellent candidates for storing quantum information. With a magneton 3 orders of magnitude weaker than electron spins, they are largely decoupled from their environment. They have long intrinsic lifetimes and the hyperfine interaction with electron spins allows one to access ensembles of nuclear spins in a controlled way [54–58]. In particular, the quantum state of an electron spin can be mapped onto the nuclear spins, giving rise to a collective quantum memory [54,55]. Nevertheless, memory lifetimes are limited, e.g., by dipole-dipole interactions among the nuclei. In this Letter we demonstrate that the presence of the electron spin substantially reduces the decoherence of this collective memory. When off-resonant, the hyperfine coupling induces a dynamic Stark shift proportional to the number of excitations in the storage spin-wave mode. This isolates the storage states from the rest of the Hilbert space energetically and protects them against nuclear spin flips and spin diffusion.

Consider a quantum dot charged with a single excess electron as indicated in Fig. 16.1. The electron spin \hat{S} is coupled to the ensemble of underlying nuclear spins \hat{I} by the Fermi

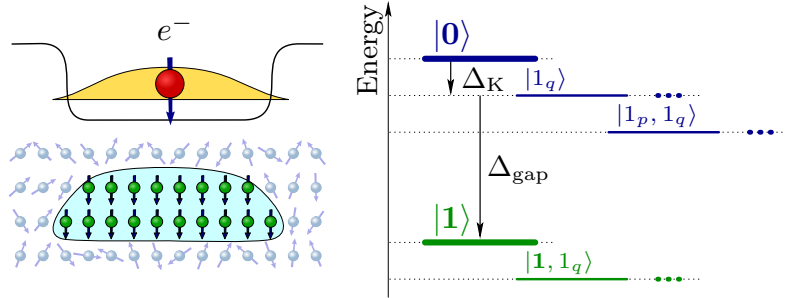


Figure 16.1: *Left*: Charged quantum dot with a single, polarized excess electron. *Right*: Spectrum of the effective nuclear Hamiltonian in the presence of a polarized electron. Off-resonant hyperfine coupling between electron and nuclei results in a gap Δ_{gap} between the storage state $|1\rangle$ and the non-storage states $|1_q\rangle$. Δ_K denotes the Zeeman shift due to the effective magnetic field associated with the electron spin (Knight shift).

contact interaction,

$$\hat{H}_{\text{hf}} = \mathcal{A} \sum_j \varrho_j \left[\hat{I}_z^j \hat{S}_z + \frac{1}{2} (\hat{I}_+^j \hat{S}_- + \hat{I}_-^j \hat{S}_+) \right], \quad (16.0.1)$$

where \mathcal{A} is the average hyperfine interaction constant, $\mathcal{A} \approx 90 \mu\text{eV}$ for GaAs, and ϱ_j is proportional to the electron density at the position of the j th nucleus, $\sum_j \varrho_j = 1$. For convenience, we introduce the collective operators $\hat{\mathbf{A}} \equiv \sum_j \varrho_j \hat{\mathbf{I}}^j$. The first term in Eq. (16.0.1) provides an effective magnetic field $B_z^{\text{OH}} = \mathcal{A} \langle \hat{A}_z \rangle / g^* \mu_B$ for the electron, known as the Overhauser field. The same also produces an energy shift for each nuclei, the so-called Knight shift. The flip-flop terms in Eq. (16.0.1), $\hat{H}_{\text{JC}} = \frac{\mathcal{A}}{2} (\hat{A}_+ \hat{S}_- + \hat{A}_- \hat{S}_+)$, can be used to polarize the nuclear spins [56, 57], and to map the electron's spin state into a collective spin mode of the nuclei [54, 55]. As will be shown here, the same can be used to provide a protective energy gap.

16.1 Fully polarized nuclei.

We start by reconsidering the storage of a qubit in a collective nuclear state [54]. In the simplest case when all the nuclear spins are initially polarized in the $-z$ direction (zero temperature limit), the $|\downarrow\rangle_e$ and $|\uparrow\rangle_e$ spin states of the electron are mapped onto the nuclear

spin states

$$|\mathbf{0}\rangle \equiv |-I, -I, \dots, -I\rangle, \quad (16.1.1)$$

$$|\mathbf{1}\rangle \equiv \frac{\mathcal{A}}{\Omega} \hat{A}_+ |\mathbf{0}\rangle \propto \sum_j \varrho_j |-I, \dots, (-I+1)_j, \dots, -I\rangle, \quad (16.1.2)$$

respectively. \hat{H}_{JC} couples the state $|\mathbf{0}\rangle|\uparrow\rangle_e$ to $|\mathbf{1}\rangle|\downarrow\rangle_e$ with an angular frequency $\Omega = \mathcal{A}(\sum_j \varrho_j^2 2I)^{1/2}$. The detuning between these two states, $\delta = \delta^{\text{el}} + \delta^{\text{OH}}$, comes from the electron's intrinsic energy splitting δ^{el} due to, e.g., an external magnetic field, and from the Zeeman splitting due to the Overhauser field, $\delta^{\text{OH}} = -\mathcal{A}I$. Coherent flip-flops between the electron and nuclear spins can be brought into resonance ($\delta \ll \Omega$) through δ^{el} , e.g., applying a spin-state dependent Stark laser pulse [59]. Then $|\mathbf{0}\rangle(\alpha|\downarrow\rangle_e + \beta|\uparrow\rangle_e)$ can be rotated to $(\alpha|\mathbf{0}\rangle + \beta|\mathbf{1}\rangle)|\downarrow\rangle_e$, and the quantum information can be transferred from the electron to the nuclear spin ensemble and back [54, 55].

Assume that, after the qubit has been written into the nuclei, the polarized electron is not removed from the quantum dot but the hyperfine flip-flops are tuned to be off-resonant ($\delta \gg \Omega$). Now real transitions can no longer take place between $|\mathbf{1}\rangle|\downarrow\rangle_e$ and $|\mathbf{0}\rangle|\uparrow\rangle_e$. However, the residual virtual transitions repel the two states from each other, in analogy to the dynamic Stark effect. As a result, after eliminating the electron, the energy of state $|\mathbf{1}\rangle$ gets shifted by $\Delta_{\text{gap}} = -\Omega^2/4\delta$. The other, orthogonal states also having exactly one spin flipped (denoted by $|1_q\rangle$ in Fig. 16.1) are “subradiant”, i.e., are not coupled via \hat{H}_{JC} to the electron. Therefore, they are unaffected by the Stark shift. This is the origin of the energy gap.

To understand the protection scheme, let us introduce *nuclear spin waves*. As long as the nuclei remain highly polarized, one can introduce bosonic operators through the Holstein-Primakoff transformation: $\hat{a}_j \approx \hat{I}_-^j / \sqrt{2I}$, $\hat{a}_j^\dagger \approx \hat{I}_+^j / \sqrt{2I}$, and $\hat{a}_j^\dagger \hat{a}_j = \hat{I}_z^j + I$. This allows us to define the bosonic spin wave modes

$$\hat{\Phi}_q \equiv \sum_j \eta_{qj} \hat{a}_j, \quad \hat{\Phi}_q^\dagger \equiv \sum_j \eta_{qj}^* \hat{a}_j^\dagger, \quad (16.1.3)$$

where the unitary matrix η_{qj} describes the mode functions of the spin waves. We identify the storage mode $q = 0$ as the one given by $\eta_{0j} = \sqrt{2I} \frac{\mathcal{A}}{\Omega} \varrho_j$, and write $|\mathbf{1}\rangle = \hat{\Phi}_0^\dagger |\mathbf{0}\rangle$. This is the mode which is directly coupled to the electron spin. In fact, $\hat{H}_{\text{JC}} \approx \frac{\Omega}{2} (\hat{\Phi}_0^\dagger \hat{S}_- + \hat{\Phi}_0 \hat{S}_+)$ is a Jaynes-Cummings coupling in the bosonic approximation. After eliminating the electron,

\hat{H}_{JC} reduces to $\hat{H}_{\text{gap}} = -\frac{\mathcal{A}^2}{4\delta}\hat{A}_+\hat{A}_- \approx \Delta_{\text{gap}}\hat{\Phi}_0^\dagger\hat{\Phi}_0$. As shown in Fig. 16.1, \hat{H}_{gap} lifts the degeneracy between states of different number of storage-mode excitations. This is the key feature of our protection scheme: Any decoherence process that is associated with a transition from the storage mode $\hat{\Phi}_0$ to any other mode $\hat{\Phi}_q$ now has to bridge an energy difference. If this energy gap is larger than the spectral width of the noise, the effect of the noise on the stored qubit is substantially reduced.

A more detailed analysis shows that the off-resonant interaction with the electron spin—which itself is coupled, e.g., to phonons—leads in general also to an additional decoherence mechanism for the nuclear spins. If the corresponding electron spin dephasing rate γ is small compared to the electron's precession frequency δ , the decay rate for the storage mode is reduced by the low probability of exciting the electron spin state: $\gamma\Omega^2/\delta^2 \ll \gamma$.

In addition to the gap, the electron is also responsible for the Knight shift $\hat{H}_{\text{K}} = \mathcal{A}\hat{A}_z\langle\hat{S}_z\rangle$. The difference of the Knight shifts for the $|\mathbf{0}\rangle$ and $|\mathbf{1}\rangle$ states, $\Delta_{\text{K}} = -\frac{\mathcal{A}}{2}\sum_j\varrho_j^3/\sum_j\varrho_j^2$, is typically much less than Δ_{gap} . When the hyperfine coupling is *inhomogeneous*, however, $|\mathbf{1}\rangle$ fails to be eigenstate of the Knight shift Hamiltonian: $\hat{H}_{\text{K}}|\mathbf{1}\rangle = (-\frac{1}{2}\delta^{\text{OH}} + \Delta_{\text{K}})|\mathbf{1}\rangle + \zeta|1^\perp\rangle$, where the state $|1^\perp\rangle$ is orthonormal to $|\mathbf{1}\rangle$ and the coupling parameter $\zeta^2 = \frac{\mathcal{A}^2}{4}\sum_j\varrho_j^4/\sum_j\varrho_j^2 - \Delta_{\text{K}}^2$ is directly related to the measure of inhomogeneities. As a consequence, the storage mode is only an approximate eigenmode, and it gets gradually mixed with non-storage modes as time passes. This causes loss of the stored qubit. $|1^\perp\rangle$ is, however, off-resonant due to the energy gap, and our calculations show that the corresponding probability of finding the system in state $|1^\perp\rangle$ is always bounded by $4\zeta^2/\Delta_{\text{gap}}^2$, so the detrimental effect of the inhomogeneous Knight shift is suppressed by the energy gap. In addition, since the admixture of $|1^\perp\rangle$ is a coherent process, it can be cancelled by refocusing methods.

A large gap can be achieved by bringing the hyperfine interaction close to resonance. For example, a non-zero external magnetic field or laser induced level shifts [59] can partially cancel the Overhauser field, such that $\delta \ll \delta_{\text{el}} \approx -\delta_{\text{OH}} = \mathcal{A}I$. (Of course, δ should be kept sufficiently large so that the hyperfine coupling remains off-resonant). The requirement of separation of time scales implies $\zeta \ll |\Delta_{\text{gap}}| \ll \Omega \ll |\delta|$. It means that the detuning should be $\delta \gtrsim 10\Omega$. To estimate the orders of magnitude of the different energies, we take an oblate Gaussian electron density of ratio (1, 1, 1/3), and we consider spin- $\frac{1}{2}$ nuclei. Then it is easy to see that Δ_{K} and ζ are inversely proportional to the number

of nuclei N , whereas $\Omega, \Delta_{\text{gap}} \propto N^{-1/2}$ only (Fig. 16.2a).

16.2 Decoherence suppression.

To analyze the decoherence suppression, we first consider a noise model where the nuclear spins are coupled to fluctuating classical fields. The corresponding interaction Hamiltonian is given by $\hat{V} = \sum_j \mathbf{B}^j \cdot \hat{\mathbf{I}}^j$. We assume isotropic Gaussian random noise with zero mean value and correlator

$$\overline{B_\mu^j(t) B_\nu^k(t')} = \delta_{\mu\nu} f_{jk} C e^{-\Gamma|t-t'|} \quad (16.2.1)$$

for $\mu, \nu = x, y, z$, where f_{jk} specifies the spatial correlations of the noise acting on different nuclei. For simplicity, the noise spectrum is assumed to be Lorentzian with a width Γ , although similar results hold for other spectra with a high-frequency cut-off.

Let us first discuss the *dephasing part*, $\hat{V}_z = \sum_j B_z^j \hat{I}_z^j$, of the noise. Using the bosonic spin-wave operators introduced in Eq. (16.1.3) we can express it as

$$\hat{V}_z = \sum_j B_z^j \hat{a}_j^\dagger \hat{a}_j = \sum_{pq} \left(\sum_j B_z^j \eta_{pj}^* \eta_{qj} \right) \hat{\Phi}_p^\dagger \hat{\Phi}_q. \quad (16.2.2)$$

As apparent from Eq. (16.2.2), dephasing of individual nuclear spins means transfer of excitations between different spin-wave modes. Especially, it leads to both real and virtual transitions from $|\mathbf{1}\rangle$ to a non-storage state $|1_q\rangle$ (with $q \neq 0$). As the latter state is “subradiant” and, thus, equivalent to $|\mathbf{0}\rangle$ when the memory is read out, this process essentially results in damping (for real transitions) and dephasing (for virtual transitions) of the stored logical qubit [60]. This can be seen using the Markov approximation by formally eliminating the classical fields and deriving a master equation for the density operator of the nuclear spins, then tracing out all non-storage modes. For that, we assume that the quantum memory operates in the zero temperature limit and all non-storage modes $\hat{\Phi}_{q \neq 0}$ are in the vacuum state. This results in

$$\frac{d}{dt} \hat{\rho} = i[\hat{\rho}, E_z \hat{\Phi}_0^\dagger \hat{\Phi}_0] + \mathcal{L}_z(\hat{\rho}), \quad (16.2.3)$$

with energy shift $E_z = (1 - F)C\Delta_{\text{gap}}/(\Gamma^2 + \Delta_{\text{gap}}^2)$ and Lindbladian

$$\begin{aligned} \mathcal{L}_z(\hat{\rho}) = & \gamma_1(2\hat{\Phi}_0\hat{\rho}\hat{\Phi}_0^\dagger - \hat{\Phi}_0^\dagger\hat{\Phi}_0\hat{\rho} - \hat{\rho}\hat{\Phi}_0^\dagger\hat{\Phi}_0) \\ & + \gamma_2(2\hat{\Phi}_0^\dagger\hat{\Phi}_0\hat{\rho}\hat{\Phi}_0^\dagger\hat{\Phi}_0 - \hat{\Phi}_0^\dagger\hat{\Phi}_0\hat{\Phi}_0^\dagger\hat{\Phi}_0\hat{\rho} - \hat{\rho}\hat{\Phi}_0^\dagger\hat{\Phi}_0\hat{\Phi}_0^\dagger\hat{\Phi}_0). \end{aligned} \quad (16.2.4)$$

Here, γ_1 is the damping rate of the stored qubit while γ_2 describes its dephasing. The two rates are given by

$$\gamma_1 = \frac{C\Gamma}{\Gamma^2 + \Delta_{\text{gap}}^2}(1 - F), \quad \gamma_2 = \frac{C}{\Gamma}F, \quad (16.2.5)$$

where we have introduced the dimensionless parameter $F \equiv \sum_{jk} f_{jk} \varrho_j^2 \varrho_k^2 / (\sum_l \varrho_l^2)^2$ containing the spatial part of the noise correlator.

When the correlation length of the classical noise is smaller than the distance between the nuclei (local uncorrelated noise, $f_{jk} \sim \delta_{jk}$), F scales inversely with the number of nuclei (Fig. 16.3). In this case, the dephasing rate γ_2 vanishes as $1/N$, which is an effect of the collective nature of the storage states [60, 61]. The storage of a qubit corresponds to an encoding of the logical state in a large, delocalized ensemble of N physical spins. As the decoherence has strongly local character, there is only a very small effect on the dephasing of the qubit. The second observation is that the loss of the stored qubit is due to transitions among states with different number of excitations in the storage mode. These transitions are strongly suppressed and the damping rate γ_1 is decreased if Δ_{gap} is large compared to the width of the noise spectrum Γ (or the corresponding cut-off frequency). Finally, we note that the opposite limit of infinite spatial correlation length ($f_{jk} = 1$) corresponds to a homogeneous random field resulting, e.g., from a global external source. In that case, $F \approx 1$ (see Fig. 16.3) and there is obviously no protection against dephasing.

Following a similar but slightly more involved procedure we can discuss the *spin-flip part* $\hat{V}_{xy} = \frac{1}{2} \sum_j (B_+^j \hat{I}_-^j + B_-^j \hat{I}_+^j)$ of the noise. When deriving a master equation for this case, we need to keep higher order terms in the Holstein-Primakoff approximation: in the next order $\hat{I}_-^j \approx \sqrt{2I}(1 - \lambda \hat{a}_j^\dagger \hat{a}_j) \hat{a}_j$ (and similarly for \hat{I}_+^j) with $\lambda = 1 - (1 - 1/2I)^{1/2}$. Here we have neglected the probability of double or more excitations on the same site j , which is reasonable in the high polarization ($T = 0$) limit and exact for spin- $\frac{1}{2}$ nuclei. Omitting the energy shifts, the Lindbladian describing decoherences due to spin flips reads, in leading

order of $1/N$,

$$\begin{aligned} \mathcal{L}_{xy}(\hat{\rho}) = & (\gamma_3 + \gamma_4)(2\hat{\Phi}_0\hat{\rho}\hat{\Phi}_0^\dagger - \hat{\Phi}_0^\dagger\hat{\Phi}_0\hat{\rho} - \hat{\rho}\hat{\Phi}_0^\dagger\hat{\Phi}_0) \\ & + \gamma_5(2\hat{\Phi}_0^\dagger\hat{\Phi}_0\hat{\rho}\hat{\Phi}_0^\dagger\hat{\Phi}_0 - \hat{\Phi}_0^\dagger\hat{\Phi}_0\hat{\Phi}_0^\dagger\hat{\Phi}_0\hat{\rho} - \hat{\rho}\hat{\Phi}_0^\dagger\hat{\Phi}_0\hat{\Phi}_0^\dagger\hat{\Phi}_0) \\ & + \gamma_3(2\hat{\Phi}_0^\dagger\hat{\rho}\hat{\Phi}_0 - \hat{\Phi}_0\hat{\Phi}_0^\dagger\hat{\rho} - \hat{\rho}\hat{\Phi}_0\hat{\Phi}_0^\dagger), \end{aligned} \quad (16.2.6)$$

which describes decay with rate γ_4 , dephasing with rate γ_5 , and additionally thermalization (relaxation to the identity matrix) with rate γ_3 . The rates read

$$\gamma_3 = \frac{C\Gamma I\tilde{F}}{\Gamma^2 + (\Delta_{\text{gap}} + \Delta_{\text{K}})^2}, \quad \gamma_4 = \frac{2C\Gamma I\lambda^2}{\Gamma^2 + (\Delta_{\text{gap}} - \Delta_{\text{K}})^2}, \quad \gamma_5 = \frac{4C\Gamma I\lambda^2}{\Gamma^2 + \Delta_{\text{K}}^2} \frac{\sum_j \varrho_j^4}{(\sum_j \varrho_j^2)^2}. \quad (16.2.7)$$

In the limit of vanishing spatial correlations of the spin-flip noise, $\tilde{F} \equiv \sum_{jk} f_{jk} \varrho_j \varrho_k / \sum_l \varrho_l^2$ tends to 1 (Fig. 16.3) and we have protection against thermalization (γ_3) because of the separation of the logical qubit states $|\mathbf{0}\rangle$ and $|\mathbf{1}\rangle$ by an energy difference of $\Delta_{\text{gap}} + \Delta_{\text{K}}$. The decay corresponding to γ_4 is due to spin-flip induced transitions between $|\mathbf{1}\rangle$ and $|1_p, 1_q\rangle$ (the latter containing a total of two excitations but none in the storage mode), and the energy to bridge is in the order of $\Delta_{\text{gap}} - \Delta_{\text{K}}$ (see Fig. 16.1). Finally, the last factor in the dephasing rate γ_5 scales as $1/N$, indicating that it is the collective nature of the storage that leads to protection. Note that the nonlinearity of the Holstein-Primakoff representation is responsible for the appearance of the dephasing: the virtual non-storage excitations are interacting with the storage mode.

Another potential source of decoherence is *nuclear spin diffusion* due to dipole-dipole interaction between nuclear spins [62]. The energy gap gives protection against this effect, too. The dipolar interaction between the pairs of spins is described in secular approximation by

$$\hat{H}_D = \sum_{j \neq k} B_{jk} (\hat{I}_+^j \hat{I}_-^k - 2\hat{I}_z^j \hat{I}_z^k) \approx 2I \sum_{j \neq k} B_{jk} \hat{a}_j^\dagger \hat{a}_k, \quad (16.2.8)$$

where $B_{jk} = \frac{1}{4}\gamma^2(3\cos^2\theta_{jk}-1)/r_{jk}^3$, γ is the gyromagnetic factor, $\mathbf{r}_{jk} = \mathbf{r}_j - \mathbf{r}_k$ is the distance between two nuclei, θ_{jk} is the zenith angle of the vector \mathbf{r}_{jk} , and we used the first order Holstein-Primakoff approximation. The dipolar Hamiltonian (16.2.8) preserves the total number of excitations and it is responsible for damping of the qubit via transitions from the storage state $|\mathbf{1}\rangle$ to non-storage states $|1_q\rangle$. Indeed, in terms of the bosonic spin wave

mode operators (16.1.3), one can write $\hat{H}_D = \sum_{pq} \tilde{B}_{pq} \hat{\Phi}_p^\dagger \hat{\Phi}_q$, with $\tilde{B}_{pq} = \sum_{j \neq k} B_{jk} \eta_{pj}^* \eta_{qk}$. Now in the interaction picture, the storage mode creation and annihilation operators ($\hat{\Phi}_0^\dagger$ and $\hat{\Phi}_0$) rotate fast with respect to the other ones due to the energy gap. Therefore, the coupling between storage and non-storage modes averages out and disappears in first order of the dipolar perturbation. In second order and on time scales between the storage and non-storage mode dynamics ($\Delta_{\text{gap}}^{-1} \ll T \ll \Delta_K^{-1}$), we find a shift $E_D = \tilde{B}_{00} + \Delta_{\text{gap}}^{-1} \sum_{q \neq 0} |\tilde{B}_{0q}|^2$ of the storage mode energy. The strength of the remaining coupling between the storage mode and mode q is only proportional to $\Delta_{\text{gap}}^{-1} \sum_{r \neq 0} \tilde{B}_{0r} \tilde{B}_{rq}$.

16.3 Non-perfect spin polarization.

Finally, we investigate the consequences of non-perfect nuclear spin polarization. It has been shown that partially polarized nuclei (at finite temperature) can also be used for storing a qubit state [55]. Instead of the fully polarized state (16.1.1), the initial preparation drives the nuclear ensemble into a statistical mixture of dark states $|\mathcal{D}_{n,\beta}\rangle$ defined by $\hat{A}_- |\mathcal{D}_{n,\beta}\rangle = 0$. These dark states can be characterized by the total number of spins flipped n and the permutation group quantum number β . As the detuning δ is adiabatically swept from far negative to far positive, a superposition of the $|\downarrow\rangle_e$ and $|\uparrow\rangle_e$ electron spin states is mapped into the mixture of superpositions of the nuclear spin states $|\mathcal{D}_{n,\beta}\rangle$ and $|\mathcal{E}_{n,\beta}\rangle \equiv \frac{\mathcal{A}}{\Omega_n} \hat{A}_+ |\mathcal{D}_{n,\beta}\rangle$, and the qubit state is efficiently written into the memory [55].

When the electron is left in the quantum dot, it feels different Overhauser fields for different dark states, hence the detuning should be adjusted such that $\overline{\delta_n^{\text{OH}} + \delta^{\text{el}}} \gg \text{Var}(\delta_n^{\text{OH}})$. Moreover, the hyperfine Rabi frequency also varies with n and the energy gap $\Delta_{\text{gap},n}$ is not the same for all the dark states. This inhomogeneous broadening would result in dephasing of the qubit, but can be avoided by the symmetric spin echo sequence prescribed in Ref. [55].

To describe inhomogeneous effects in the case of non-perfect polarization, first we note that the storage state $|\mathcal{D}_{n,\beta}\rangle$ is no longer an eigenstate of the Knight shift operator, but it is partially mapped into an orthogonal state: $\hat{H}_K |\mathcal{D}_{n,\beta}\rangle = -\frac{1}{2} \delta_n^{\text{OH}} |\mathcal{D}_{n,\beta}\rangle + \omega_n |\mathcal{D}_{n,\beta}^\perp\rangle$. This is due to the fact that the inhomogeneous $\hat{A}_{z,\pm}$ operators do not follow the angular momentum commutation relation. Furthermore, $|\mathcal{E}_{n,\beta}\rangle$ is neither an eigenstate of \hat{H}_{gap} nor of \hat{H}_K : $\hat{H}_K |\mathcal{E}_{n,\beta}\rangle = (-\frac{1}{2} \delta_n^{\text{OH}} + \Delta_{K,n} + \Delta_{\text{gap},n}) |\mathcal{E}_{n,\beta}\rangle + \zeta_n |\mathcal{E}_{n,\beta}^\perp\rangle$. The parameters can be expressed

as expectation values in $|\mathcal{D}_{n,\beta}\rangle$:

$$\begin{aligned}
\Omega_n^2 &= \mathcal{A}^2 \langle \hat{A}_- \hat{A}_+ \rangle, & \omega_n^2 &= \mathcal{A}^2 \langle \hat{A}_z^2 \rangle - \langle \hat{A}_z \rangle^2, \\
\Delta_{\text{gap},n} &= \mathcal{A}^4 \langle \hat{A}_- \hat{A}_+ \hat{A}_- \hat{A}_+ \rangle / 4\delta_n \Omega_n^2, \\
\Delta_{\text{K},n} &= \frac{\mathcal{A}}{2} \langle \hat{A}_z \rangle - \mathcal{A}^3 \langle \hat{A}_- \hat{A}_z \hat{A}_+ \rangle / 2\Omega_n^2, \\
\zeta^2 &= \langle \mathcal{E}_{n,\beta} | \hat{H}^2 | \mathcal{E}_{n,\beta} \rangle - \langle \mathcal{E}_{n,\beta} | \hat{H} | \mathcal{E}_{n,\beta} \rangle^2.
\end{aligned} \tag{16.3.1}$$

The explicit form of the inhomogeneous dark states [55] allows us to estimate these values. The results are shown in Fig. 16.2b.

In summary, we have demonstrated that it is possible to suppress the influence of spin-dephasing and spin-flips on a quantum memory consisting of a delocalized ensemble of nuclear spins in a quantum dot if the noise has a highly local character and the spectral width or cut-off frequency of the noise spectrum is small compared to the energy gap. We have shown in particular that the memory can be protected against nuclear spin diffusion mediated by dipole-dipole interaction. We have also analyzed the effects of inhomogeneous hyperfine couplings and imperfect initial nuclear spin polarization.

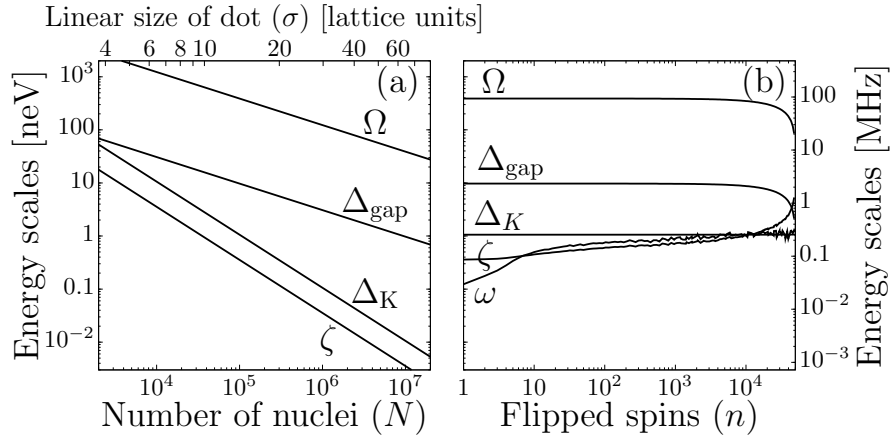


Figure 16.2: Hyperfine Rabi frequency (Ω), protective energy gap (Δ_{gap}), Knight shift difference between the logical states (Δ_K), and symmetry breaking couplings (ζ and ω) due to inhomogeneities. (a) The fully polarized (zero temperature) case is displayed as function of the number of spin- $\frac{1}{2}$ nuclei (N) taking part in the storage, i.e., located within 3σ away from the center of the oblate Gaussian electron density distribution with in-plane variance σ . (b) Estimated energies in dark states $|\mathcal{D}_{n,\beta}\rangle$ with n spins flipped from the fully polarized state for $N = 10^5$. The energy units are obtained in both plots by taking the average hyperfine constant of GaAs, $\mathcal{A} = 90 \mu\text{eV}$.

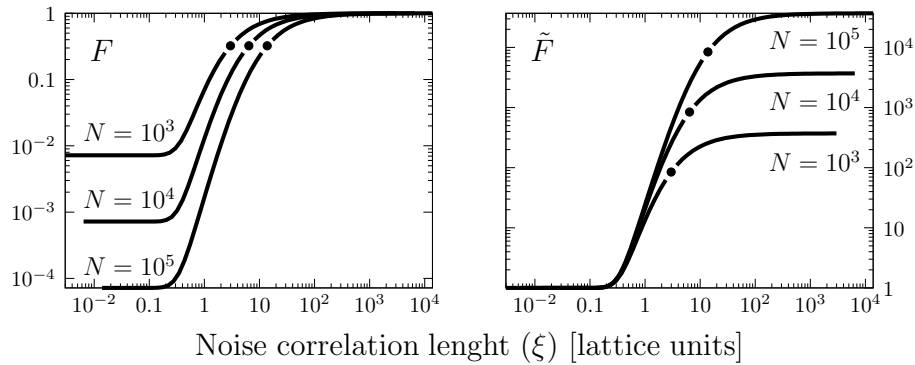


Figure 16.3: The parameters F and \tilde{F} describing the effects of spatial correlations in the classical noise ($f_{jk} = e^{-r_{jk}/\xi}$) for different number of nuclei. The same family of Gaussian electron densities was used as in Fig. 16.2. The bullets on the curves denote the linear size of the dot given by the variance σ .

Part V

Conclusions

Conclusions

Here we summarize the main results presented in the thesis.

In Part Two we investigated the approximations often used in quantum optics where the transverse nature of the interacting light is completely ignored. We did that by developing a full three-dimensional theory describing the interaction between light and an ensemble of atoms. We showed how to separate the problem into an average effect and an effect arising from the atoms being point particles, and showed how spontaneous emission from the atoms naturally appear as an effect caused by the fluctuations in the random position of the atoms. The main feature of the theory is that we only make a perturbative expansion of the system dynamics in the fluctuations of the interaction Hamiltonian. The theory therefore has a much wider range of applicability. The conclusions drawn concerning the validity of the one-dimensional theories are that the system of light and atoms has to apply to the paraxial approximation, and in particular for the interaction considered here, that the Fresnel number describing the geometry of the atomic ensemble has to be much larger than one. The main purpose however of the work presented in part two, was to derive a full and consistent three-dimensional description of light-matter interactions.

In Part Three we turned to the problem of superradiance. Our main focus was to develop a theory that could describe in detail the spatial distribution of superradiation, depending on parameters such as the optical depth and the Fresnel number. The system

in consideration was cylindrically symmetric, and we showed that a natural description of the dynamics of the electric field involved the decomposition in transverse momentum. We then argued that the conditions for superradiance naturally sets a cut in the allowed transverse momenta. This way we developed a consistent theory that gives finite results. One of the motivations for developing the theory was, similarly to Part two, to understand in what limit the simple one-dimensional description derived by Raymer and Mostowski will agree with a true three-dimensional theory. We showed that here the requirement is that the Fresnel number must be of order unity. In the derivation of the one-dimensional theory it is assumed that the atomic ensemble, or the gain medium, is cylindrically symmetric and has a transverse area of infinite size. When this assumption is relaxed, we showed that the one-dimensional model over-estimates the total superradiance. Finally we compared the analytical result for the total superradiated power with the total superradiated power that can be found from a numerical calculation of the point particle mode. Here we found that the analytical result did not agree very convincingly. In fact we showed that the numerical calculation seems to have an unexplained behavior depending on the number of atoms. We thus had to conclude that we are able to explain the connection between the three-dimensional theory and the one-dimensional theory, but we can not yet explain the numerical results for superradiance in detail.

In Part Four we look at the problem of storing information from an electron spin, in an ensemble of nuclear spins. The idea was that distribution the information stored in one spin particle among an ensemble of spin particles makes the stored information more robust against individual spin flips and other decoherence processes. In the work we show that this way of distributing the information in a de-localized ensemble of atomic spins suppresses the influence of spin-dephasing and spin-flips, if the noise has a local character. We also show that the noise coming from dipole-dipole interactions are suppressed. In addition the effect of inhomogeneous coupling between electron spin and nuclei was analyzed, as also the effect of imperfect nuclear spin polarization.

Appendix for Part 1

A.1 Adiabatic elimination

In this appendix we derive an effective Hamiltonian involving only the atomic ground state. The Hamiltonian (3.1.1) can be expanded on the complete set of states describing the atom. Let such a set be comprised of a set of excited states $\{|e_j\rangle\}$ and a set of ground states $\{|g_i\rangle\}$ so that the Hamiltonian reads

$$\mathcal{H} = \sum_j (\omega_j + \omega_0) |e_j\rangle\langle e_j| + \sum_i \omega_0 |g_i\rangle\langle g_i| + \mathcal{H}_{\text{int}}. \quad (\text{A.1.1})$$

For convenience we have here set $\hbar = 1$ and only consider a single atom. The set of ground states are assumed to have the same energy, ω_0 and ω_j is the transition frequency from the ground state to the excited state $|e_j\rangle$. The interaction Hamiltonian is given in Eq. (3.1.3), and when expanded on the set of internal atomic states it reads

$$\mathcal{H}_{\text{int}} = -\frac{1}{\epsilon_0} \sum_{ij} \hat{\mathbf{D}}^{(-)}(t) \cdot \langle g_i | \hat{\mathbf{P}} | e_j \rangle |g_i\rangle\langle e_j| + \langle e_j | \hat{\mathbf{P}} | g_i \rangle |e_j\rangle\langle g_i| \cdot \hat{\mathbf{D}}^{(+)}(t), \quad (\text{A.1.2})$$

where we have used the rotating wave approximation as well as the fact that the matrix elements $\langle e_j | \hat{\mathbf{P}} | e_{j'} \rangle$ and $\langle g_i | \hat{\mathbf{P}} | g_{i'} \rangle$ vanish. To shorten the notation we suppress the spatial

dependence. We will use that the displaced electric field primarily oscillate at the laser frequency, and change to the interaction picture

$$\hat{\mathbf{D}}^{(-)}(t) \propto e^{i\omega_L t}. \quad (\text{A.1.3})$$

Using Heisenberg's equations of motion we may derive an equation of motion for $|g_i\rangle\langle e_j|$

$$\frac{d}{dt}|g_i\rangle\langle e_j| = -i\Delta_j|g_i\rangle\langle e_j| - \frac{i}{\epsilon_0} \sum_{j'} \left\{ \langle e_j|\hat{\mathbf{P}}|g_i\rangle|e_{j'}\rangle\langle e_j| - \langle e_j|\hat{\mathbf{P}}|g_{j'}\rangle|g_i\rangle\langle g_{j'}| \right\} \cdot \tilde{\mathbf{D}}^{(+)}(t), \quad (\text{A.1.4})$$

where $\tilde{\mathbf{D}}^{(\pm)}$ is slowly varying. In the limit of weak driving we may set $\frac{d}{dt}|g_i\rangle\langle e_j| = 0$, and obtain an approximate solution

$$|g_i\rangle\langle e_j| \approx \frac{1}{\epsilon_0\Delta_j} \sum_{j'} \langle e_j|\hat{\mathbf{P}}|g_{j'}\rangle|g_i\rangle\langle g_{j'}| \cdot \hat{\mathbf{D}}^{(+)}(t), \quad (\text{A.1.5})$$

where we have neglected the excited state population. The atomic part of the Hamiltonian can be written

$$\mathcal{H}_0 = \sum_j \Delta_j|e_j\rangle\langle g_0|g_0\rangle\langle e_j| + \sum_i \omega_L|g_i\rangle\langle g_i| + \sum_{ij} (\omega_0 - \omega_L)|e_j\rangle\langle e_j| + |g_i\rangle\langle g_i|, \quad (\text{A.1.6})$$

where $|g_0\rangle$ is any ground state. By inserting expression (A.1.5) and the Hermitian conjugate into Eq. (A.1.2) and (A.1.6) we find the simple result

$$\mathcal{H} = -\frac{1}{\epsilon_0} \left(\hat{\mathbf{D}}^{(-)}(t) \cdot \sum_{jii'} \frac{1}{\epsilon_0\Delta_j} \langle g_i|\hat{\mathbf{P}}|e_j\rangle \right) |g_i\rangle\langle g_{i'}| \left(\langle e_j|\hat{\mathbf{P}}|g_{i'}\rangle \cdot \hat{\mathbf{D}}^{(+)}(t) \right). \quad (\text{A.1.7})$$

(neglecting a zero-point energy term in the Hamiltonian). We may now identify the matrix operator $\bar{\mathbf{V}}[\hat{J}]$

$$\bar{\mathbf{V}}[\hat{J}] = \sum_{jii'} \frac{1}{\epsilon_0\Delta_j} \langle g_i|\hat{\mathbf{P}}|e_j\rangle \langle e_j|\hat{\mathbf{P}}|g_{i'}\rangle |g_i\rangle\langle g_{i'}|, \quad (\text{A.1.8})$$

and we immediately get the result stated in equation (3.1.3). The notation “ \cdot ” in this expression means usual vector product with the vector to the right. Furthermore we may

also find the relation between the polarization and the displaced electric field

$$\begin{aligned}
\hat{\mathbf{P}}^{(-)}(t) &= \sum_{ij} |e_j\rangle\langle e_j| \hat{\mathbf{P}} |g_i\rangle\langle g_i| \\
&= \sum_{jii'} \frac{1}{\epsilon_0 \Delta_j} \langle e_j | \hat{\mathbf{P}} | g_i \rangle \langle g_{i'} | \hat{\mathbf{P}} | e_j \rangle | g_i \rangle \langle g_{i'} | \cdot \hat{\mathbf{D}}^{(-)}(t) \\
&= \bar{\mathbf{V}}^t [\hat{\mathbf{J}}] \hat{\mathbf{D}}^{(-)}(t).
\end{aligned} \tag{A.1.9}$$

We have here only written the positively oscillating component, the negatively oscillating component is found by Hermitian conjugation, which from equation (A.1.8) is the same as transposition of the matrix.

A.2 Calculation of infinitely short propagator

In this appendix we calculate the infinitely short propagator in the local density approximation. We will for simplicity only consider the simple interaction given by

$$\bar{\mathcal{V}}[\mathbf{J}] = \beta\rho(\mathbf{r}) \left(c_0 \mathbf{J}(\mathbf{r})^2 - ic_1 \mathbf{J}(\mathbf{r}) \times \right). \tag{A.2.1}$$

We further shorten the notation by introducing the coefficients $a_0 = 1 - \beta\rho(\mathbf{r})c_0 \mathbf{J}(\mathbf{r})^2$ and $a_1 = \beta\rho(\mathbf{r})c_1 |\mathbf{J}(\mathbf{r})|$.

If we Fourier-transform equation (3.2.9), the equation we wish to solve is

$$\hat{\mathbf{k}} \times \hat{\mathbf{k}} \times (a_0 + ia_1 \hat{\mathbf{j}} \times) \epsilon^{\mathbf{k}} = - \frac{\omega_{\mathbf{k}}^2}{c^2 k^2} \tag{A.2.2a}$$

$$\hat{\mathbf{k}} \cdot \epsilon^{\mathbf{k}} = 0, \tag{A.2.2b}$$

where the vectors $\hat{\mathbf{k}}$ and $\hat{\mathbf{j}}$ are unit vectors representing respectively the direction of the plane wave solution and the orientation of the atomic spin. The solutions to the above equations is the following set of polarization-vectors

$$\epsilon_{\pm}^{\mathbf{k}} = N_{\pm}^{\mathbf{k}} \left(\frac{\hat{\mathbf{j}} \times \hat{\mathbf{k}}}{|\hat{\mathbf{j}} \times \hat{\mathbf{k}}|} \pm i \frac{\hat{\mathbf{k}} \times (\hat{\mathbf{j}} \times \hat{\mathbf{k}})}{|\hat{\mathbf{k}} \times (\hat{\mathbf{j}} \times \hat{\mathbf{k}})|} \right) \equiv N_{\pm}^{\mathbf{k}} (\hat{\mathbf{v}}_1 \pm i \hat{\mathbf{v}}_2), \tag{A.2.3}$$

where $\hat{\mathbf{v}}_1$ and $\hat{\mathbf{v}}_2$ are unit vectors given by the first and second fraction respectively. The

normalization constant $N_{\pm}^{\mathbf{k}}$ is determined by using the inner product in Eq. (3.2.10). In this way we find the real space representation of the basis-functions $\mathbf{f}_{\mathbf{k}}(\mathbf{r})$

$$\mathbf{f}_{\pm}^{\mathbf{k}}(\mathbf{r}) = \frac{1}{\sqrt{2(2\pi)^3(a_0 \pm a_1(\hat{\mathbf{j}} \cdot \hat{\mathbf{k}}))}} (\hat{\mathbf{v}}_1 \pm i\hat{\mathbf{v}}_2) e^{i\mathbf{k} \cdot \mathbf{r}}. \quad (\text{A.2.4})$$

The dispersion relation is then derived from (A.2.2a)

$$\omega_{\mathbf{k}\pm}^2 = c^2 k^2 (a_0 \pm a_1(\hat{\mathbf{j}} \cdot \hat{\mathbf{k}})). \quad (\text{A.2.5})$$

The infinitely short propagator can then be calculated to be the following

$$\bar{\bar{P}}^{(-)}(\mathbf{r}, t - t') = \frac{-i}{2\omega_L c^2} \sum_{s \in \{+, -\}} \int d^3k \omega_{\mathbf{k}s}^2 (\mathbf{f}_{\mathbf{k}s}^{\mathbf{k}}(\mathbf{r}))^* \mathbf{f}_{\mathbf{k}s}^{\mathbf{k}}(\mathbf{r}) e^{\frac{i(t-t')}{2\omega_L} (\omega_{\mathbf{k}s}^2 - \omega_L^2)}. \quad (\text{A.2.6})$$

We introduce the matrix given by the following juxtaposition:

$$\bar{\bar{M}}(\hat{\mathbf{k}}, \hat{\mathbf{j}}, s) = (\hat{\mathbf{v}}_1 - is\hat{\mathbf{v}}_2)(\hat{\mathbf{v}}_1 + is\hat{\mathbf{v}}_2). \quad (\text{A.2.7})$$

Changing to spherical coordinates and making the substitutions $x = \cos \theta$ and $k' = k\sqrt{1 - a_0 + sa_1x}$ as well as using the dispersion relations given in equation (A.2.5) the integral reduce to

$$\bar{\bar{P}}^{(-)}(\mathbf{r}, t - t') = \frac{-i}{2\omega_L c^2} \sum_{s \in \{+, -\}} \int_0^\infty dk' \int_{-1}^1 dx \int_0^{2\pi} d\phi \frac{c^2 k'^4}{2(2\pi)^3 (a_0 + sa_1x)^{5/2}} \bar{\bar{M}}(x, \phi, s) e^{ic(t-t')(k'^2 - k_L^2)/(2k_L)}. \quad (\text{A.2.8})$$

Neglecting the dependence of k' outside the exponential and using that the difference $k'^2 - k_L^2$ for large k_L runs from $-\infty$ to ∞ , the k' integral gives a delta-function in time. Including the ϕ integration in a matrix $\bar{\bar{M}}$ we finally get

$$\bar{\bar{P}}^{(-)}(\mathbf{r}, t - t') = \frac{-ik_L^3 \delta(t - t')}{16\pi^2 c^2} \sum_{s \in \{+, -\}} \int_{-1}^1 dx \frac{\bar{\bar{M}}(x, s)}{(a_0 + sa_1x)^{\frac{5}{2}}}, \quad (\text{A.2.9})$$

with the matrix \bar{M} given by

$$\bar{M}(x, s) = \pi \begin{bmatrix} 2(1-x^2) & 0 & 0 \\ 0 & 1+x^2 & 2isx \\ 0 & -2isx & 1+x^2 \end{bmatrix}. \quad (\text{A.2.10})$$

The s -sum is evaluated by substitution in the integral and the final expression for the infinitely short propagator is

$$\bar{P}^{(-)}(\mathbf{r}, t-t') = \frac{-ik_L^3 \delta(t-t')}{8\pi c^2} \int_{-1}^1 dx \frac{\bar{M}(x, +)}{\pi(a_0 + a_1 x)^{5/2}}. \quad (\text{A.2.11})$$

These integral may be evaluated, and we will express the infinitely short propagator as

$$\bar{P}^{(-)}(\mathbf{r}, t-t') = \frac{-i\delta(t-t')}{c^2} \begin{bmatrix} \varrho_{\parallel} & 0 & 0 \\ 0 & \varrho_{\perp} & -i\varrho_{\Gamma} \\ 0 & i\varrho_{\Gamma} & \varrho_{\perp} \end{bmatrix}. \quad (\text{A.2.12})$$

The coefficients are for $a_0 - a_1 > 0$, given by

$$\varrho_{\parallel} = \frac{-k_L^3}{3\pi a_1^3} \left\{ \frac{-4a_0 + 2a_1}{\sqrt{a_0 - a_1}} + \frac{4a_0 + 2a_1}{\sqrt{a_0 + a_1}} \right\} \quad (\text{A.2.13a})$$

$$\varrho_{\perp} = \frac{-k_L^3}{3\pi a_1^3} \left\{ \frac{2a_0^2 - 3a_0 a_1 + \frac{1}{2}a_1^2}{(a_0 - a_1)^{3/2}} - \frac{2a_0^2 + 3a_0 a_1 + \frac{1}{2}a_1^2}{(a_0 + a_1)^{3/2}} \right\} \quad (\text{A.2.13b})$$

$$\varrho_{\Gamma} = \frac{k_L^3}{6\pi a_1^2} \left\{ \frac{2a_0 - 3a_1}{(a_0 - a_1)^{3/2}} - \frac{2a_0 + 3a_1}{(a_0 + a_1)^{3/2}} \right\}. \quad (\text{A.2.13c})$$

A.3 Reciprocal equation for Green's function

In this appendix we derive the reciprocal equation for the Green's function. Before doing so we will need some results concerning the representation of the Green's function. Let us define the following inner product:

$$\langle \phi | \psi \rangle = \int d^3 r dt \bar{M}(\mathbf{r}) \phi(\mathbf{r}, t) \cdot \psi^{\dagger}(\mathbf{r}, t). \quad (\text{A.3.1})$$

We will generally work in the L^2 -space equipped with this inner product. Using that the matrix operator $\bar{\bar{M}}$ is Hermitian, one finds the differential operator \mathcal{D} given in equation (5.0.1) to be Hermitian in our inner product space

$$\langle \phi | \mathcal{D} \psi \rangle = \langle \mathcal{D} \phi | \psi \rangle. \quad (\text{A.3.2})$$

That \mathcal{D} is Hermitian means that the eigenfunctions F_k to \mathcal{D}

$$\mathcal{D} \mathbf{F}_k(\mathbf{r}, t) = \lambda_k \mathbf{F}_k(\mathbf{r}, t), \quad (\text{A.3.3})$$

define a complete basis of our inner product space $\{\mathbf{F}_k\}$. A representation of the identity functional given in equation (5.0.2) may therefore be

$$\sum_{\mathbf{k}} \mathbf{F}_k^\dagger(\mathbf{r}, t) \mathbf{F}_k(\mathbf{r}_0, t_0). \quad (\text{A.3.4})$$

It can be checked that this is exactly a functional identity representation in our inner product space by expanding any function on the basis $\{\mathbf{F}_k\}$.

To get a formal expression of the Green's function defined in equation (5.0.2) we expand the Green's function in this basis, and using equation (A.3.3) and (A.3.4) we find

$$\bar{\bar{G}}(\mathbf{r}, t | \mathbf{r}_0, t_0) = \sum_{\mathbf{k}} \frac{1}{\lambda_k} \mathbf{F}_k^\dagger(\mathbf{r}, t) \mathbf{F}_k(\mathbf{r}_0, t_0). \quad (\text{A.3.5})$$

Starting from equation (5.0.2) we make the substitution $t \rightarrow -t$, $t_0 \rightarrow -t_1$ and $\mathbf{r}_0 \rightarrow \mathbf{r}_1$ and we write:

$$\mathcal{D}^* \bar{\bar{G}}(\mathbf{r}, -t | \mathbf{r}_1, -t_1) = \bar{\bar{I}} \delta(\mathbf{r}, \mathbf{r}_1) \delta(t, t_1). \quad (\text{A.3.6})$$

In the next step we take inner product with equation (5.0.2) and $\bar{\bar{G}}(\mathbf{r}, -t | \mathbf{r}_1, -t_1)$ from the left with respect to unprimed coordinates, and equation (A.3.6) and $\bar{\bar{G}}(\mathbf{r}, t | \mathbf{r}_0, t_0)$ also from the left with respect to unprimed coordinates. The resulting two equations are then subtracted. The term containing ω_L^2 vanish trivially, and using rules for differentiating a

product, the resulting equation may be written as

$$\begin{aligned}
& 2i\omega_L \iint d^3 r dt \bar{\mathcal{M}}(\mathbf{r}) \frac{\partial}{\partial t} [\bar{G}(\mathbf{r}, -t|\mathbf{r}_1, -t_1) \cdot \bar{G}(\mathbf{r}, t|\mathbf{r}_0, t_0)] \\
& + c^2 \iint d^3 r dt [\bar{\mathcal{M}}(\mathbf{r}) \bar{G}(\mathbf{r}, -t|\mathbf{r}_1, -t_1) \cdot \nabla \times \nabla \times \bar{\mathcal{M}}(\mathbf{r}) \\
& \bar{G}(\mathbf{r}, t|\mathbf{r}_0, t_0) - \bar{\mathcal{M}}(\mathbf{r}) \bar{G}(\mathbf{r}, t|\mathbf{r}_0, t_0) \cdot \nabla \times \nabla \times \bar{\mathcal{M}}(\mathbf{r}) \\
& \bar{G}(\mathbf{r}, -t|\mathbf{r}_1, -t_1)] = \bar{G}(\mathbf{r}_1, t_1|\mathbf{r}_0, t_0) - \bar{G}(\mathbf{r}_0, -t_0|\mathbf{r}_1, -t_1). \tag{A.3.7}
\end{aligned}$$

Using the cut-off property of the Green's function, the first term on the left hand side is seen to vanish. Using the explicit expression for the Green's function (A.3.5) along with Gauss' theorem, one may show that the second term also vanish. The final result is therefore

$$\bar{G}(\mathbf{r}_1, t_1|\mathbf{r}_0, t_0) = \bar{G}(\mathbf{r}_0, -t_0|\mathbf{r}_1, -t_1). \tag{A.3.8}$$

From Eq. (5.0.2), (A.3.8) and using the substitutions $t \rightarrow -t'$, $t_0 \rightarrow t$, $\mathbf{r} \rightarrow \mathbf{r}'$ and $\mathbf{r}_0 \rightarrow \mathbf{r}$ we end up with the *reciprocal equation*

$$\left(-2i\omega_L \frac{\partial}{\partial t'} - \omega_L^2 + c^2 \nabla' \times \nabla' \times \bar{\mathcal{M}}(\mathbf{r}') \right) \bar{G}(\mathbf{r}, t|\mathbf{r}', t') = \bar{I} \delta(\mathbf{r}, \mathbf{r}') \delta(t, t'). \tag{A.3.9}$$

In the following we derive the general solution to the equation

$$\left(2i\omega_L \frac{\partial}{\partial t} - \omega_L^2 + c^2 \nabla \times \nabla \times \bar{\mathcal{M}}(\mathbf{r}) \right) \psi(\mathbf{r}, t) = \rho(\mathbf{r}, t), \tag{A.3.10}$$

where $\psi(\mathbf{r}, t)$ is an unknown field, $\rho(\mathbf{r}, t)$ is a source term effecting the solution, and $\bar{\mathcal{M}}$ is some Hermitian matrix operator, which may depend on position. We make an inner product of equation (A.3.10) with $\bar{G}(\mathbf{r}, t|\mathbf{r}', t')$ from the left and an inner product of equation (A.3.9) with $\psi(\mathbf{r}, t)$ from the right and subtract these two equations. In this calculation we are integrating over the time interval $t' \in]t_0, t^+[$, where we understand $t^+ = \lim_{\epsilon \rightarrow 0} [t + \epsilon]$. Again we find that terms containing ω_L^2 vanish. Similar to above we

will use rules for differentiation a product, and we eventually end up with

$$\begin{aligned}
\psi(\mathbf{r}, t) - \iint_{t_0}^{t^+} d^3 r' dt' \bar{M}(\mathbf{r}') \bar{G}(\mathbf{r}, t | \mathbf{r}', t') \cdot \rho(\mathbf{r}', t') = \\
- 2i\omega_L \iint_{t_0}^{t^+} d^3 r' dt' \bar{M}(\mathbf{r}') \frac{\partial}{\partial t} [\bar{G}(\mathbf{r}, t | \mathbf{r}', t') \cdot \psi(\mathbf{r}', t')] \\
+ c^2 \iint_{t_0}^{t^+} d^3 r' dt' \bar{M}(\mathbf{r}') \{ \\
\psi(\mathbf{r}', t') \cdot \nabla' \times \nabla' \times \bar{M}(\mathbf{r}') \bar{G}(\mathbf{r}, t | \mathbf{r}', t') \\
- \bar{G}(\mathbf{r}, t | \mathbf{r}', t') \cdot \nabla' \times \nabla' \times \psi(\mathbf{r}', t') \}. \tag{A.3.11}
\end{aligned}$$

Using the same boundary conditions as was done in the calculation leading to the reciprocal equation we conclude that the last term in equation (A.3.11) vanish. The right hand side of the equation thus reduce to

$$-2i\omega_L \int d^3 r' \bar{M}(\mathbf{r}') [\bar{G}(\mathbf{r}, t | \mathbf{r}', t') \cdot \psi(\mathbf{r}', t')]_{t_0}^{t^+} = 2i\omega_L \int d^3 r' \bar{M}(\mathbf{r}') \bar{G}(\mathbf{r}, t | \mathbf{r}', t_0) \cdot \psi(\mathbf{r}', t_0). \tag{A.3.12}$$

Here we have used that the upper time limit vanish due to the cut-off in the Green's function. Rearranging terms we finally arrive at the general solution to the diffusion equation

$$\begin{aligned}
\psi(\mathbf{r}, t) = 2i\omega_L \int d^3 r' \bar{M}(\mathbf{r}') \bar{G}(\mathbf{r}, t | \mathbf{r}', t_0) \cdot \psi(\mathbf{r}', t_0) \\
+ \iint_{t_0}^t d^3 r' dt' \bar{M}(\mathbf{r}') \bar{G}(\mathbf{r}, t | \mathbf{r}', t') \cdot \rho(\mathbf{r}', t'). \tag{A.3.13}
\end{aligned}$$

A.4 Lorentz-Lorenz relation

In the main text we mainly consider lowest order corrections to the index of refraction. To verify that our theory can also correctly reproduce higher order corrections, we shall in this appendix show how to derive the so called Lorentz-Lorenz or Clausius-Mossotti relation for the electric permittivity within our theoretical framework [48]. To lowest

order the permittivity is given by Eq. (4.0.11)

$$\bar{\bar{\epsilon}}(\mathbf{r})^{-1} = 1 - \bar{\bar{V}}'[\mathbf{J}]. \quad (\text{A.4.1})$$

To calculate the higher order correction it is convenient to first Fourier transform the Dyson equation (5.1.1) describing the light field with respect to time

$$\tilde{\mathbf{D}}^{(-)}(\mathbf{r}, \omega) = \tilde{\mathbf{D}}_0^{(-)}(\mathbf{r}, \omega) + c^2 \int d^3 r' \bar{\bar{P}}^{(-)}(\mathbf{r}, \mathbf{r}', \omega) \cdot \bar{\bar{m}}[\hat{\mathbf{J}}]' \tilde{\mathbf{D}}^{(-)}(\mathbf{r}', \omega). \quad (\text{A.4.2})$$

This equation is the starting point for the analysis. (The Fourier transformation is here defined as

$$f(\omega) = \int_0^\infty dt e^{i(\omega-\eta)t} f(t), \quad (\text{A.4.3})$$

where η is an infinitely small convergence factor.)

From Eq. (5.3.7) we find the Fourier transformed propagator $\bar{\bar{P}}^{(-)}$ to read

$$\bar{\bar{P}}^{(-)}(\mathbf{r}, \mathbf{r}', \omega) = \frac{1}{c^2} \sum_{\mathbf{k}} \frac{\omega_{\mathbf{k}}^2 \mathbf{f}_{\mathbf{k}}^*(\mathbf{r}) \mathbf{f}_{\mathbf{k}}(\mathbf{r}')}{\omega_{\mathbf{k}}^2 - \omega_{\mathbf{L}}^2 + 2\omega_{\mathbf{L}}(\omega + i\eta)}. \quad (\text{A.4.4})$$

The real space representation of this propagator is in general difficult to calculate, however, for a scalar interaction the calculation simplify considerably. For $\omega \approx 0$ which is reasonable in our case, since we are dealing with slowly varying operators, the propagator reads

$$\begin{aligned} \bar{\bar{P}}^{(+)}(\mathbf{n}) &= \int \frac{d^3 k}{c^2 (2\pi)^3} \sum_{\boldsymbol{\varepsilon} \perp \mathbf{k}} \boldsymbol{\varepsilon} \boldsymbol{\varepsilon} \frac{\mathbf{k}^2 e^{i\mathbf{k} \cdot \mathbf{n}}}{\mathbf{k}^2 - k_{\mathbf{L}}^2} \\ &= -\frac{k_{\mathbf{L}}^3}{c^2 4\pi} \frac{e^{ik_{\mathbf{L}} n}}{k_{\mathbf{L}} n} \left[\left(1 + \frac{3i}{k_{\mathbf{L}} n} - \frac{3}{(k_{\mathbf{L}} n)^2} \right) \frac{\mathbf{n}\mathbf{n}}{n^2} - \left(1 + \frac{i}{k_{\mathbf{L}} n} - \frac{1}{(k_{\mathbf{L}} n)^2} \right) \bar{\bar{I}} \right] + \frac{2}{3} \bar{\bar{I}} \delta(\mathbf{n}), \end{aligned} \quad (\text{A.4.5})$$

where $\mathbf{n} = \mathbf{r} - \mathbf{r}'$, $n = |\mathbf{n}|$, and $\bar{\bar{I}}$ is the identity matrix. We notice that the propagator gives us the well known result for the radiated field of an oscillating dipole. In addition we have a term describing a self-interaction. This propagator is also discussed in Ref. [63]. In the following we shall only be considering the self interaction part of the propagator.

When considering the density correlation function to second order $\langle \rho(\mathbf{r}_1) \rho(\mathbf{r}_2) \rangle$ we

have so far used the ideal gas approximation in Eq. (5.2.1), where there are no correlations between different atoms. In reality we can never have two atoms at the same position and this give a small correction to $\langle \rho(\mathbf{r}_1)\rho(\mathbf{r}_2) \rangle$, which must vanish for $\mathbf{r}_1 = \mathbf{r}_2$ (apart from the delta function, which represent the single atom contribution). This can formally be described by introducing so called irreducible correlation functions h_2 such that

$$\langle \rho(\mathbf{r}_1)\rho(\mathbf{r}_2) \rangle = \langle \rho(\mathbf{r}_1) \rangle \langle \rho(\mathbf{r}_2) \rangle + h_2(\mathbf{r}_1, \mathbf{r}_2), \quad (\text{A.4.6})$$

where h_2 now takes care of the core-repulsion of the atoms (here we exclude the delta function). For $\mathbf{r}_1 = \mathbf{r}_2$ we thus finds that $h_2(\mathbf{r}_1, \mathbf{r}_1) = -\langle \rho(\mathbf{r}_1) \rangle^2$.

The above can be used along with the real space representation of the propagator to give the second order correction to the permittivity. We will not consider terms that vanish when we take quantum mechanical mean. The relevant part of the second order term thus gives in shorthand notation $-\int \bar{P}^{(-)}(2/3)(\bar{V}'[\mathbf{J}])^2 \bar{D}^{(-)}$. When we introduce this interaction to the differential equation (4.0.11) we find the permittivity to second order

$$\bar{\epsilon}(\mathbf{r})^{-1} = 1 - \bar{V}'[\mathbf{J}] + \frac{2}{3}(\bar{V}'[\mathbf{J}])^2. \quad (\text{A.4.7})$$

The calculation can be continued to infinite order [64], and the result reads

$$\begin{aligned} \bar{\epsilon}(\mathbf{r})^{-1} &= 1 - \bar{V}'[\mathbf{J}] - \bar{V}'[\mathbf{J}] \sum_{n=1}^{\infty} \left(\frac{-2}{3} \bar{V}'[\mathbf{J}] \right)^n \\ &= \frac{1 - \frac{1}{3} \bar{V}'[\mathbf{J}]}{1 + \frac{2}{3} \bar{V}'[\mathbf{J}]} \end{aligned} \quad (\text{A.4.8})$$

This is the Lorenz-Lorenz relation, and we thus see that the effect can be included in the theory by dressing the spatial mode functions according to the result above.

A.5 Calculations of second-order Stokes generator

In this appendix we present detailed calculations of the second-order terms of Eq. (6.4.4). We will denote the fourth term of the right hand side of Eq. (6.4.4) as $\bar{\mathcal{S}}_A^{(2)}$, and one finds

$$K \langle\langle \tilde{\mathbf{f}}_{kmj}^*(\mathbf{r}, t) | \bar{\mathcal{S}}_A^{(2)} | \tilde{\mathbf{f}}_{km'j'}^*(\mathbf{r}, t) \rangle\rangle = \left(\frac{1}{2}\right)^2 (k_l \beta c_1)^2 \iint d^3 r d^3 r' \sum_{\substack{ln \\ l'n'}} \rho(\mathbf{r}) \rho(\mathbf{r}') \Theta_{jl}^{mn}(\mathbf{r})^* \Theta_{j'l'}^{m'n'}(\mathbf{r}') \hat{a}_{knl}^\dagger \hat{a}_{kn'l'}. \quad (\text{A.5.1})$$

The seventh term of the right hand side of Eq. (6.4.4) plus its complex conjugate we will denote as $\bar{\mathcal{S}}_B^{(2)}$. To calculate this term we extend the limits of the time integration from minus to plus infinity. This we can do by introducing a factor of one half, and approximating the imaginary term $i \int_{-\infty}^0 dt \sin(\omega t)$ to be zero. This corresponds to the usual treatment of such terms in the Markov approximation to spontaneous emission when one ignores the Lamb shift. We then find the following contribution to the Stokes operators

$$K \langle\langle \tilde{\mathbf{f}}_{kmj}^*(\mathbf{r}, t) | \bar{\mathcal{S}}_B^{(2)} | \tilde{\mathbf{f}}_{km'j'}^*(\mathbf{r}, t) \rangle\rangle = \left(\frac{1}{2}\right)^3 (k_l \beta c_1)^2 \iint d^3 r d^3 r' \sum_{\substack{ln \\ l'n'}} \rho(\mathbf{r}) \rho(\mathbf{r}') \left\{ \Theta_{jl}^{mn}(\mathbf{r})^* \Theta_{l'l'}^{nn'}(\mathbf{r}')^* \hat{a}_{kn'l'}^\dagger \hat{a}_{km'j'} + \Theta_{j'l}^{m'n}(\mathbf{r}) \Theta_{ll'}^{mm'}(\mathbf{r}') \hat{a}_{kmj}^\dagger \hat{a}_{kn'l'} \right\}. \quad (\text{A.5.2})$$

One notice that the factors of 1/2 in Eq. (A.5.1) and (A.5.2) exactly add up to give one half of the square of the first-order term, as is shown in Eq. (7.2.1)

The sixth term on the right hand side of Eq. (6.4.4), plus its Hermitian conjugate, we

will denote as $\bar{\bar{S}}_C^{(2)}$, and we find

$$\begin{aligned}
K \langle\langle \tilde{\mathbf{f}}_{kmj}^*(\mathbf{r}, t) | \bar{\bar{S}}_C^{(2)} | \tilde{\mathbf{f}}_{km'j'}^*(\mathbf{r}, t) \rangle\rangle = \\
\left(\frac{1}{2}\right)^3 (k_L \beta c_1)^2 \int d^3 r' \sum_{\substack{ln \\ ql'n' \\ n'l''}} \rho(\mathbf{r}') \{ C_{jl}^{l'l''}(\mathbf{r}') \Psi_k^{mn}(\mathbf{r}')^* \Psi_q^{n'n''}(\mathbf{r}') \hat{a}_{qn'l'}^\dagger \hat{a}_{qn''l''} \hat{a}_{knl}^\dagger \hat{a}_{km'j'} \\
+ \hat{a}_{kmj}^\dagger \hat{a}_{qn'l'}^\dagger \hat{a}_{qn''l''} \hat{a}_{knl} C_{j'l}^{l'l''}(\mathbf{r}') \Psi_k^{m'n}(\mathbf{r}') \Psi_q^{n'n''}(\mathbf{r}')^* \}, \tag{A.5.3}
\end{aligned}$$

where we have introduced the coefficients

$$C_{jl}^{l'l''}(\mathbf{r}) = \mathbf{e}_j(\mathbf{r}) \cdot \{ (\bar{\mathbf{J}}(\mathbf{r}) \times [\mathbf{e}_{l'}(\mathbf{r}) \times \mathbf{e}_{l''}(\mathbf{r})]) \times \mathbf{e}_l(\mathbf{r}) \}. \tag{A.5.4a}$$

This term can be shown to vanish by expanding the spin-operator $\bar{\mathbf{J}}$ on the basis defined by the polarization vectors $\mathbf{e}_x(\mathbf{r})$, $\mathbf{e}_y(\mathbf{r})$ and $\mathbf{e}_z(\mathbf{r})$ and using that the indices j, l, l' and l'' only run over x and y .

Finally we will calculate the effect of the fifth term on the right hand side of Eq. (6.4.4), which we will denote $\bar{\bar{S}}_D^{(2)}$. In this calculation it is important to remember that the term will scale as $\beta^2 \rho$, and reads

$$\begin{aligned}
K \langle\langle \tilde{\mathbf{f}}_{kmj}^*(\mathbf{r}, t) | \bar{\bar{S}}_D^{(2)} | \tilde{\mathbf{f}}_{km'j'}^*(\mathbf{r}, t) \rangle\rangle = \\
\left(\frac{1}{2}\right)^2 (k_L \beta)^2 \int d^3 r \sum_{\substack{ln \\ l'n'}} \rho(\mathbf{r}) \Psi_k^{nm}(\mathbf{r}) \Psi_k^{m'n'}(\mathbf{r}) \hat{a}_{knl}^\dagger \hat{a}_{kn'l'} \left\{ \right. \\
c_1^2 (\bar{\mathbf{J}}(\mathbf{r}) \cdot \mathbf{e}_z(\mathbf{r}))^2 (\delta_{jy} \delta_{lx} - \delta_{jx} \delta_{ly}) (\delta_{j'y} \delta_{l'x} - \delta_{j'x} \delta_{l'y}) \\
\left. + c_0^2 \mathbf{J}(\mathbf{r})^4 \delta_{jl} \delta_{j'l'} \right\}. \tag{A.5.5}
\end{aligned}$$

A.6 Calculation of second-order Spin-terms

In this section we calculate the second order terms for the atomic spin, represented as the third and fourth term of the right-hand side of Eq. (6.4.15). These terms we will denote

$\mathcal{J}_A^{(2)}$, and using the previous notation one finds

$$\mathcal{J}_A^{(2)} = \frac{-i}{2} \left(\frac{\beta c_1 k_L}{2} \right)^2 \sum_k \int d^3 r' \sum_{m' m''} (\bar{\mathbf{J}}(\mathbf{r}) \times \mathbf{e}_z(\mathbf{r})) \left(\begin{array}{c} 0 \\ \bar{J}_y(\mathbf{r}') \\ \bar{J}_z(\mathbf{r}') \end{array} \right) \cdot \mathbf{e}_z(\mathbf{r}') \rho(\mathbf{r}') \hat{a}_{km'l}^\dagger \hat{a}_{km''l} \\ \sum_m \{ \Psi_k^{mm''}(\mathbf{r}) \Psi_k^{m'm}(\mathbf{r}') - \Psi_k^{m'm}(\mathbf{r}) \Psi_k^{mm''}(\mathbf{r}') \}. \quad (\text{A.6.1})$$

We can examine this term by assuming that the only photon carrying modes of the light are the two modes \mathbf{k}_{kox} and \mathbf{k}_{koy} and neglect all other modes. In this case the term reduce to

$$\mathcal{J}_A^{(2)} = \left(\frac{\beta c_1 k_L}{2} \right)^2 \sum_k \int d^3 r' \sum_{(n,l) \in \{(o,x), (o',y)\}} \cdot \\ (\bar{\mathbf{J}}(\mathbf{r}) \times \mathbf{e}_z(\mathbf{r})) \left(\begin{array}{c} 0 \\ \bar{J}_y(\mathbf{r}') \\ \bar{J}_z(\mathbf{r}') \end{array} \right) \cdot \mathbf{e}_z(\mathbf{r}') \rho(\mathbf{r}') \hat{a}_{knl}^\dagger \hat{a}_{knl} \text{Im}[\Psi_k^{mn}(\mathbf{r}) \Psi_k^{nm}(\mathbf{r}')]. \quad (\text{A.6.2})$$

This term represents an atom at position \mathbf{r}' interacting with the light field and emitting a photon into mode m , which propagates to the position \mathbf{r} , where it is absorbed by an atom followed by stimulated emission into the classical beam. This process is also known as optically induced dipole-dipole interaction, and indeed the sum over all modes m can be used to introduce the dipole propagator in (A.4.5). Note, however, that above we have written the term in the paraxial approximation, where we ignore the dependence of the polarization vector on the mode number. Since the sum over m involves all modes, and not just the paraxial modes, an accurate treatment requires a more complicated expression involving the polarization vectors along the lines of Appendix A.8 (we use this more complicated expression in our estimates of the size of the effect).

The last term we will consider is the term describing an atom interacting with the light field at two different times. This term is represented as the fifth term on the right hand side of Eq. (6.4.15), and is given on vector component form in Eq. (6.1.13). We will

denote this term with $\mathcal{J}_B^{(2)}$. A short calculation gives

$$\mathcal{J}_B^{(2)} = -\frac{1}{2} \left(\frac{\beta c_1 k_L}{2} \right)^2 \sum_{kk'} \sum_{\substack{mm' \\ mm'}} \sum_{\substack{jj' \\ l}} \mathbf{e}_l (\mathbf{J} \cdot \mathbf{e}_{j'}) \left\{ \right. \\ \left. \Psi_k^{mn} \Psi_{k'}^{m'n'} \left[\hat{a}_{kml}^\dagger \hat{a}_{k'm'l}^\dagger \hat{a}_{knj} \hat{a}_{k'n'j'} - \hat{a}_{kmj}^\dagger \hat{a}_{k'm'l}^\dagger \hat{a}_{knj'} \hat{a}_{k'n'l} \right] + \text{H.c.} \right\}, \quad (\text{A.6.3})$$

where we have suppressed the spatial dependence to shorten the notation. Doing the sum over j, j' and l we obtain

$$\mathcal{J}_B^{(2)} = -\frac{1}{2} \left(\frac{\beta c_1 k_L}{2} \right)^2 \sum_{kk'} \sum_{\substack{mm' \\ mm'}} (\mathbf{J} - \mathbf{e}_z (\mathbf{J} \cdot \mathbf{e}_z)) \cdot \\ \Psi_k^{mn} \Psi_{k'}^{m'n'} \left\{ 2 \hat{a}_{kmx}^\dagger \hat{a}_{k'm'y}^\dagger \hat{a}_{kny} \hat{a}_{k'n'x} - \hat{a}_{kmy}^\dagger \hat{a}_{k'm'y}^\dagger \hat{a}_{knx} \hat{a}_{k'n'x} - \hat{a}_{kmx}^\dagger \hat{a}_{k'm'x}^\dagger \hat{a}_{kny} \hat{a}_{k'n'y} \right\}. \quad (\text{A.6.4})$$

The first order term in Eq. (6.4.16) describe the first order effect of rotation of the spin around the $e_z(\mathbf{r})$ axis. The second order term in (A.6.4) describe the second order term of this rotation. From the rotation frequency in the first order term $\propto s_3$ (assuming Ψ to be real), one would thus expect this term to scale as $\beta^2 (s_3)^2$ which is different from the term in (A.6.4). This difference arises because we have separated the term into normal ordered components such that the second order term in (A.6.4) only contributes when at least two photons are present. When we did the normal ordering in the diagram we introduced an additional term, which we described by the third term in Eq. (6.1.4)

A.7 Calculation of spontaneous emission

In this section we calculate the corrections to Eq. (7.2.1) and Eq. (7.2.2), due to the incoherent interaction. To do this we need a result for the infinitely short propagator. From the definition of the propagator (5.3.7) and the calculation of in it (6.1.8), we find the relation

$$\sum_n |U_n(\mathbf{r}_\perp)|^2 = \frac{2}{k_L} \varrho(\mathbf{r}_\perp) \quad (\text{A.7.1})$$

where $\varrho(\mathbf{r}_\perp) = k_\perp^3/(16\pi^2)$ is the zeroth order term of the expansion of $\varrho_\parallel(\mathbf{r})$ in β given in Eq. (A.2.13). This result is important when calculating $\bar{\mathcal{S}}_d^{(2)}$ and for relating this term with the incoherent interactions, responsible for spontaneous emission. When including this term and the decay described in Sec. 6.2, the incoherent interaction reduce to

$$\hat{s}_{1,out}(\mathbf{r}_\perp) = \dots - \frac{\beta^2 k_\perp \varrho(\mathbf{r}_\perp)}{2} \int dz' \rho(z') \left\{ c_1^2 (\bar{J}_y^2(z') - \bar{J}_z^2(z')) \hat{s}_{0,in}(\mathbf{r}_\perp) + (c_0^2 \mathbf{J}^4(z') + c_1^2 [4J_z^2(z') + J_y^2(z')]) \hat{s}_{1,in}(\mathbf{r}_\perp) \right\}, \quad (\text{A.7.2a})$$

$$\hat{s}_{2,out}(\mathbf{r}_\perp) = \dots - \frac{\beta^2 k_\perp \varrho(\mathbf{r}_\perp)}{2} \int dz' \rho(z') \left\{ c_0^2 \mathbf{J}^4(z') + c_1^2 [3J_z^2(z') + J_y^2(z') + J_x^2(z')] \right\} \hat{s}_{2,in}(\mathbf{r}_\perp), \quad (\text{A.7.2b})$$

$$\hat{s}_{3,out}(\mathbf{r}_\perp) = \dots - \frac{\beta^2 k_\perp \varrho(\mathbf{r}_\perp)}{2} \int dz' \rho(z') \left\{ c_0^2 \mathbf{J}^4(z') + c_1^2 [J_z^2(z') + J_y^2(z') + J_x^2(z')] \right\} \hat{s}_{3,in}(\mathbf{r}_\perp), \quad (\text{A.7.2c})$$

where we have only kept terms that are nonvanishing after taking quantum mechanical average of the atomic spin. The operators $\hat{s}_{0,in}(\mathbf{r}_\perp)$ measures the total photon flux, and is given as

$$\hat{s}_0(\mathbf{r}_\perp) = \sum_{kmm'} \frac{1}{2} \left(U_m^*(\mathbf{r}_\perp) \hat{a}_{kmx}^\dagger \hat{a}_{km'x} U_{m'}(\mathbf{r}_\perp) + U_m^*(\mathbf{r}_\perp) \hat{a}_{kmy}^\dagger \hat{a}_{km'y} U_{m'}(\mathbf{r}_\perp) \right) \quad (\text{A.7.3})$$

It is important to note that in a discussion of the various contributions to decay one should include all terms in the perturbative expansion, including the loop diagrams (6.2.2). If these are not included one finds the contribution from the term in Eq. (A.5.5) to increase the the operator \hat{s}_3 .

Similarly we find the effect of spontaneous emission on the spin equation to read

$$\bar{J}_{x,out}(z) = \dots - \beta^2 c_1^2 k_\perp \varrho(\mathbf{r}_\perp) \sum_k \left\{ \bar{J}_{x,in}(z) [\hat{s}_{0,in}^k(\mathbf{r}_\perp) + \frac{1}{2} \hat{s}_{1,in}^k(\mathbf{r}_\perp)] + \frac{1}{2} \bar{J}_{y,in}(z) \hat{s}_{2,in}^k(\mathbf{r}_\perp) \right\} \quad (\text{A.7.4a})$$

$$\bar{J}_{y,out}(z) = \dots - \beta^2 c_1^2 k_\perp \varrho(\mathbf{r}_\perp) \sum_k \left\{ \bar{J}_{y,in}(z) [\hat{s}_{0,in}^k(\mathbf{r}_\perp) + \frac{1}{2} \hat{s}_{1,in}^k(\mathbf{r}_\perp)] + \frac{1}{2} \bar{J}_{x,in}(z) \hat{s}_{2,in}^k(\mathbf{r}_\perp) \right\} \quad (\text{A.7.4b})$$

$$\bar{J}_{z,out}(z) = \dots - \beta^2 c_1^2 k_\perp \varrho(\mathbf{r}_\perp) \sum_k \bar{J}_{z,in}(z) \hat{s}_{0,in}^k(\mathbf{r}_\perp). \quad (\text{A.7.4c})$$

The above result is derived from Eq. (6.1.9) by using the paraxial approximation and only keeping terms of order β^2 . A minor correction is introduced since we in Eq. (7.2.2) chose a representation that was in fact not normal ordered.

A.8 Beyond paraxial approximation

In this section we will go slightly beyond the approximation made in Eq. (6.4.3), and consider the set

$$\mathbf{f}_q(\mathbf{r}) = \frac{1}{\sqrt{2\pi}} U_{nq}(\mathbf{r}) \mathbf{e}_{nj}(\mathbf{r}). \quad (\text{A.8.1})$$

We will consider the correction this generalization makes to the result given in Eq. (7.3.4), and therefore define spin-components in the local basis given by the set $\mathbf{e}_{mx}(\mathbf{r})$, $\mathbf{e}_{my}(\mathbf{r})$ and $\mathbf{e}_{mz}(\mathbf{r})$

$$\bar{\mathcal{J}}_{\mathbf{e}_{mi}}(\mathbf{r}) = \begin{pmatrix} 0 \\ \bar{J}_y(\mathbf{r}) \\ \bar{J}_z(\mathbf{r}) \end{pmatrix} \cdot \mathbf{e}_{mi}(\mathbf{r}) \quad (\text{A.8.2})$$

for $i \in \{x, y, z\}$. These vectors are defined by the fact that, e.g., $\mathbf{e}_{oy}(\mathbf{r})$ should be transverse and perpendicular to the polarization vector arising from the mode function $U_{ok}(\mathbf{r})\mathbf{e}_{ox}(\mathbf{r})$. \mathbf{e}_{oz} is then defined by $\mathbf{e}_{oz} = \mathbf{e}_{ox} \times \mathbf{e}_{oy}$. Similarly for the quantum modes m the definition of \mathbf{e}_{mx} follow from the fact that it should be perpendicular to the polarization vector from the mode $U_{mk}(\mathbf{r})\mathbf{e}_{my}(\mathbf{r})$.

With these definitions Eq. (7.3.4) gives

$$\hat{X}_{out}^m = \hat{X}_{in}^m + k_L \beta c_1 \sqrt{\frac{N_x^o}{2}} \int d^3 r' \rho(\mathbf{r}') \text{Re}[\Psi_k^{mo}(\mathbf{r})] \{ \bar{\mathcal{J}}_{\mathbf{e}_{oz}}(\mathbf{r}) [\mathbf{e}_{ox}(\mathbf{r}) \cdot \mathbf{e}_{mx}(\mathbf{r})] - \bar{\mathcal{J}}_{\mathbf{e}_{ox}}(\mathbf{r}) [\mathbf{e}_{ox}(\mathbf{r}) \cdot \mathbf{e}_{mz}(\mathbf{r})] \} \quad (\text{A.8.3a})$$

$$\hat{P}_{out}^m = \hat{P}_{in}^m + k_L \beta c_1 \sqrt{\frac{N_x^o}{2}} \int d^3 r' \rho(\mathbf{r}') \text{Im}[\Psi_k^{mo}(\mathbf{r})] \{ \bar{\mathcal{J}}_{\mathbf{e}_{oz}}(\mathbf{r}) [\mathbf{e}_{ox}(\mathbf{r}) \cdot \mathbf{e}_{mx}(\mathbf{r})] - \bar{\mathcal{J}}_{\mathbf{e}_{ox}}(\mathbf{r}) [\mathbf{e}_{ox}(\mathbf{r}) \cdot \mathbf{e}_{mz}(\mathbf{r})] \}. \quad (\text{A.8.3b})$$

Similarly we find the correction to Eq. (7.3.5) to give

$$\bar{\mathbf{J}}_{out}(\mathbf{r}) \approx \bar{\mathbf{J}}_{in}(\mathbf{r}) + k_L \beta c_1 \sqrt{\frac{N_x^o}{2}} \sum_n \left[\text{Re}[\Psi_k^{no}(\mathbf{r})] \hat{P}_{in}^n - \text{Im}[\Psi_k^{no}(\mathbf{r})] \hat{X}_{in}^n \right] \{ \bar{\mathbf{J}}_{in}(\mathbf{r}) \times (\mathbf{e}_{ox}(\mathbf{r}) \times \mathbf{e}_{ny}(\mathbf{r})) \}. \quad (\text{A.8.4})$$

Appendix for Part 2

B.1 Deriving the first order correction to the matrix $M_{k'm'n'}^{kmn}$

By introducing the dummy variable $\alpha = 2\sigma_{\perp}^2$ in the Gaussian function, the series expansion of the x -integral in Eq. (12.0.13) may be written as

$$\sum_{l=0}^{\infty} (-\partial_{\alpha})^l \int_0^{\infty} e^{-\alpha x^2} I_m(2\sigma_{\perp}^2 \gamma_n x) I_m(2\sigma_{\perp}^2 \gamma_{n'} x) \Big|_{\alpha=2\sigma_{\perp}^2} \quad (\text{B.1.1})$$

Using the above expansion along with the relation $I_m(x) = i^{-m} J_m(ix)$ together with the result [50]

$$\int_0^{\infty} r dr e^{-\alpha^2 r^2} J_m(\beta r) J_m(\gamma r) = \frac{1}{2\alpha^2} e^{-\frac{\beta^2 + \gamma^2}{4\alpha^2}} I_m\left(\frac{\beta\gamma}{2\alpha^2}\right) \\ |\arg[\alpha]| < \frac{\pi}{4}, \Re[m] > -1, \beta > 0, \gamma > 0, \quad (\text{B.1.2})$$

Equation (B.1.1) may be rewritten as

$$\sum_{l=0}^{\infty} \frac{(-\partial_{\alpha})^l}{(-1)^m} \int_0^{\infty} e^{-\alpha x^2} J_m(2i\sigma_{\perp}^2 \gamma_n x) J_m(2i\sigma_{\perp}^2 \gamma_{n'} x) \Big|_{\alpha=2\sigma_{\perp}^2} \quad (\text{B.1.3})$$

From Eq. (12.0.12) we find the integral to give

$$\sum_{l=0}^{\infty} (-\partial_{\alpha})^l \frac{e^{\frac{\sigma_{\perp}^4(\gamma_n^2 + \gamma_{n'}^2)}{\alpha}}}{2\alpha} I_m\left(\frac{2\sigma_{\perp}^4 \gamma_n \gamma_{n'}}{\alpha}\right) \Bigg|_{\alpha=2\sigma_{\perp}^2}. \quad (\text{B.1.4})$$

We see that in terms of an expansion in the variable $1/\sigma_{\perp}^2$ each differentiation will give a factor of $1/\sigma_{\perp}^2$. We shall therefore only consider a sum up to the first order in the differential. To zeroth order the x -integral simply gives

$$\frac{e^{\frac{\sigma_{\perp}^2(\gamma_n^2 + \gamma_{n'}^2)}{2}}}{4\sigma_{\perp}^2} I_m(\sigma_{\perp}^2 \gamma_n \gamma_{n'}). \quad (\text{B.1.5})$$

To first order we find the x -integral to give

$$\begin{aligned} -\partial_{\alpha} \frac{e^{\frac{\sigma_{\perp}^4(\gamma_n^2 + \gamma_{n'}^2)}{\alpha}}}{2\alpha} I_m\left(\frac{2\sigma_{\perp}^4 \gamma_n \gamma_{n'}}{\alpha}\right) \Bigg|_{\alpha=2\sigma_{\perp}^2} &= \frac{e^{-\frac{\sigma_{\perp}^2}{2}(\gamma_n^2 + \gamma_{n'}^2)}}{8\sigma_{\perp}^4} \left[I_m(\sigma_{\perp}^2 \gamma_n \gamma_{n'}) \right. \\ &\quad \left. - \frac{\sigma_{\perp}^2}{2}(\gamma_n^2 + \gamma_{n'}^2) I_m(\sigma_{\perp}^2 \gamma_n \gamma_{n'}) + \frac{\sigma_{\perp}^2}{2} \gamma_n \gamma_{n'} (I_{m-1}(\sigma_{\perp}^2 \gamma_n \gamma_{n'}) + I_{m+1}(\sigma_{\perp}^2 \gamma_n \gamma_{n'})) \right]. \end{aligned} \quad (\text{B.1.6})$$

To understand the above expression let us assume a sufficiently large σ_{\perp} so that the modified Bessel function $I_{m\pm 1}$ can be approximated with I_m . In this way we get

$$-\partial_{\alpha} \frac{e^{\frac{\sigma_{\perp}^4(\gamma_n^2 + \gamma_{n'}^2)}{\alpha}}}{2\alpha} I_m\left(\frac{2\sigma_{\perp}^4 \gamma_n \gamma_{n'}}{\alpha}\right) \Bigg|_{\alpha=2\sigma_{\perp}^2} = \frac{e^{-\frac{\sigma_{\perp}^2}{2}(\gamma_n^2 + \gamma_{n'}^2)}}{8\sigma_{\perp}^4} I_m(\sigma_{\perp}^2 \gamma_n \gamma_{n'}) \left[1 - \frac{\sigma_{\perp}^2}{2}(\gamma_n - \gamma_{n'})^2 \right]. \quad (\text{B.1.7})$$

The above approximation gets worse for increasing values of m , however we argue in Sec. 14.2, that for a finite width of the sample, higher order modes in m has less influence. Finally the exponential function along with the modified Bessel function express a conservation of transverse momentum given by the variables γ_n since for increasing values of the transverse momentum, Eq. (B.1.7) can be approximated with

$$\frac{e^{-\frac{\sigma_{\perp}^2}{2}(\gamma_n - \gamma_{n'})^2}}{8\sigma_{\perp}^4 \sqrt{2\pi \gamma_n \gamma_{n'}}} \left[1 - \frac{\sigma_{\perp}^2}{2}(\gamma_n - \gamma_{n'})^2 \right]. \quad (\text{B.1.8})$$

We shall then make the approximation

$$1 - \frac{\sigma_{\perp}^2}{2}(\gamma_n - \gamma_{n'})^2 \approx e^{-\frac{\sigma_{\perp}^2}{2}(\gamma_n - \gamma_{n'})^2}, \quad (\text{B.1.9})$$

thus the expression in Eq. (B.1.8) can to first order in the difference $\gamma_n - \gamma_{n'}$ be written as

$$\frac{e^{-\sigma_{\perp}^2(\gamma_n - \gamma_{n'})^2}}{8\sigma_{\perp}^4 \sqrt{2\pi\gamma_n\gamma_{n'}}} \quad (\text{B.1.10})$$

This result is the large size limit, and we therefore conclude that to give this limit as $\sigma_{\perp} \rightarrow \infty$ the term in Eq. (B.1.6) must be approximated with

$$\sqrt{2} \frac{e^{-\sigma_{\perp}^2(\gamma_n^2 + \gamma_{n'}^2)} I_m(2\sigma_{\perp}^2 \gamma_n \gamma_{n'})}{8\sigma_{\perp}^4}. \quad (\text{B.1.11})$$

From this we conclude the result given in Eq. (12.0.15).

B.2 Commutation relation for $\Lambda_{nn'}^m$ and $\Lambda_{nn'}^{1m}$

Here we show that the two matrices $\Lambda_{nn'}^m$ and $\Lambda_{nn'}^{1m}$ commute. Since both matrices are symmetric, it is enough to show that the product $\sum_p \Lambda_{np}^m \Lambda_{pn'}^{1m}$ is symmetric. Again we make the continuation $\sum_p \frac{1}{a_c} \rightarrow \int \frac{d\gamma_p}{\pi}$ for $a_c \rightarrow \infty$. In this way we get

$$\sum_p \Lambda_{np}^m \Lambda_{pn'}^{1m} = \frac{4\sigma_{\perp}^4 e^{-\frac{\sigma_{\perp}^2}{2}\gamma_n^2 - \frac{\sigma_{\perp}^2}{2}\gamma_{n'}^2}}{a_c^2 J_{m+1}(X_{mn}) J_{m+1}(X_{mn})} \int d\gamma_p \gamma_p \frac{(-1)^m}{2} e^{-\frac{3\sigma_{\perp}^2}{2}\gamma_p^2} J_m(i\sigma_{\perp}^2 \gamma_n \gamma_p) J_m(2i\sigma_{\perp}^2 \gamma_{n'} \gamma_p). \quad (\text{B.2.1})$$

After making the γ_p -integral we end up with

$$\sum_p \Lambda_{np}^m \Lambda_{pn'}^{1m} = \frac{4\sigma_{\perp}^4 e^{-\frac{\sigma_{\perp}^2}{3}(\gamma_n^2 + \gamma_{n'}^2)} I_m\left(\frac{2\sigma_{\perp}^2}{3}\gamma_n \gamma_{n'}\right)}{3a_c^2 J_{m+1}(X_{mn}) J_{m+1}(X_{mn})}. \quad (\text{B.2.2})$$

Since the matrix Eq. (B.2.2) is symmetric we conclude that the matrices $\Lambda_{nn'}^m$ and $\Lambda_{nn'}^{1m}$ commute.

B.3 Beyond the delta function approximation of the Gaussian $\eta(k)$.

In general the matrix M , Eq. (12.0.9) can be diagonalized using a unitary transformation described by U . Let us denote the eigenvalues corresponding to this diagonalization with $\Lambda_{\mathbf{q}}$. From this formal diagonalization we will in complete analogy with the problem of $\Lambda_{mm'}^m$, eventually have to look at summations such as

$$\sum_{\mathbf{q}} U_{\mathbf{q},kmn} \Lambda_{\mathbf{q}}^N U_{\mathbf{q},k'm'n'}^* \quad (\text{B.3.1})$$

The index \mathbf{q} has a dimensionality to fit the Hilbert space spanned by k, m, n . Again we introduce the unit,

$$\mathbb{1} = \sum_{\mathbf{q}_1} \int dk_1 \sum_{m_1 n_1} U_{\mathbf{q}_1, kmn} U_{\mathbf{q}_1, k_1 m_1 n_1}^* \quad (\text{B.3.2})$$

so that the expression in Eq. (B.3.1), can be written as the sum

$$\sum_{\substack{m_1, \dots, m_{N-1} \\ n_1, \dots, n_{N-1}}} \int \prod_{i=1}^{N-1} dk_i M_{k_1 m_1 n_1}^{kmn} M_{k_2 m_2 n_2}^{k_1 m_1 n_1} \dots M_{k' m' n'}^{k_{N-1} m_{N-1} n_{N-1}} \quad (\text{B.3.3})$$

Thus to find the effect of the finite width of the Gaussian function we have to make the following type of integrals

$$\int dk_1 M_{k_1 m_1 n_1}^{kmn} M_{k_2 m_2 n_2}^{k_1 m_1 n_1} \quad (\text{B.3.4})$$

The product of two Gaussian functions $\eta(k - k_1)\eta(k_1 - k_2)$ integrated over k_1 gives

$$\frac{\sigma_{\parallel}}{\sqrt{2\pi}} e^{-\frac{\sigma_{\parallel}^2}{2}(k-k_2)^2}, \quad (\text{B.3.5})$$

a Gaussian with a width increased by a factor of $\sqrt{2}$. In the delta function approximation the functional form is unchanged by such integrations, thus the end result remains a delta function. As we increase the number of integrations k_1, k_2, \dots, k_{N-1} the width of the Gaussian increases thus making the delta function approximation worse. The figure of merit

is now the power N and as the width only increases with the square root of the power, we expect that for reasonably fast converging series Eq. (13.0.9), the delta-function approximation is acceptable. However as time and also Δz increases one would have to reconsider the approximation. We note that to treat this effect one should also include the poles $1/(k^2 - k_1^2), \dots$ in the calculation and not only the Gaussian function as done here.

B.4 Additional material to Sec. 14.3

Here we will show Eq. (14.3.2). Our starting point is the orthogonality relation given by

$$\int_0^\infty r dr J_m(\gamma_n r) J_m(\gamma_{n'} r) = \frac{\delta_{nn'} a_c^2}{2J_{m+1}(X_{mn})^2}, \quad (\text{B.4.1})$$

where the variable $\gamma_n = \frac{X_{mn}}{a_c}$ and X_{mn} is the n 'th zero of the m 'th order Bessel function J_m . We will assume that X_{mn} is large, which does not require γ_n to be so, since we can choose the cut-off a_c to be anything. In this way we can write Eq. (B.4.1) as

$$\int_0^\infty r dr J_m(\gamma_n r) J_m(\gamma_{n'} r) = \frac{\delta_{nn'} a_c}{\pi \gamma_n} \quad (\text{B.4.2})$$

We will then take the sum over n on both sides and use the standard continuation $\sum_n \frac{1}{a_c} \rightarrow \int \frac{d\gamma_n}{\pi}$ so that

$$\int d\gamma_n \gamma_n \int r dr J_m(\gamma_n r) J_m(\gamma_{n'} r) = 1. \quad (\text{B.4.3})$$

Since γ_n is now a continuous variable, we conclude that the measure of the distribution

$$f(x, x') = x \int r dr J_m(xr) J_m(x'r), \quad (\text{B.4.4})$$

where x, x' is some real and positive number is unity. The next step is to show that for $x \neq x'$ the function $f(x, x')$ vanish. This follows when choosing a zero point X_{mn} and a cut-off a_c such that say $x = \gamma_n$. This does not necessarily mean that x' has a similar representation with the chosen cut-off. On the other hand this is not necessary as one may

show, see e.g. [48], that

$$(\gamma_n^2 - x'^2) \int_0^{\alpha_c} r dr J_m(\gamma_n r) J_m(x' r) = 0. \quad (\text{B.4.5})$$

from here we conclude that when γ_n and x' are different the function $f(\gamma_n, x')$ vanish. This concludes the derivation of Eq. (14.3.2).

B.5 The Sum rule

Here we derive the sum rule Eq. (14.3.6) used in Sec. 14.3. The starting point is the total radiated intensity of Stokes-photons

$$\oint_S \{ \mathbf{D}^- \times (\nabla \times \mathbf{A}^+) - (\nabla \times \mathbf{A}^-) \times \mathbf{D}^+ \}, \quad (\text{B.5.1})$$

where S is a sphere surrounding the atoms. Using the Divergence theorem as well as the Maxwell equations, the total radiated intensity can be written as

$$-\mu_0 \epsilon_0 \int_V d^3 r \frac{\partial(\mathcal{H}_F + \mathcal{H}_I)}{\partial t} - \mu_0 \int_V d^3 r G[\mathbf{P}, \mathbf{D}] \quad (\text{B.5.2})$$

where

$$G[\mathbf{P}, \mathbf{D}] = \frac{\partial \mathbf{P}^-}{\partial t} \cdot \mathbf{D}^+ + \mathbf{D}^- \cdot \frac{\partial \mathbf{P}^+}{\partial t}. \quad (\text{B.5.3})$$

To first order in ω_s , Eq. (B.5.2) reduce to

$$\mu_0 \omega_s \hbar \epsilon_0 \left[\sum_j \Gamma \hat{b}_j(t) \hat{b}_j^\dagger(t) + \sum_{j \neq j'} \left\{ \hat{b}_j(t) M_{jj'} \hat{b}_{j'}^\dagger(t) + H.c. \right\} \right], \quad (\text{B.5.4})$$

where we have used Eqs. (10.1.7), (10.2.6) and (10.2.7). When measuring the intensity infinitely far away from the atomic ensemble, the expression in Eq. (B.5.1) reduce to the electric field squared times $2\mu_0 c$, thus the normalized sum-rule reads

$$\frac{2}{k_s \hbar \epsilon_0} \int d\Omega \mathbf{D}^- \cdot \mathbf{D}^+ = \sum_j \Gamma \hat{b}_j(t) \hat{b}_j^\dagger(t) + \sum_{j \neq j'} \left\{ \hat{b}_j(t) M_{jj'} \hat{b}_{j'}^\dagger(t) + H.c. \right\}. \quad (\text{B.5.5})$$

Bibliography

- [1] M. W. Sørensen and A. S. Sørensen. *Phys. Rev. A*, 77:013826, 2008.
- [2] P. Zoller L.-M. Duan, J. I. Cirac and E. S. Polzik. *Phys. Rev. Lett.*, **85**, 005643, 2000.
- [3] M. G. Raymer and J. Mostowski. *Phys. Rev. A*, 24:4, 1981.
- [4] H. J. Briegel et al. *Phys. Rev. Lett.*, **81**, 5932, 1998.
- [5] A. Kuzmich L. M. Duan and H. J. Kimble. *Phys. Rev. A*, **67**, 032305, 2003.
- [6] I. Schuster N. Syassen P. W. H. Pinkse P. Maunz, T. Puppe and G. Rempe. *Nature*, **428**, 50, 2004.
- [7] L. M. Duan B. B. Blinov, D. L. Moehring and C. Monroe. *Nature*, **428**, 153–157, 2004.
- [8] A. Scherer J. Vučković, M. Pelton and Y. Yamamoto. *Phys. Rev. A*, **66**, 023808, 2002.
- [9] M. Atatüre J. Dreiser E. Hu P.M. Petroff A. Badolato, K. Hennessy and A. Imamoglu. *Science*, **308**, 1158, 2005.
- [10] A. Kozhekin B. Julsgaard and E. S. Polzik. *Nature*, **413**, 400, 2001.
- [11] J. I. Cirac J. Fiurasek B. Julsgaard, J. Sherson and E. S. Polzik. *Nature*, **432**, 482, 2004.
- [12] R. K. Olsson B. Julsgaard K. Hammerer J. I. Cirac J. F. Sherson, H. Krauter and E. S. Polzik. *Nature*, **443**, 557, 2006.

-
- [13] J. K. Stockton J. M. Geremia and H. Mabuchi. *Science*, **304**, 270, 2004.
- [14] N. P. Bigelow A. Kuzmich and L. Mandel. *Europhys. Lett*, **42**, 481, 1998.
- [15] J. I. Cirac L.-M. Duan, M. D. Lukin and P. Zoller. *Nature*, **414**, 413, 2001.
- [16] D. N. Matsukevich and A. Kuzmich. *Science*, **306**, 663, 2004.
- [17] C. H. van der Wal *et al.* *Science*, **301**, 196, 2003.
- [18] C. W. Chou *et al.* *Nature*, **438**, 828, 2005.
- [19] S. Chen *et al.* *Phys. Rev. Lett.*, **97**, 173004, 2006.
- [20] A.T. Black H.W. Chan and V. Vuletić. *Phys. Rev. Lett.*, **90**, 063003, 2003.
- [21] M. D. Lukin. *Rev. Mod.Phys.*, **75**, 457, 2003.
- [22] M. Nilsson S. Kröll B. Kraus W. Tittel, N. Gisin and J. I. Cirac. *Phys. Rev. A*, **73**, 020302, 2006.
- [23] I. M. Sokolov B. Julsgaard D. V. Kupriyanov, O. S. Mishina and E. S. Polzik. *Phys. Rev. A*, **71**, 032348, 2005.
- [24] J. H. Müller O. S. Mishina, D. V. Kupriyanov and E. S. Polzik. *Phys. Rev. A*, **75**, 042326, 2007.
- [25] J. Mostowski and B. Sobolewska. *Phys. Rev. A*, **28**, 2573, 1983.
- [26] J. Mostowski and B. Sobolewska. *Phys. Rev. A*, **30**, 610, 1984.
- [27] J. I. Cirac L. M. Duan and P. Zoller. *Phys. Rev. A*, **66**, 023818, 2002.
- [28] J. Dupont-Roc C. Cohen-Tannoudji and G. Grynberg. *Photons and Atoms, Introduction to Quantum Electrodynamics*. Wiley, 1997.
- [29] Brian Julsgaard. *Entanglement and Quantum Interactions with Macroscopic Gas Samples*. PhD thesis, University of Århus, Denmark, October 2003.
- [30] R. J. Glauber and M. Lewinsein. *Phys. Rev. A*, **43**, 467, 1991.
- [31] S. J. van Enk and H. J. Kimble. *Phys. Rev. A*, **63**, 023809, 2000.

-
- [32] I. V. Sokolov D. V. Vasilyev and E. S. Polzik. *Phys. Rev. A*, **77**, 020302, 2008.
- [33] I. Ali-Khan R. M. Camacho, C. J. Broadbent and J. C. Howell. *Phys. Rev. Lett.*, **98**, 043902, 2007.
- [34] P. W. Milonni and J. H. Eberly. *Lasers*. Wiley, 1988.
- [35] E. S. Polzik C. A. Muschik and J. I. Cirac. *Detecting entanglement in two mode squeezed states by particle counting*. arXiv:0806.3448v2, 2008.
- [36] E. J. Woodbury and W. N. Ng. *Proc. IRE*, **50**, 2347, 1962.
- [37] R. W. Hellwarth. Theory of stimulated raman scattering. *Phys. Rev.*, **130**, 5:1850–1852, Jun 1963.
- [38] N. E. Rehler and J. Eberly. *Phys. Rev. A*, **3**, 5, 1971.
- [39] R. H. Dicke. *Phys. Rev.*, **93**, 1, 1954.
- [40] R. Bonifacio and L. A. Lugiato. *Phys. Rev. A*, **11**, 5, 1975.
- [41] J. Mostowski M. G. Raymer, I. A. Walmsley and B. Sobolewska. *Phys. Rev. A*, **32**, 1, 1985.
- [42] D. M. Stamper-Kurn-J. Stenger D. E. Pritchard S. Inouye, A.P. Chikkatur and W. Ketterle. *Science*, **285**, 571, 1999.
- [43] R. Bonifacio *et. al.* *Phys. Rev. Lett.*, **233**, 155–160, 2004.
- [44] M. G. Moore and P. Meystre. *Phys. Rev. Lett.*, **83**, 25, 1999.
- [45] A. Gero E. Akkermans and R. Kaiser. *Phys. Rev. Lett.*, **101**, 103602, 2008.
- [46] L. H. Pedersen and Klaus Mølmer. *Few qubit atom-light interfaces with collective encoding*. arXiv:0807.3610v2.
- [47] D. Porras and J. I. Cirac. *Collective generation of quantum states of light by entangled atoms*. arXiv:0808.2732v1.
- [48] John David Jackson. *Classical Electrodynamics*. John Wiley & Sons, inc., 3rd edition edition, 1998.

-
- [49] V.V.Klimow and M.Ducloy. *Phys. Rev. A*, **69**, 013812, 2004.
- [50] Gradshteyn and Ryzhik. *Tables of integrals, Series and Products*. Academic Press, 1965.
- [51] G.N.Watson. *Theory of Bessel functions*. Cambridge university press, 1944.
- [52] A. S. Sørensen K. Hammerer and E. Polzik. *Quantum interface between light and atomic ensembles*. arXiv:0807.3358v2.
- [53] Andrew Hilliard. *Collective Rayleigh scattering in a Bose Einstein condensate*. PhD thesis, Copenhagen University, October 2008.
- [54] C. M. Marcus J. M. Taylor and M. D. Lukin. *Phys. Rev. Lett.*, , 206803, 2003.
- [55] A. Imamoglu J. M. Taylor and M. D. Lukin. *Phys. Rev. Lett.*, **91**, 246802, 2003.
- [56] L. Tian A. Imamoglu, E. Knill and P. Zoller. *Phys. Rev. Lett.*, **91**, 017402, 2003.
- [57] J. I. Cirac H. Christ and G. Giedke. *Phys. Rev. B*, **75**, 155324, 2007.
- [58] A. Badolato. C. W. Lai, P. Maletinsky and A. Imamoglu. *Phys. Rev. Lett.*, **96**, 167403, 2006.
- [59] J. A. Gupta and D. D. Awschalom. *Phys. Rev. B*, **63**, 085303, 2001.
- [60] C. Mewes and M. Fleischhauer. *Phys. Rev. A*, **72**, 022327, 2005.
- [61] C. Mewes. PhD thesis, University of Kaiserslautern, Germany, 2002.
- [62] C. Deng and X. Hu. *IEEE Trans. Nanotechnol.*, **4**, 35, 2005.
- [63] Y. Castin O. Morice and J. Dalibard. *Phys. Rev. A*, **51**, 3896, 1995.
- [64] B.A. van Tiggelen A. Lagendijk, B. Nienhuis and P. de Vries. *Phys. Rev. Lett.*, **79**, 657, 1997.